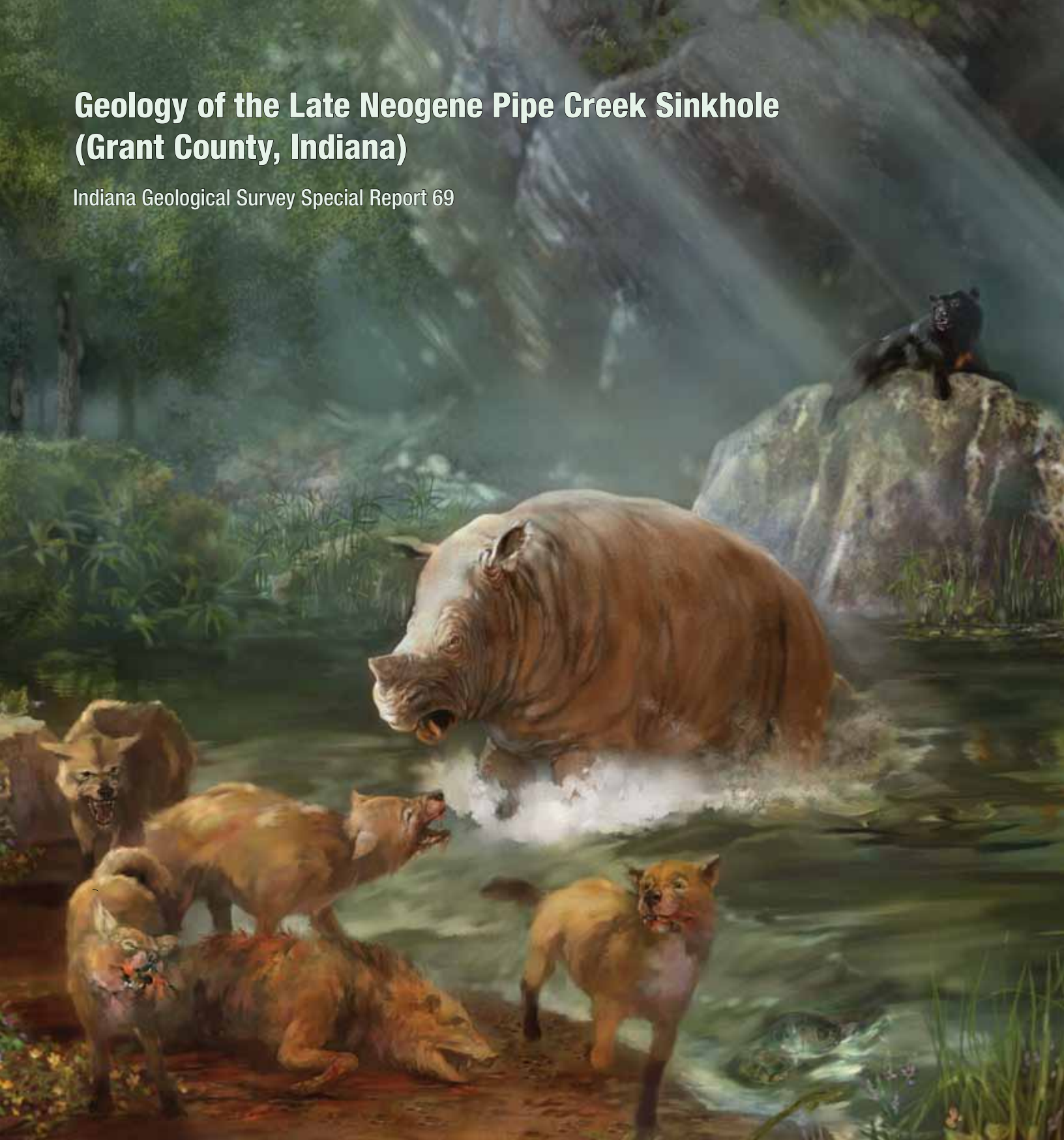


Geology of the Late Neogene Pipe Creek Sinkhole (Grant County, Indiana)

Indiana Geological Survey Special Report 69



INDIANA
GEOLOGICAL SURVEY

INDIANA UNIVERSITY

Indiana Geological Survey Staff

Administration (812) 855-5067

John C. Steinmetz, Director and State Geologist
Glenda K. Bitner, Assistant Director for Business
Teresa J. Blevins, Administrative Secretary
and Licensing Coordinator
Richard T. Hill, Assistant Director for Information
Technology and Chief Information Officer
Todd A. Thompson, Assistant Director for Research
Helen C. Stephenson, Financial Records Assistant

Center for Geospatial Data Analysis (CGDA) (812) 855-7428

Shawn C. Naylor, Hydrogeologist and Section Head
Chris R. Dintaman, Geologist and GIS Specialist
John T. Haddan, Field Laboratory Specialist
Denver Harper, Environmental Geologist
Sally L. Letsinger, Hydrogeologist
Deann Reinhart, Grants Compliance Monitor

Coal and Industrial Minerals Section (812) 855-2687

Nelson R. Shaffer, Geologist and Section Head
Megan E. Divine, Grants Compliance Monitor
Agnieszka Drobniak, Coal Geologist
Carolyn M. Estell, Database Manager
and Geological Assistant
Walter A. Hasenmueller, Geologist
Maria D. Mastalerz, Coal Geologist
Rebecca A. Meyer, GIS/Database Analyst
Licia A. Weber, Geologist

Environmental Geology Section (812) 855-7428

Nancy R. Hasenmueller, Environmental Geologist
and Section Head
Marni Dickson Karaffa, Glacial Geologist
Michael L. Prentice, Glacial Geologist
Deann Reinhart, Grants Compliance Monitor
Robin F. Rupp, Geologist

Geochemistry Section (812) 855-2687

Shawn C. Naylor, Acting Section Head
Tracy D. Branam, Geochemist
Megan E. Divine, Grants Compliance Monitor
Margaret V. Ennis, Geochemist
Ronald T. Smith, Geochemist

Information Technology Section (812) 855-3951

Richard T. Hill, Section Head
Michael S. Daniels, Systems Analyst/Programmer
Deborah A. DeChurch, Senior Editor
Janis D. Fox, Sales Office Manager
Walter E. Gray, Education and Outreach Coordinator
Kathleen M. Griffin, Network Support Specialist
David A. Held, Cartographic Specialist
Paul D. Rohwer, Database Administrator/Developer
Kathryn R. Shaffer, Minerals Statistician
Kimberly H. Sowder, Cartographic Coordinator
Renée D. Stubenrauch, Cartographic Specialist
Donna M. Webb, Accounting Representative
and Publication Sales

Photography and Imaging Section (812) 855-1370

Barbara T. Hill, Photography Manager and Section Head
John M. Day, Photographic Specialist
Donna M. Webb, Accounting Representative

Physical Facilities and Field Services Section (812) 855-3596

Drew M. Packman, Laboratory and Field Assistant
Donna M. Webb, Accounting Representative

Subsurface Geology Section (812) 855-5412

Charles W. Zuppann, Petroleum Geologist
and Section Head
Sherry K. Cazee, Sample and Core Library Supervisor
Kevin Ellett, Senior Research Geophysicist/Hydrologist
David M. Jacob, Laboratory and Field Assistant
Brian D. Keith, Petroleum Geologist
Cristian R. Medina, Research Geologist
Mary A. Parke, Petroleum Geologist
John A. Rupp, Geologist

Research Affiliates

Lewis M. Brown
John B. Comer
John B. Droste
Henry H. Gray
Richard Lahann
Greg A. Olyphant
Richard L. Powell
Carl B. Rexroad

Geology of the Late Neogene Pipe Creek Sinkhole (Grant County, Indiana)

Edited by James O. Farlow, John C. Steinmetz, and Deborah A. DeChurch

Indiana University
Indiana Geological Survey Special Report 69



PRINCIPAL AUTHORS

James O. Farlow is Professor of Geology in the Department of Geosciences at Indiana-Purdue University Fort Wayne.

Anne Argast is Professor of Geology in the Department of Geosciences at Indiana-Purdue University Fort Wayne.

Jack A. Sunderman is Professor Emeritus, Department of Geosciences, Indiana University-Purdue University Fort Wayne. While a staff member of the Indiana Geological Survey, he discovered the ancient rocks of the Pipe Creek Jr. Quarry.

Cover: Reconstruction of the Pipe Creek Sinkhole. A rhinoceros (*Teleoceras*) confronts a pack of canids (*Borophagus*) feeding on the carcass of a pecary, while a bear (*Plionarctos*) lazily watches the drama, and frightened turtles and a frog scramble into the water for safety. Painting by paleoartist Karen Carr; used by permission of the Indiana State Museum.

CONTENTS

Occurrence and features of fossiliferous sediments of the Pipe Creek Sinkhole (Late Neogene, Grant County, Indiana).....	1
<i>James O. Farlow, Ronald L. Richards, Rexford C. Garniewicz, Michele Greenan, William R. Wepler, Aaron J. Shunk, Greg A. Ludvigson, Nelson R. Shaffer, and Amzie L. Wenning</i>	
Interstratified kaolinite-smectite from a sediment derived from terra rossa in the Pipe Creek Sinkhole, Indiana.....	61
<i>Anne Argast and James O. Farlow</i>	
Course of the Tertiary Teays River southwest of Lake Erie Lowlands, USA: Evidence from petrologic and lead isotopic characteristics of pebbles found in the northern Indiana Pipe Creek Sinkhole.....	75
<i>Jack A. Sunderman, E. Troy Rasbury, and Sidney R. Hemming</i>	

Occurrence and Features of Fossiliferous Sediments of the Pipe Creek Sinkhole (Late Neogene, Grant County, Indiana)

By James O. Farlow, Ronald L. Richards, Rexford C. Garniewicz, Michele Greenan, William R. Wepler, Aaron J. Shunk, Greg A. Ludvigson, Nelson R. Shaffer, and Amzie L. Wenning

ABSTRACT

The Pipe Creek Sinkhole (Pipe Creek Jr. Quarry, Irving Materials, Inc., Grant County, Indiana) preserves a diverse paleobiota of late Neogene (late Hemphillian or early Blancan) age. Part of the site was destroyed by quarry operations before it could be studied, but intensive interdisciplinary field and laboratory work has revealed much about the microstratigraphic context and characteristics of the fossiliferous deposit and associated units.

Despite frequent complications of postdepositional sagging around large limestone boulders in the sinkhole, a typical stratigraphic sequence of distinct layers (zones) was recognized. The fossiliferous sediment (Zone A) was a dark-colored, mud-rich, organic-rich diamicton overlying a yellow-brown clay (Zone B), which in turn overlay (in situ sediments no longer exist in the sinkhole) thick red clays (Zone C). Zone C was so thick that its lower limit could not be detected, either by mechanical digging or by ground penetrating radar.

Sediment microfabrics of Zones A and C were similar in containing reworked mudballs presumably transported into the sinkhole from the surrounding landscape. Zone B appeared to be a product of weathering of the uppermost parts of the red clays; Zone B and parts of Zone C preserved root traces, and appear to have undergone alternating oxidizing and reducing conditions.

In contrast, Zone A experienced reducing conditions and poor drainage through most of its history, as indicated by its dark color and abundant siderite nodules, and by stable carbon and oxygen isotope ratios of the siderites. Such reducing conditions presumably were associated with large quantities of organic matter (5 to 10 percent dry weight of the noncoarse sediment fraction) that accumulated in the Zone A depositional environment. Reducing conditions in turn facilitated preservation of plant and other fossils. In one part of the sinkhole, Zone A

contained a laterally extensive layer of wood, seeds, and other detritus. The organic content of Pipe Creek Sinkhole fossil plant material (as a percentage of dry weight) is very little, less than that of modern plant tissues.

In addition to large plant fragments, fossils preserved in Zone A included vertebrates, invertebrates, and charophyte gyrogonites. Because Zone A was mostly unconsolidated, screen-washing was used to concentrate fossils. Vertebrate bones occurred in concentrates collected on 4-mm, 2-mm, 1-mm, and 0.5-mm mesh screens. The most common small vertebrates were frogs and turtles, but snakes, small mammals, and fishes were also present. Small molluscs, seeds, and charophyte gyrogonites were abundant in the 1-mm and 0.5-mm fractions. With few exceptions, large mammals were represented by isolated bones.

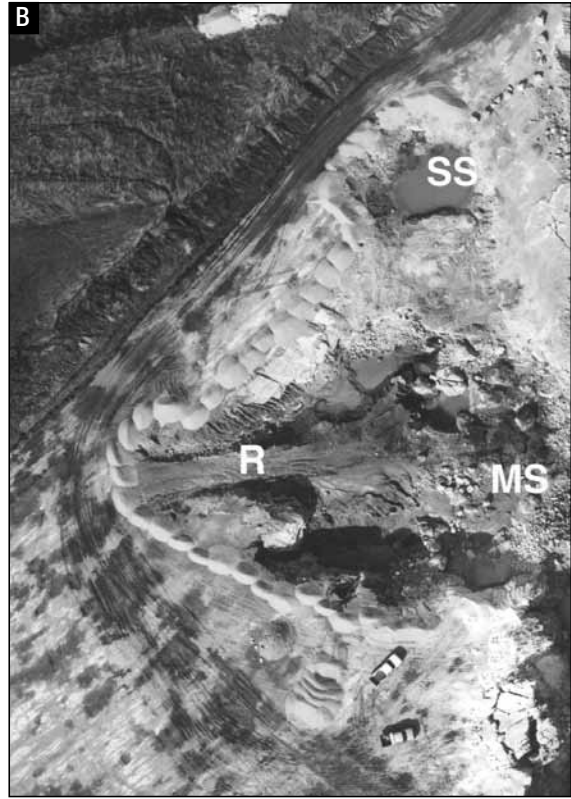
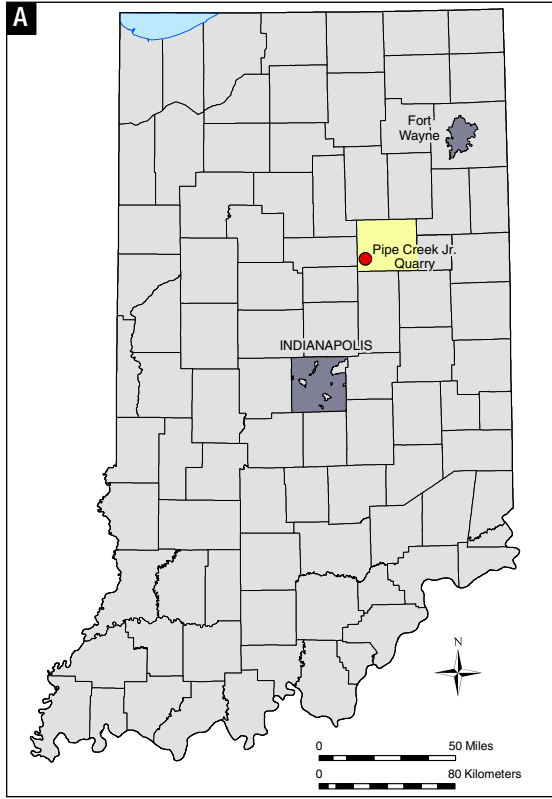
Zone C probably derived from terra rossa clays on the surrounding landscape that filtered into the future site of the sinkhole while it was still a cave that was largely closed to the surface. Zone B constitutes the end product of weathering of the uppermost portions of Zone C after the sinkhole had opened, permitting plants to grow and pedogenesis to occur. Along with sedimentary features of Zone A, the dominance of the biota by aquatic taxa indicates deposition in a wetland at least and, more likely, a pond.

INTRODUCTION

Karst features frequently constitute important sites for accumulation and preservation of vertebrate fossils (for example, Sutcliffe and others, 1976; Andrews, 1990; Latham, 1999; Moriarty and others, 2000; Hulbert, 2001; Worthy and Holdaway, 2002; Schubert and others, 2003; Bechtel and others, 2005; Lundelius, 2006; Reed, 2006; George and others, 2007; Richards, 2007). In 1996, quarry workers at the Pipe Creek Jr. limestone quarry (Irving

Materials, Inc.) near Swayzee in Grant County, Indiana, stripped away the cover of Wisconsin till as they expanded the quarry into a new area. To their surprise, they did not find limestone bedrock immediately beneath the till, but rather a preglacial sinkhole filled with a thick deposit of largely unconsolidated sediment (fig. 1). The greater part of this sediment was dumped in a heap (designated the "Spoil Pile" to label samples collected from it) beside the quarry in an attempt to reach bedrock, but this proved too difficult to do, even

Figure 1 (opposite page). The Pipe Creek Sinkhole. A) Map of Indiana showing the geographic location of the sinkhole in Grant County. B) Aerial photograph of the sinkhole in March 1997, prior to large-scale processing of in situ sediments, north roughly toward the top of the picture. Note pickup trucks near bottom of picture for scale. The flat surface on which the trucks are parked, and which extends around the sinkhole on the left, is glacially scoured bedrock. Note a small satellite sinkhole (SS) (which contained no fossiliferous sediments) to the north of the main sink. A ramp (R) of sediment was graded from the flat bedrock surface downward and to the right into the main sink (MS, center right). Quarrying operations altered the sinkhole before our main field work began in 2003, destroying much of the doline's south rim, but not greatly affecting the remaining in situ fossiliferous sediments. C) The sinkhole as positioned in the Pipe Creek Jr. limestone quarry, spring 2007, view to the west. The sinkhole developed in Silurian reef flank beds of the Wabash Formation. Much of the sinkhole had been destroyed by quarry operations by the time this photograph was taken, but its remnants constitute the depression just beyond (above) the orange-brown stained area near the center of the photograph. D) View across the sinkhole, looking to the southwest, June 25, 2003. Landmark Rocks A (1), B (2), and C (3) are labeled, as is Trench 1 (Tr 1) just beyond Rock B (partly covered by a white tarp).



using heavy machinery. When fossil bone was found in Spoil Pile material, it became clear that the Pipe Creek Sinkhole (PCS) preserved an important fossil assemblage.

Since 1996, Jack Sunderman of Indiana-Purdue University Fort Wayne (IPFW) has studied PCS sediments and their depositional history. From 1997 to the present, James Farlow has coordinated study of the sinkhole's fossils, doing surface collecting and also screen-washing sediments remaining in situ in the sinkhole and material dumped in the Spoil Pile. In June 1998 a field crew from the Indiana State Museum (INSM; the repository for PCS fossils) and IPFW wet-screened a large amount of Spoil Pile sediments on site. Fossiliferous Spoil Pile sediments were similar to and yielded the same kinds of fossils as in situ fossiliferous sediments that we removed from the sinkhole.

A preliminary account of the diverse assemblage of plants, vertebrates, and microinvertebrates recovered from PCS sediments, along with a preliminary interpretation of sinkhole structure and history, was published by Farlow and others (2001). Small mammals from the PCS were described by Martin and others (2002), who determined the biostratigraphic age of the fossil assemblage to be late Hemphillian (latest Miocene-earliest Pliocene—but see Bell and others [2004] for a slightly different interpretation of the age of the site), and by Dawson and others (2008). Farlow and Argast (2006) characterized the diagenesis and preservation of PCS fossil bone. Shunk and others (2009) provided interpretations of the late Neogene paleoclimate and paleoenvironment in Indiana based on features of PCS sediments and fossils. Farlow and others (2010) described carnivore coprolites from the site.

From 2003 to 2005, joint Indiana State Museum/Indiana-Purdue University Fort Wayne field crews studied in situ sediments remaining in the sinkhole and wet-screened sediment on site. A large number of additional fossils were obtained, along with information about the sediments in which they were entombed.

Like the Gray Fossil Site of Tennessee (Wallace and Wang, 2004; Shunk and others, 2006), the PCS provides a rare glimpse of late Neogene plants and animals from the interior of the eastern half of North America; all other presently known sites are from western North America or the Gulf and Atlantic Coasts (Janis and others, 1998; Woodburne, 2004; Prothero, 2005, 2006). The PCS paleobiota is, therefore, of considerable importance for reconstructing the paleoclimate, biogeography, and paleoecology of the continent during this time interval. Whether the Pipe Creek Sinkhole is a unique occurrence in Indiana, or whether similar sites will turn up now that we have a search image for them, is obviously unknown. However, on the chance that the PCS remains the only site of its kind in the state, it is critical that it be thoroughly documented.

This report describes features of the fossiliferous PCS sediments, the procedures used to obtain this information, the names assigned to particular parts of the sinkhole deposit, and samples collected from those parts of the deposit. It provides a repository of provenance and sample data that will be cited in future descriptions of the various components of the paleobiota.

We first describe the occurrence of late Neogene fossiliferous and associated sediments as observed in the field, in terms of gross stratigraphic features, texture (for example, abundance of coarse clasts, and clay content as crudely determined by feel), fossil content, and color. When characterizing colors according to the Munsell Color (2000) system, the formal color written names will be followed by the standard Munsell color code. However, in some places informal color descriptions will be used, and these do not have a code associated with them.

The term “saprolite” is used in an informal sense to mean decomposed rock, without implying any composition of that decayed material. However, most of this material was calcareous. Another informal term used is “zone” (for example, Zones A, B, and C), used to characterize distinct sedimentary units or subunits in the sinkhole.

Figure 2. Plan map of excavations in the Pipe Creek Sinkhole during 2003. Large breakdown boulders shown in gray; Rocks A, B, and C were landmarks throughout the project (Rock B was also named the “Bear Rock” because paleoartist Karen Carr painted an ancient bear draped over this rock in her reconstruction of the Pipe Creek Sinkhole [see fig. 27]). Arrow indicates true north. In 2003 Trench 1 (figs. 6 and 7) was dug, and Zone A fossiliferous sediment from the SW and SE Quadrants adjacent to it were removed and screened. The Funnel was an area between breakdown boulders in which a thick sequence of sagging fossiliferous material was collected (figs. 7 and 8).

We report the results of ground penetrating radar (GPR) surveys of the sinkhole carried out prior to our excavations. GPR was used for two purposes: first, to see if it could ascertain anything about the deepest parts of the sinkhole (for example, where it bottomed out in bedrock); and second, to see how well interpretations of sinkhole structure based on GPR matched the results of our actual digging.

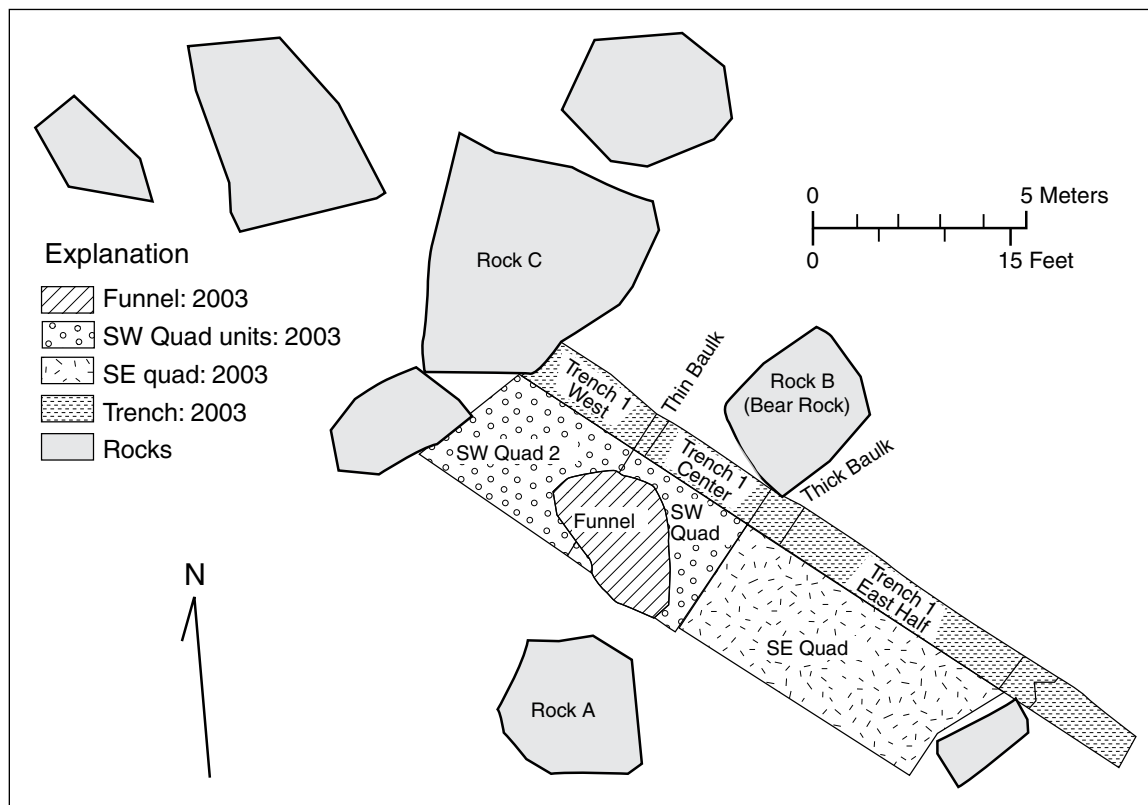
Fossiliferous sediments were wet-screened in the field and laboratory to concentrate fossils. The effects of mesh size on the quantitative composition of fossil faunas has been investigated by invertebrate paleontologists (Kowalewski and Hoffmeister, 2003; Bush and others, 2007); although vertebrate paleontologists are aware that mesh size affects sampling of microvertebrates (McKenna and others, 1994; Cifelli, 1996; Sankey and Baszio, 2008), quantitative analyses of such effects are limited. Because our future work will examine this topic, sediment size fractions generated by screen-washing during our work will be characterized in detail.

Micromorphological features of fossiliferous and associated sediments, based on oriented thin sections, are described. Geochemical and stable isotope data about siderite nodules from the fossiliferous

sediment are presented. Finally, modifications to an earlier scenario of the depositional history and taphonomy of the sinkhole (Farlow and others, 2001) necessitated by our observations are discussed.

FIELD WORK AND SITE DESCRIPTION

The Pipe Creek Sinkhole (fig. 1) is located at latitude $40^{\circ} 27' 25.4''$ N., longitude $85^{\circ} 47' 37.2''$ W. (NAD 83), NE1/4, NW1/4, SE1/4, Sec. 12, T. 23 N., R. 6 E., Point Isabel quadrangle, U.S. Geological Survey 7.5-Minute Series Topographic Map, Grant County, Indiana. The bedrock comprises the famous Silurian Pipe Creek Jr. Reef (Wabash Formation: Pinsak and Shaver, 1964; Shaver and others, 1970; Sunderman and Mathews, 1975; Shaver and Sunderman, 1982, 1989; Shaver and others, 1983; Devaney and others, 1986; Lehmann and Simo, 1988; Simo and Lehmann, 2000). The sinkhole developed in limestone flank beds of the reef. When field work on the in situ material began in 2003, only a thin cover of fossiliferous sediment was thought to remain. The plan was to remove and process this material quickly, and then move on to finish washing the Spoil Pile sediments. Once work was initiated (figs.



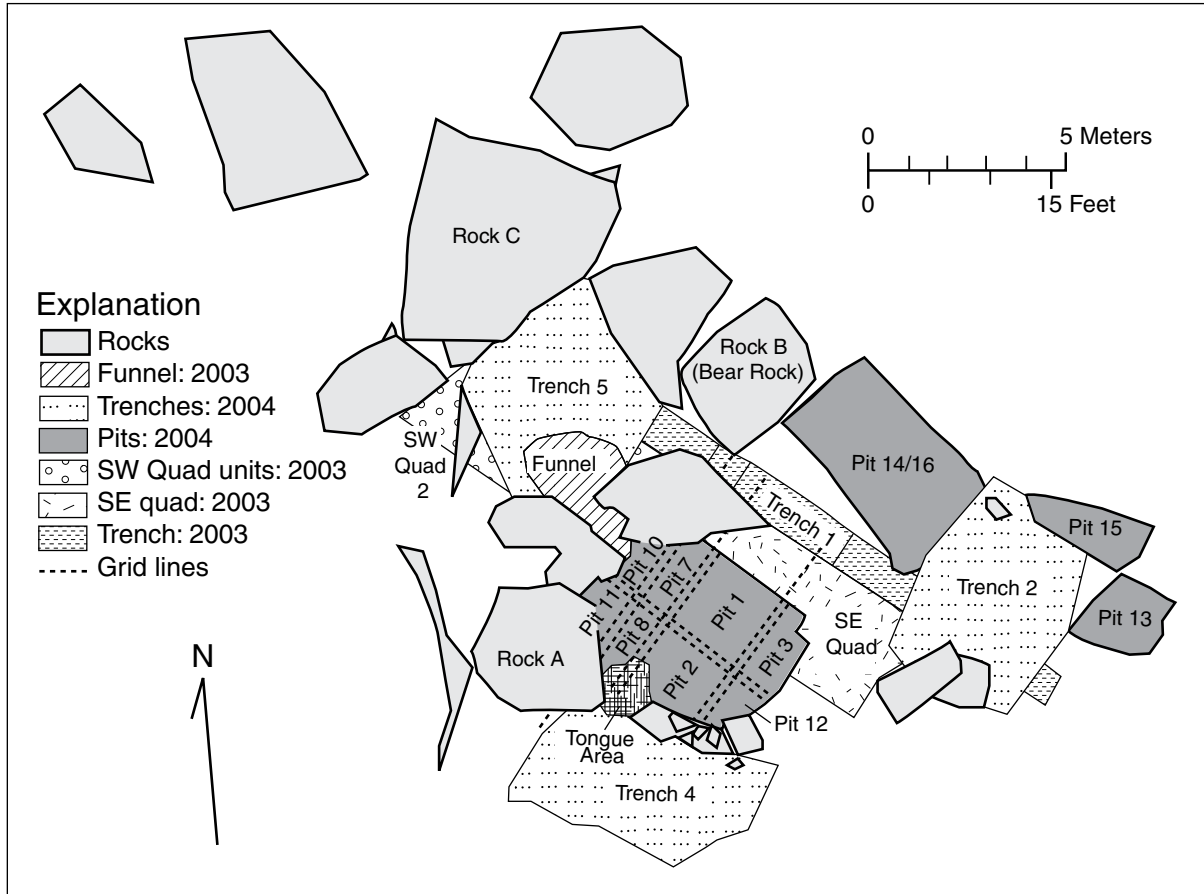


Figure 3. Plan map of the Pipe Creek Sinkhole showing 2004 excavations. Several new trenches and excavation pits were dug, and Zone A sediment from them was screened. The gridded Excavation Plateau of numbered pits was stratigraphically beneath the 2003 SW and SE Quadrants, but is shown above them in the map for clarity.

2–4), it quickly became apparent that a far greater amount of fossiliferous sediment remained in the sinkhole than was realized.

2003 field season

A northwest- to southeast-running trench was dug along the edge of the remaining in situ sinkhole sediments (figs. 2, 5, 6, and 7A, B), to get a preliminary idea of the attitude and distribution of the sediments. The northwest edge of the trench abutted Rock C, one of three large limestone boulders (interpreted as breakdown) that constituted important landmarks throughout our excavations. About midway along its length, the trench passed adjacent to Rock B, another landmark boulder. The segment of Trench 1 from Rock B to the southeast end of the trench was designated the “East Half” of Trench 1. The portion of Trench 1 adjacent to Rock B was des-

ignated its “Center,” and the segment northwest of the trench Center was designated the “West Edge.” Two baulks of sediment, one considerably thicker than the other, were left as most of the sediment was removed while digging the trench.

The surface layer of Trench 1 sediments (and in all other parts of the remaining in situ sinkhole deposits) constituted a Disturbed Zone of mixed origin. Some of these disturbed sediments may reflect depositional or ancient postdepositional events within the sinkhole, while other disturbance (particularly in the East Half) reflected modern plant growth and our previous spot sample collecting. Thickness of the Disturbed Zone varied, but was as much as 20 cm (~ 8 inches). Material removed from the Disturbed Zone of Trench 1 was designated “Level 1” throughout; for Trench 1 the two names are synonymous.

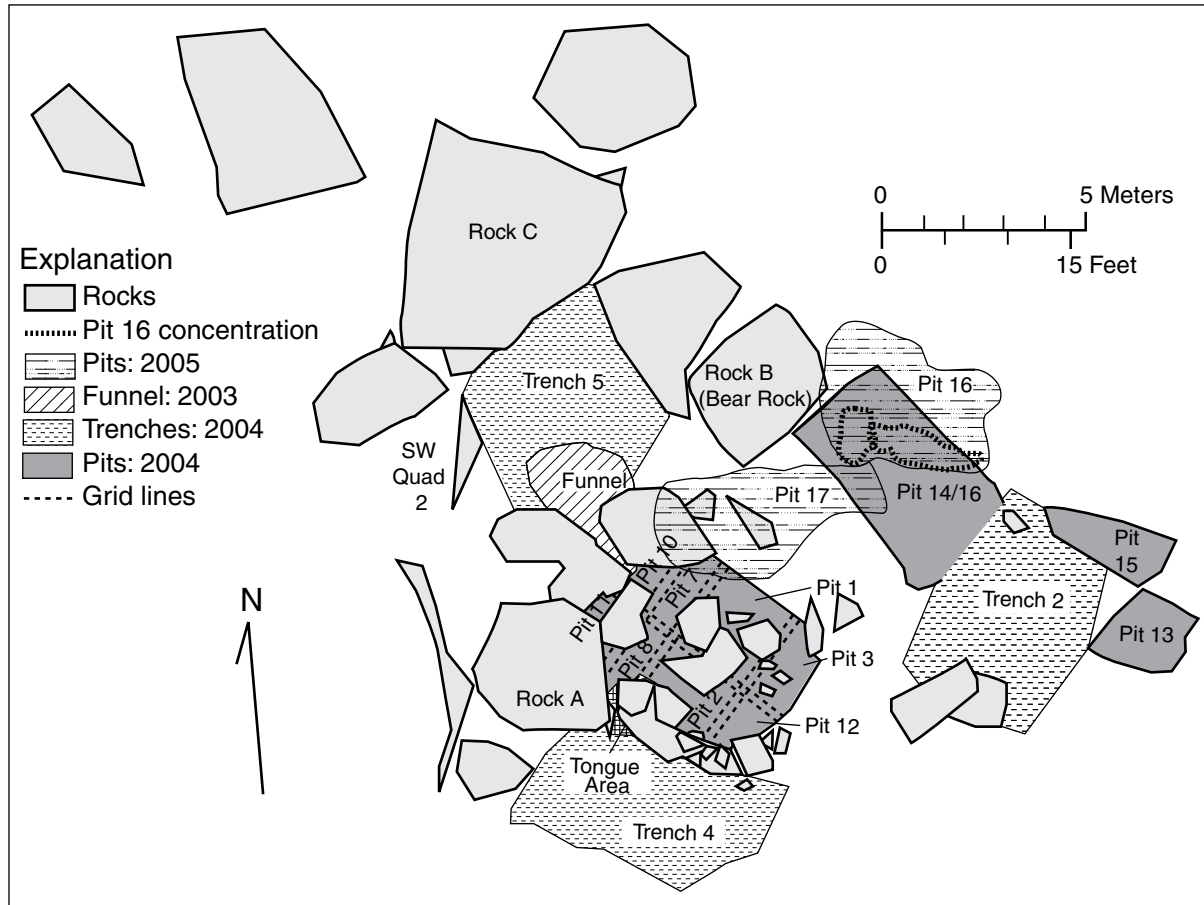


Figure 4. Plan map of the Pipe Creek Sinkhole showing 2005 excavations. Two final excavation pits were dug, and an attempt to hit bedrock beneath the 2004 Excavation Plateau was made. However, as deeply as we were able to dig by hand or using heavy machinery, limestone boulders surrounded by Zone C terra rossa were found. The map shows several of these boulders, drawn on top of the 2004 excavation platform for clarity, even though these rocks were stratigraphically beneath the 2004 surface. By the end of fieldwork in 2005 all fossiliferous Zone A sediment remaining in situ in the sinkhole had been removed and screened.

Features of the sediment immediately beneath the Disturbed Zone varied along the length of Trench 1 (fig. 6). In a few places sediment was a very dark gray (10 YR 3/1) organic layer (designated Zone A) rich in plant material, bone fragments, limestone fragments, and rounded quartzite pebbles (Sunderman and others, 1998).

Over much of the length of Trench 1, the material just beneath the Disturbed Zone comprised a layer (Zone B) of clay-rich sediment in varying shades of brown (ranging from 10 YR 4/6 [dark yellowish brown] to 5 YR 4/4-4/6 [reddish brown-yellowish red]). Zone B contained scattered lenses or strings of calcareous, saprolitic sand, a few patches of sediment comparable to that in Zone A, and once again limestone fragments and rounded quartzite pebbles.

Over most of the length of Trench 1, Zone B was underlain by a heavy, sticky, dark red (2.5 YR 3/6) clay, designated "Zone C." In several places the clay contained strings of yellowish brown (10 YR 5/8), calcareous, saprolitic sand. Individual chunks of calcite crystal were fairly common. Just west of the thin baulk, two vertical patches of Zone B punched downward into Zone C. These were likely smaller-scale versions of the down-sagging sediment structures seen elsewhere in the sinkhole.

One such larger feature occurred adjacent to the thick baulk in the Center portion of Trench 1, where Zone C sediments wrapped in a plastic fashion around the margins of limestone rocks (presumed breakdown boulders) (figs. 6 and 7B). The exposed portion of Zone C was much thicker

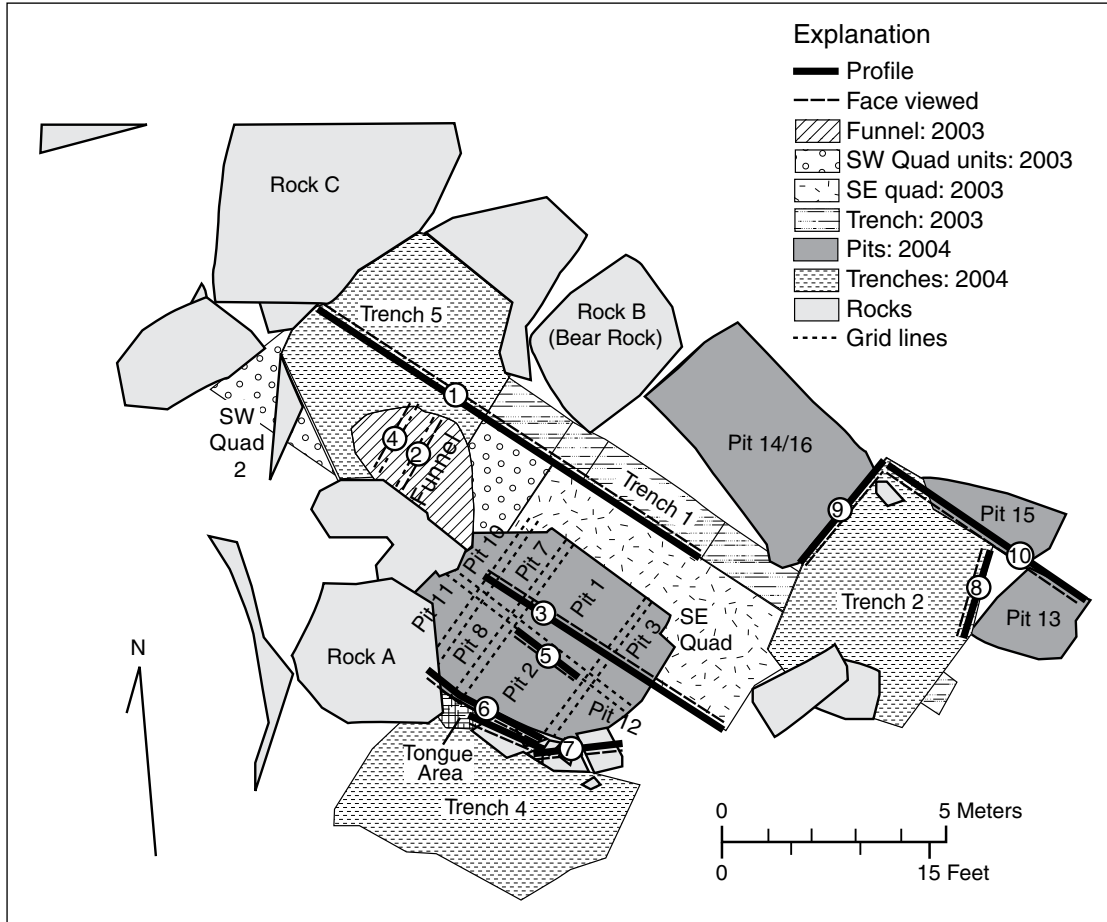


Figure 5. Combined maps of excavations, 2003 through 2005, of the Pipe Creek Sinkhole showing locations of section profiles (circled numbers on solid bars plus dashed lines). "Face viewed" (dashed pattern) shows where a viewer of the section would have stood while examining the section. Key to profiles: 1) South (north-facing) wall of 2003 Trench 1; 2) Profile across the 2003 Southwest Quadrant Funnel; 3) South (north-facing) edge of 2003 Southeast Quadrant; 4) Periphery of the 2003 SW Quadrant Funnel, as exposed in 2004; 5) Northeast (southwest-facing) wall of 2004 Excavation Pit 2; 6) North (south-facing) wall of 2004 Trench 4; 7) Two profiles of the north (south-facing) wall of 2004 Trench 4, stratigraphically and topographically beneath Profile 6; 8) East (west-facing) wall of 2004 Trench 2; 9) West (east-facing) wall of 2004 Trench 2; 10) North(east) (south[west]-facing) wall of Pit 13 and associated parts of 2004 Trench 2. After Profile 10 was drawn, Pit 15 was excavated to the northeast of the profile location. Some of the profiles drawn during fieldwork were later determined to be relatively uninformative, and so are not included in this report.

here than in other parts of Trench 1, except in other places where Zone C filled the gap between other limestone boulders (for example, near the eastern end of the trench). In addition to having a thicker accumulation of sediment in this feature, sediment microstratigraphy was more complex, because two additional sediment zones were intercalated between Zones B and C. Zone D, just beneath Zone B, was a strong brown (7.5 YR 4/6) laminated clay that was relatively clean of rubble, in contrast to the overlying Zone B and underlying Zone E. Zone E, positioned beneath Zone D and above Zone C, was a reddish brown (2.5 YR 5/4) clay unit that had abundant chert and limestone fragments, and also

quartzite pebbles, near its base. Clear laminations characterized the top of Zone E, but were absent at its base.

Zones A, B, and C, although initially defined from Trench 1, could be recognized in other parts of the sinkhole as well, and these sediment categories were used throughout the rest of our field work; in their paleoclimatic study, Shunk and others (2009) characterized our Zone A as the PCS dark facies, our Zone C as the red facies, and our Zone B as the PCS paleosol. Sunderman and others (this volume) used the term "Diamicton-2" to characterize the sediments that we called Zone A. Our Zones B

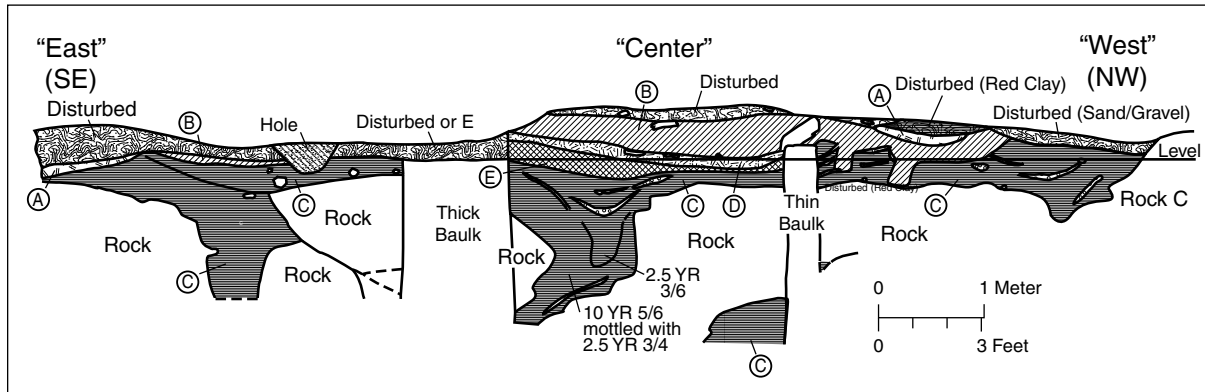


Figure 6. Illustration of Profile 1 (fig. 5), the south (north-facing) wall of 2003 Trench 1. Limestone boulders and smaller pieces of limestone and chert, and individual large crystals of calcite, are shown in a plain white pattern in the profile, as are baulks; other (unconsolidated) materials are designated by pattern and letter label. Beneath a cover of material greatly disturbed by modern plant growth and human activity, five sediment units (zones) were recognized in Trench 1. Zone A (identified on the profile by a circled letter A) was a very dark gray (see text for Munsell color codes) clay containing numerous pieces of limestone and chert, along with rounded quartzite pebbles, as well as abundant plant material and bones. Zone B (circled letter B) was mostly a dark yellowish brown clay with saprolitic sand lenses, a few intermixed pieces of Zone A material, and once again pieces of limestone and chert, and quartzite pebbles. Zone C (circled letter C) was a dark red clay, marked in places by strings of yellowish brown, saprolitic, calcareous sand and isolated large calcite crystals. Zone C material surrounded large limestone breakdown boulders, in some places clearly having sagged into gaps between boulders. Zones A, B, and C could be recognized in other sediment profiles, but two other facies (or subfacies of Zone B) were unique to Trench 1. Zone D (circled letter D) was strong brown laminated clay that was relatively free of rubble compared with overlying Zone B and underlying Zone E. Zone E (circled letter E) was reddish brown clay with chert and limestone fragments, and quartzite pebbles, particularly abundant near its base. Laminations were distinct at the top of the zone, but not visible at its base.

and C together represent different aspects of Sunderman and others Diamicton-1. Zones D and E are best regarded as variants or subzones of Zone B. Such letter subdivisions of Zone B were not subsequently used in other excavation pits or trenches.

Southwest Quadrant: After Trench 1 was dug, sediment was removed from a region (SW Quadrant) immediately southwest of the Trench 1 Center, after removing disturbed material to reach Zone A. Based on our observations in Trench 1, it was expected that Zone A would be very thin in the SW Quadrant. Instead Zone A turned out to be more than 2 m (6.5 ft) thick in part of the quadrant, forming a very large feature (2003 SW Quadrant Funnel) positioned among large limestone breakdown boulders (figs. 2, 7C, D, and 8). Sediments in the funnel showed significant sagging into it; large rock fragments were positioned nearly vertically in the sediment. These observations suggest that the funnel may have been a route for materials moving downward through the sinkhole.

A baulk roughly aligned with the thin baulk of Trench 1 was left temporarily across the funnel to allow drawing a profile of sediment within the

funnel. This baulk separated the SW Quadrant into two portions, the northwestern portion of which was designated "SW Quadrant 2." Subtle differences in Zone A materials in different parts of the funnel allowed recognition of three subzones. Zone A1 was mostly dark gray to grayish brown (10 YR 4/1 to 5/2) clay with abundant limestone and chert pieces, siderite nodules, and quartzite pebbles. Zone A2 was dark yellowish brown (10 YR 3/4) clay, but had patches of red clay mixed in; Zone A2 had less rubbly material than Zone A1. (This kind of numerical subdivision of sediment zones was used in all our profile descriptions; sediments assigned zone letters with no numerical suffix or with 1 as the suffix contained a higher proportion of coarse material than sediments with the number 2 or higher as a suffix.) Zone A3 was very dark grayish brown (10 YR 3/2) to black (10 YR 2/1) clay with few rock fragments. Zone A sediments finally bottomed out in typical Zone B yellow-brown sediment 310 cm below the surface.

About 700 3.5-gallon buckets (about 9 m³) of Zone A sediments were removed from the SW Quadrant for on-site screen-washing. Some significant vertebrate fossils were found in this material. Among these



Figure 7. Photographs showing features of 2003 Trench 1 and the 2003 Southwest Quadrant. A) Western portion of Trench 1, looking to the west. Note thin baulk of sediment cutting transversely across the trench, and large limestone boulders (presumed to be breakdown) in the wall and floor of the trench. B) Sagging of sediment around the margin of a limestone boulder in Trench 1. C) Funnel structure cutting across the SW Quadrant and SW Quadrant 2 (fig. 2), looking to the northwest. Note the presence of large, flat rocks dipping steeply into the funnel. The thick section of Zone A sediment in this feature yielded several important vertebrate fossils. Nineteen sediment samples were taken at 10-cm (4-inch) intervals vertically along this profile for geochemical and pollen analyses (Shunk and others, 2009). D) Peripheral view of the funnel, looking toward the southeast, after removal of nearly all Zone A sediment.

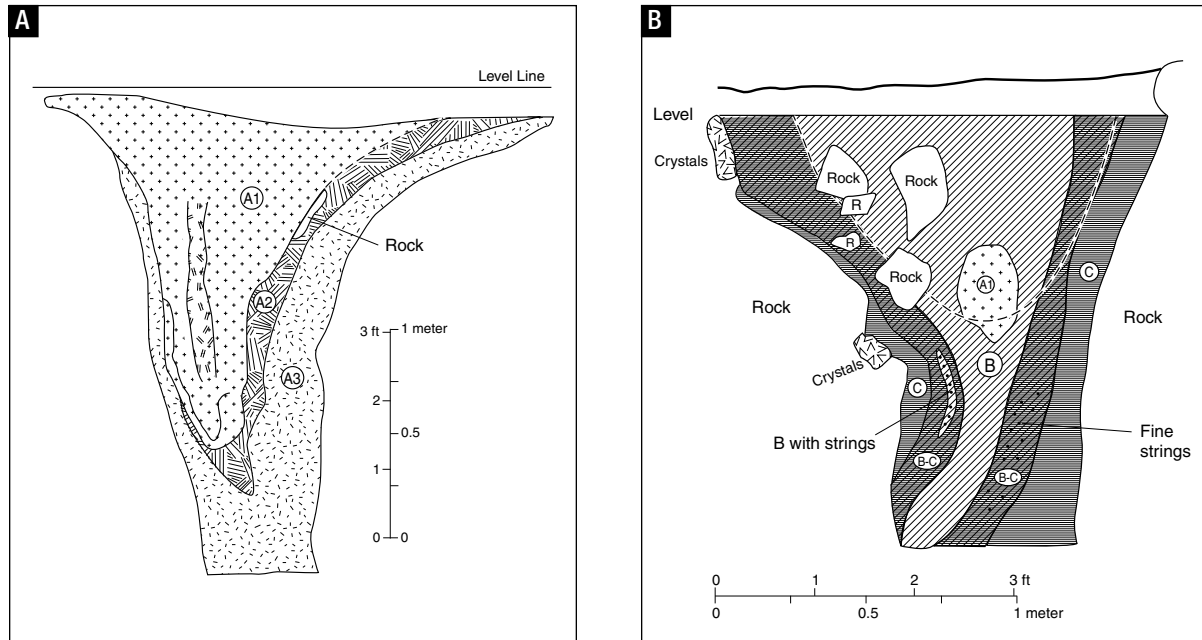


Figure 8. Illustrations of the Southwest Quadrant sediment funnel structure. A) Profile 2 (fig. 5), looking toward the northwest, as seen in 2003 (fig. 7C). All of the sediment was Zone A material, which was variable enough that it was subdivided into three zones (Zones A1–A3 [labeled on profile with circles surrounding A1, A2, and A3]; see text). B) Profile 4 (fig. 5), looking toward the southeast (fig. 7D). Apart from a patch of Zone A1 material, sediment was entirely Zone B and Zone C material (labeled as circled B and circled C), or a transition between them (labeled by B-C inside an ellipse). Several large pieces of limestone (labeled as Rock or R) were embedded in Zone B or transitional B-C sediment. Nearly vertically oriented strings of fine calcareous saprolite occurred in the B-C transitional material. Patches of large calcite crystals were present on the surfaces of some of the limestone boulders bounding the funnel. The area above the curved, dashed line indicates a concave depression in the top of the deposit at the time the profile was drawn (fig. 7D).

were the metapodium of a large carnivore (*Borophagus*) preserved in partial articulation (found in sediment from the baulk across the funnel), some fairly complete (but broken by sediment compaction) chelonian shells, and a large camel cervical vertebra.

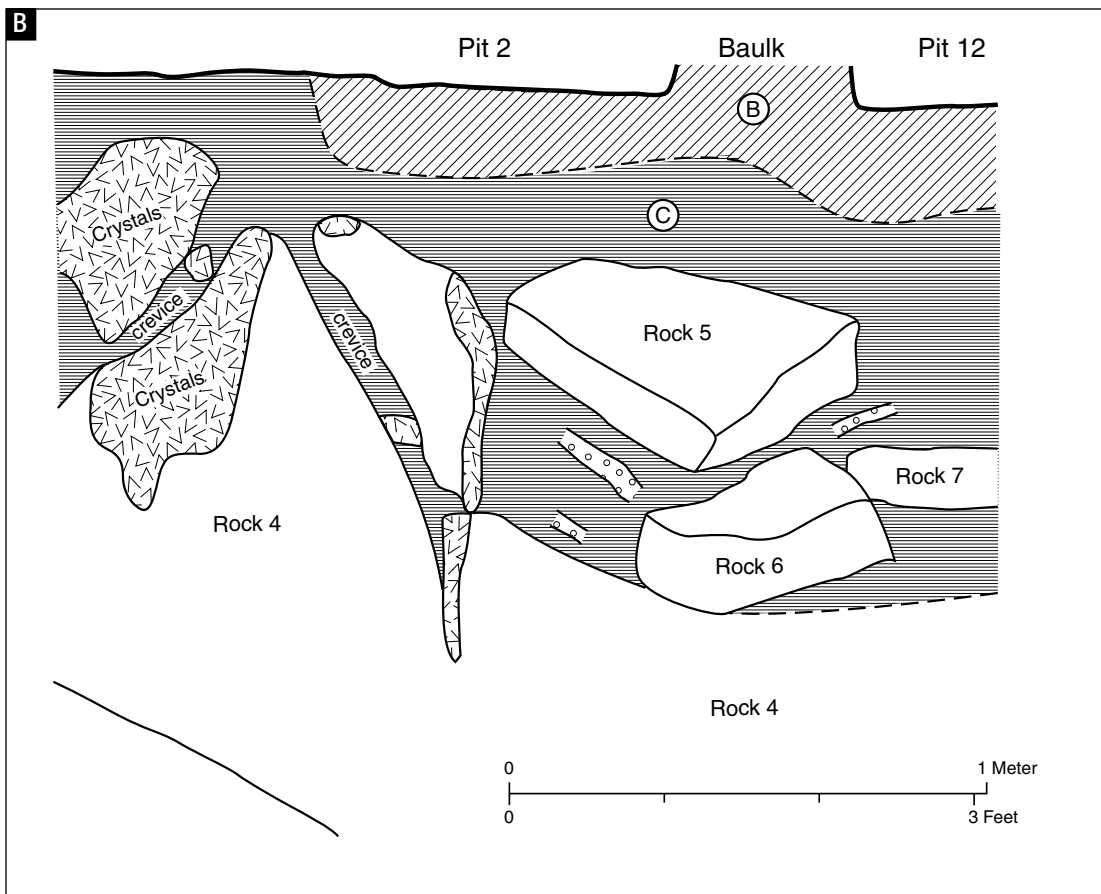
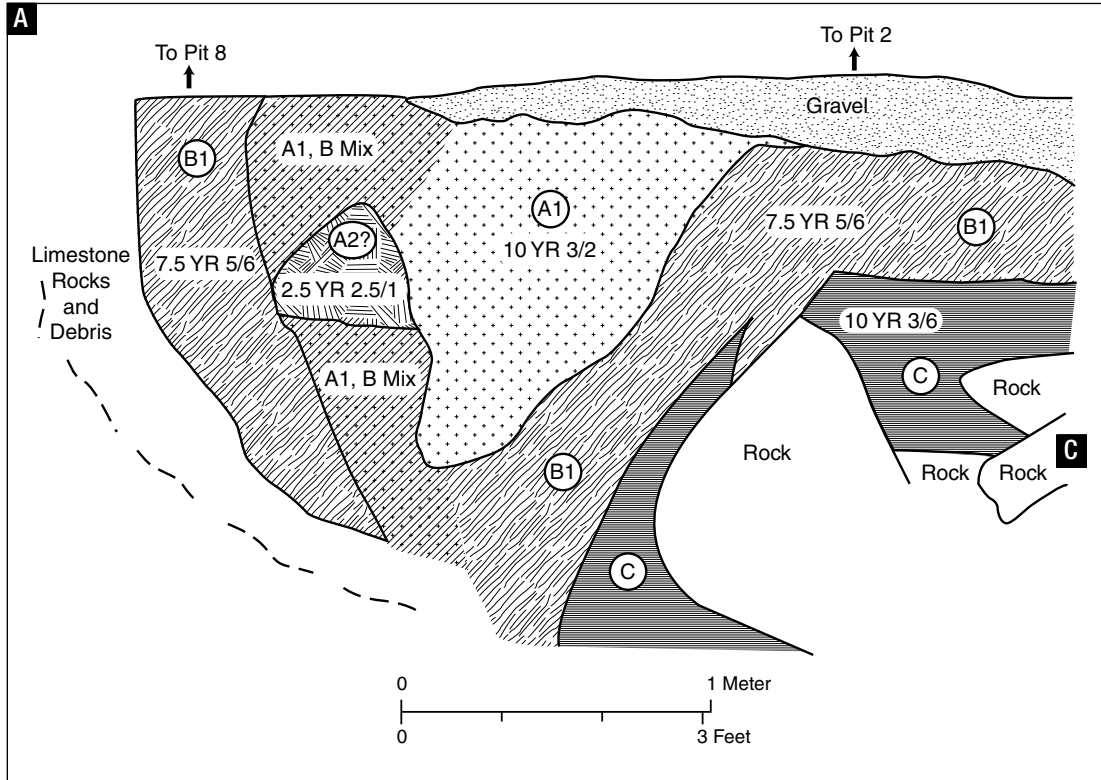
Southeast Quadrant: A third area of sediment removal was established to the southeast of the SW Quadrant, adjacent to the East Half of Trench 1 (fig. 2). The remaining in situ fossiliferous sediments here were fairly thin, generally made up of a mixture of Zone A and Zone C material above more typical Zone C red clay.

2004 field season

A large backhoe was used to dig trenches around the northwest and southeast edges of the sinkhole area to determine the limits of fossiliferous sediment (mainly Zone A materials). During this operation several patches of Zone A sediment were seen in spoil removed from the southeastern

trench; this material was collected and designated “SE Trench Zone A Disturbed.” The SE Trench encompassed such a large portion of the site that it was deemed appropriate to subdivide it into Trenches 2 through 4 (fig. 3). Trench 3 (not shown on fig. 3) exposed limestone with no overlying sediment, and so received no further attention. Some of the fossiliferous spoil from the SE Trench was determined to have come from its Trench 2 portion, and so this material was designated “Trench 2 Zone A Disturbed.” The trench cut along the northwest side of the site was designated “Trench 5.” Digging these trenches left behind a centrally located, topographically higher area that we named the “Excavation Plateau” (figs. 3, 9A, and 10A, B).

A layer of Zone A material could be seen in the walls of the various segments of the SE Trench, so this sediment was removed from above, in a series of pits in the Excavation Plateau, rather than laterally from the trench. Two reference lines were laid out across this area. One of these, which extended southwestward from a conspicuous pointed projection on Rock B



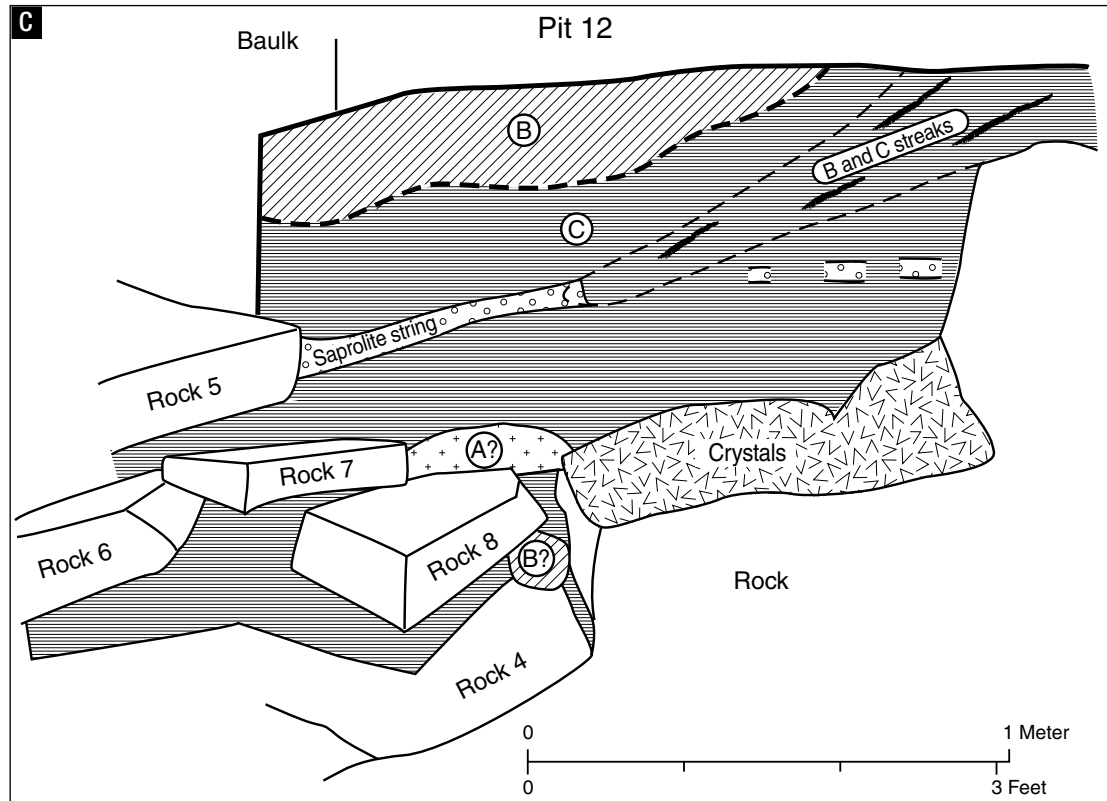


Figure 9. Wall profiles of 2004 Trench 4 (fig. 3). A) Profile 6 (fig. 5), “north” (actually northeast; southwest-facing) profile, adjacent to Pits 2 and 8. Digging Trench 4 cut through a funnel-shaped sag of sediment similar to the 2003 Southwest Quadrant funnel (figs. 7C, D, and 8), leaving behind a tongue of sediment projecting from Pit 2 into Trench 4. Zones A, B, and C (labeled on the profile) were present in their usual order from top to bottom (fig. 10B). B) Western portion of Profile 7 (fig. 5), “north” (southwest-facing) wall of Trench 4, immediately southeast of and stratigraphically beneath the funnel projecting from Pit 2 (figs. 9A and 10B). C) Eastern continuation of Profile 7, north (south-facing) wall of Trench 4. Note large limestone boulders with extensive fields of large calcite crystals covering some rock surfaces (identified on the profile as patches marked with V's), and strings of saprolitic limestone (identified on the profile as patches containing small circles) embedded in red Zone C clay in both portions of Profile 7.

(fig. 3), marked by the boundary between the 2003 SW and SE Quadrants. This first reference line was crossed at a right angle by the second reference line, which itself marked the boundary between the two quadrants and Trench 1. The excavation pits (fig. 3) were established with respect to the two reference lines; the boundary between Pits 8 and 11 corresponds to the boundary between the 2003 SW and SE Quadrants. Some of the defined pits turned out to have no fossiliferous sediment, and so are not delimited in our excavation diagrams.

Some of the pits were associated with, but stratigraphically beneath, excavation areas established in 2003. Most of these were associated with the 2003 SE Quadrant; Pits 4 and 5 were in the SE Quadrant adjacent to the East Half of 2003 Trench 1. Pits 6 and 9 were associated with the Center of 2003 Trench 1. Pit 10 was located at the base of the 2003 SW Quad-

rant Funnel, immediately above where this feature terminated against a slab of breakdown limestone. Portions of Pits 1, 3, and 7 were also beneath the 2003 SE Quadrant, but parts of these pits extended to the southwest beyond the edge of this quadrant. Pits 2, 8, 11, and 12 were completely beyond the edge of the 2003 SE Quadrant.

The surface of the Excavation Plateau defined by the 2004 trenches and subdivided into excavation pits was very irregular when digging began, partly reflecting the disturbance created by our trenching, and partly owing to the disposition of sedimentary materials prior to trenching. Disturbed material from the pits was removed and screened, beginning with Pit 1. Digging in Pit 1 removed sediment to a depth about 80 cm (31 inches) below our local datum, the south stake used to define this pit. At this level, material in the pit consisted

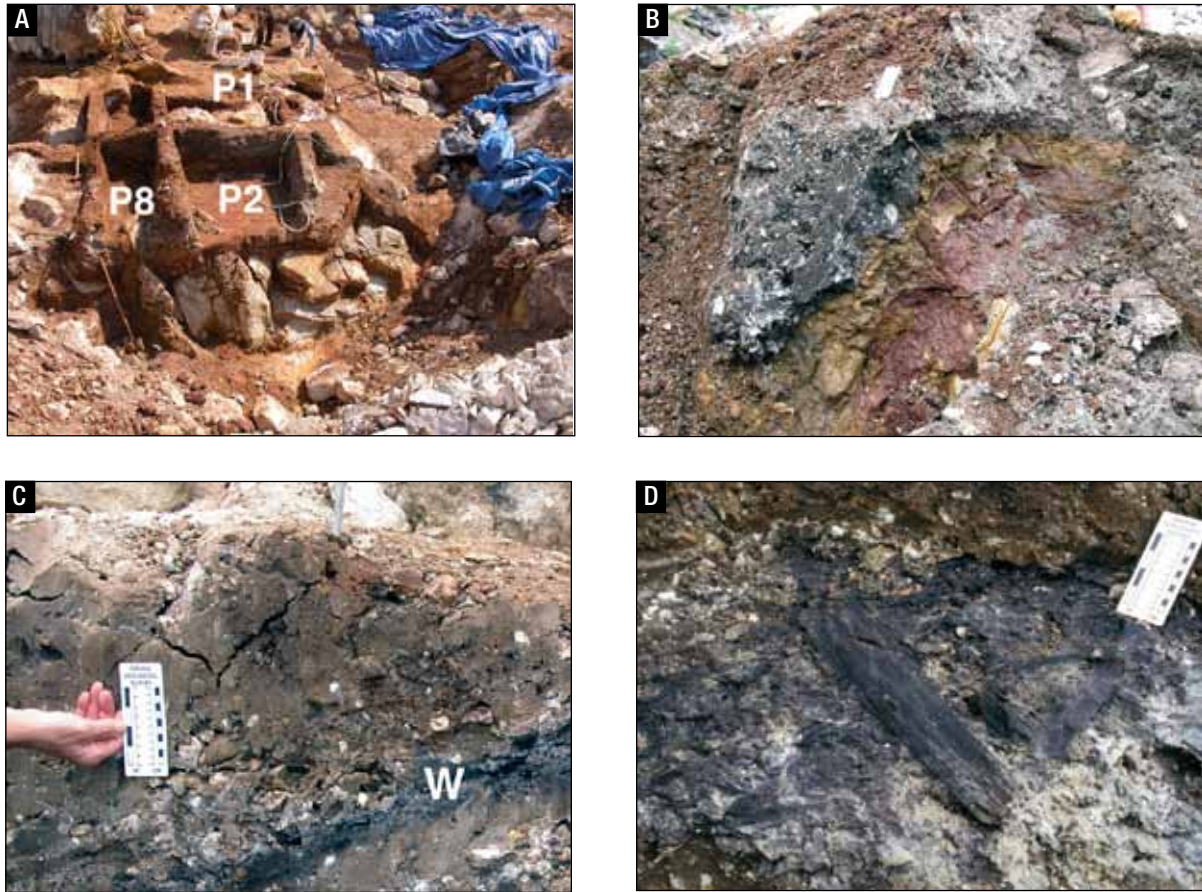


Figure 10. Photographs showing features of the 2004 Excavation Plateau and Trenches 2 and 4 (fig. 3). A) View of the Excavation Plateau from the southwest, showing excavation pits (some of which are labeled). The pits were floored with Zone C red clay. Trench 4 ran around the margin of the Excavation Plateau on the side toward the viewer; note large limestone breakdown boulders in a jumbled mass beneath the plateau (fig. 9C). B) Tongue of sediment lapping from Pit 2 into the southwest-facing wall of Trench 4; this tongue had been removed by the time the photograph in A of this figure was taken. Note the characteristic vertical succession of black Zone A sediment above brown Zone B sediment, and Zone B sediment above red Zone C clay (fig. 9A). C) “North” (northeast; southwest-facing) wall of Pit 13; note the diagonally running Zone A1 plant layer (W = wood). D) View from above of part of the Pit 13 Zone A1 plant layer; note large piece of wood in center of view, surrounded by dark mat of smaller plant fragments.

of large blocks of limestone (probable breakdown boulders) surrounded by a mixture of Zone B and C sediment. Similar materials occurred in most of the other pits on the Excavation Plateau.

Pit 2, however, was different. A significant tongue of sediment projected off Pit 2 into the north (south-facing) wall of Trench 4 as a cone-shaped deposit similar to but smaller than the 2003 SW Quadrant Funnel (figs. 9A and 10B). Zones A (subdivided into Zones A1 and A2), B, and C could readily be distinguished in this tongue, in that order from top to bottom, steeply dipping toward the presumed center of the cone, which had been destroyed in the creation of Trench 4. Sediment in Zones A through

C could be peeled off in layers from the underlying limestone breakdown boulders. Zone A1 was very dark grayish brown (10 YR 3/2), and Zone A2 reddish black (2.5 YR 2.5/1). Zone B1 was a strong brown (7.5 YR 5/6) color. Zone C did not always show its usual bright red color, attributable to its mixing with decomposed limestone, as in the spot where the Munsell color reading was taken, which was a dark yellowish brown (10 YR 3/6). To reduce the threat of collapse of this tongue of material into Trench 4, it was removed simultaneously from above (Pit 2) and from the side (Trench 4). Zone A sediment removed from this funnel was designated Pit 2 A1 Funnel. Even so, some sediment from the periphery of Pits 2 and 8 did fall into Trench 4.

In some cases it was possible to assign collapsed material to a specific zone from Pit 2 or 8, but most of the fallen material was too mixed for that. Such collapsed sediment was variously labeled as "Pit 2" or "Pit 8 A1, B, C," "Pit 2" or "8 A1, B, C, T4 wall collapse," or "funnel wall collapse."

In the main part of Pit 2, the material present was characterized at four vertical levels beneath the local datum (fig. 11). Although sediment like that seen in Zones A, B, and C could be recognized, microstratigraphy in this pit was rather jumbled and, frequently, material of the three zones was chaotically intermixed. Level 1 was about 25 to 30 cm (10–11 inches) below the local datum. Material here consisted of limestone in large blocks and smaller pieces surrounded by a mixture of very dark grayish brown (10 YR 3/2) Zone A1 and C material, but also a small patch of yellowish red (5 YR 5/8) Zone B, and well-rounded, lithologically heterogeneous gravels. Level 2 was about 20 cm (8 inches) below Level 1. Material here comprised dark brown (10 YR 3/3) Zone A1, very dark brown (10 YR 2/2) Zone A2, light red (2.5 YR 6/6) Zone B, and dusky red (10 R 3/4) Zone C sediment (in some places intermixed), again also mixed with significant amounts of gravel. Level 3 was another 20 cm (8 inches) below Level 2. Although some Zone A1 material was observed, in one place mixed with Zone B sediment, the bulk of sediment exposed at this level was a mixture of Zone B and C sediment, with gravel still also present. Level 4 (not illustrated in Figure 11) was 80 cm (31 inches) below the local datum; material here was mainly Zone C sediment, albeit with patches of Zone B material. A profile of the NE (SW-facing) wall of Pit 2 shows Zone A materials (at the top of the profile mixed with gravel) roughly overlying Zone B and C sediments (fig. 11D). In the SE (NW-facing) wall (not drawn), Zone A1 sediment, mixed with gravel, overlay a Zone B/C mixture. A distinct line of gravel existed, separating A1 and B/C sediment, which angled downward toward the southwest and Trench 4.

Material deeper than at Level 4 in Pit 2 could be seen in the adjacent Trench 4 north (south-facing) wall profile (figs. 9B, C, and 10A). Large limestone boulders—probable breakdown—occurred beneath the level of the Excavation Plateau all along the north wall of Trench 4. Layers of Zone A, B, and C could be sequentially peeled away in that order from the limestone boulders (Zone C being immediately against the rocks). Some of the limestone boulders had conspicuous patches of large calcite crystals.

In general, sediment was removed for screening from pits in the Excavation Plateau down to about 80 cm below the local datum. This was the lower limit of Zone B material. Beneath this, Zone C red clay made up nearly all the sediment encountered; extensive screening of Zone C here (and elsewhere in the sinkhole) produced no fossils. In Pit 2, Zones A through C were so mixed vertically that sediment was mostly removed and labeled in terms of the above-described 20-cm (8-inch) levels, rather than the sediment zones. Material above Zone C in Pit 12 was a mixture of Zone A sediment and gravel, which was designated "Pit 12 A1 Level 1." Pits 6 and 9 had little Zone A material, so this was pooled as "Pits 6 + 9 A1." Sediment in Pits 1, 3, 7, and 10 was entirely a mixture of Zones B and C.

Another funnel-shaped structure or slump could be seen in the west (east-facing) wall of the Trench 2 portion of the SE Trench (fig. 12A). As in the 2003 SW Quadrant funnel and the 2004 Pit 2 funnel, the order of materials passed from Zone A sediments at the top of the structure, through Zone B to Zone C in the lowest material. Zone A2 was a black (10 YR 2/1) dense clay containing traces of white saprolite. Zone A3 was a very dark gray (10 YR 3/1) to dark yellowish brown (10 YR 3/6) clay with horizontally oriented saprolite strings. Zone B1 was a yellowish brown (10 YR 5/6) to dark yellowish brown (10 YR 4/6) clay having a considerable amount of heterogeneous gravel mixed therein. Zone B2 was similar to Zone B1 except for lacking gravel. Zone C was dark red (2.5 YR 3/6) clay having a high content of saprolitic debris.

The most remarkable feature observed during 2004 field work was uncovered in the east (west-facing) wall of Trench 2, and more extensively in Pits 15 and especially 13 (fig. 5, profile 10), two extensions of Trench 2 (figs. 10C, D, and 12B). Zone A1 was recognized here, but was split into upper and lower portions by a layer of concentrated plant material. Above the wood layer, Zone A1 was a dark gray (10 YR 4/1) to dark grayish brown (10 YR 4/2) clay-silt-sand mixture, in part laminated, containing angular pieces of limestone and rounded quartzite pebbles, as well as the fragments of organic material commonly found in Zone A. The wood zone was a black (10 YR 2/1), peaty mat nearly devoid of clay or silt but having abundant pieces of wood (some as much as 60 cm long), twigs, leaf fragments, and seeds (fig. 10D). Although plant debris was abundantly dispersed throughout Zone A sediments in the sinkhole, this was the densest accumulation of

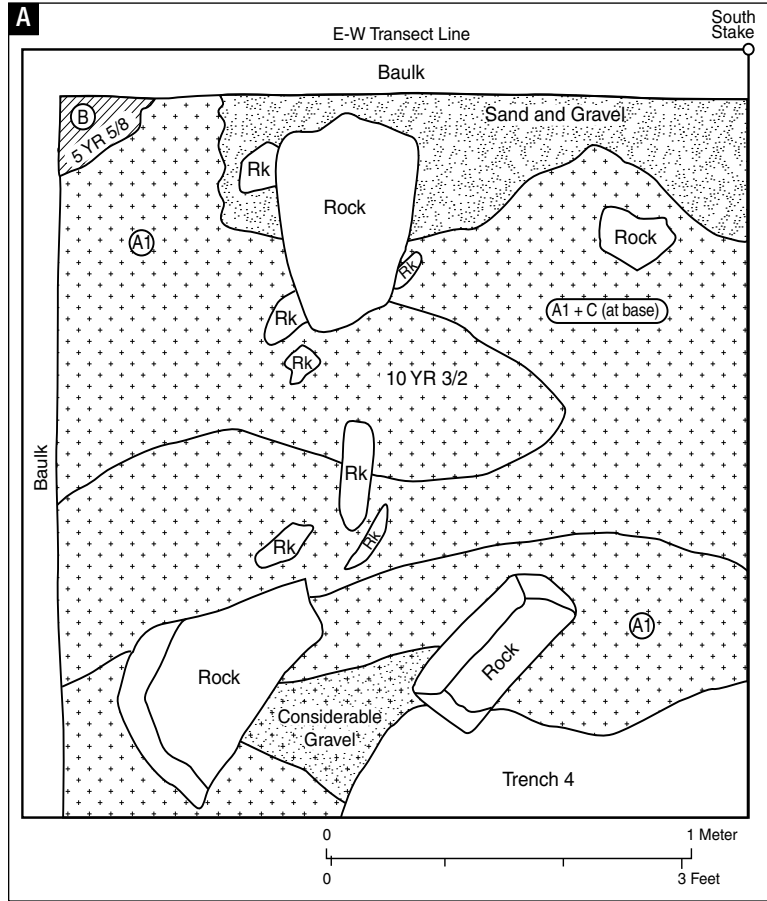
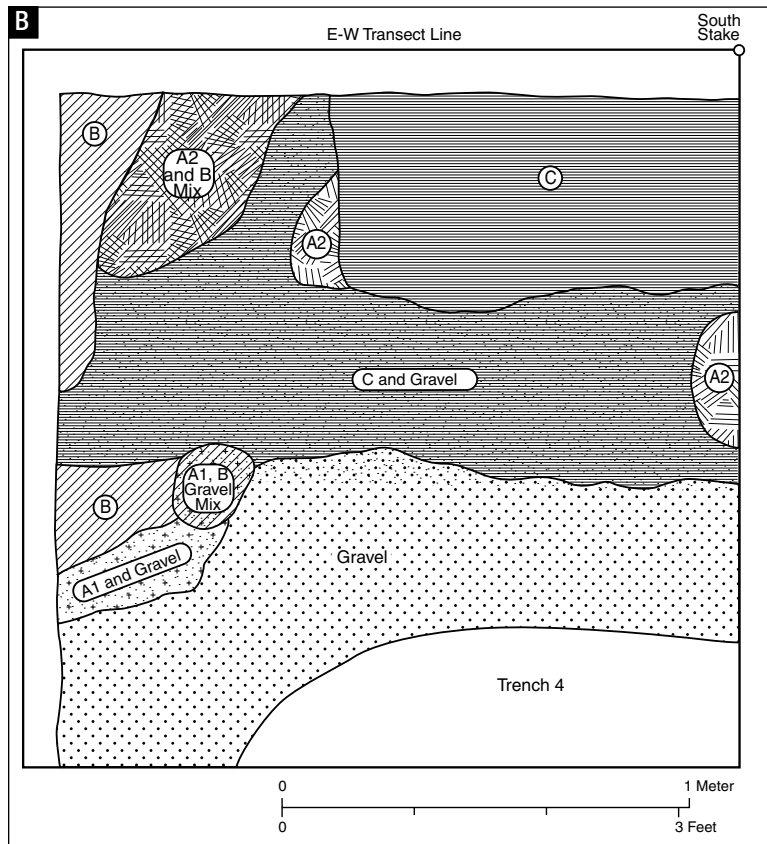


Figure 11. Illustrations showing features of Pit 2 of the 2004 Excavation Plateau (fig. 3). Individual sediment zones are labeled on the plans and profile. A–C) Vertical dissection showing plan views of three sequential horizontal levels of the pit. The “E-W Transect Line” actually ran in a northwest-southeast direction (fig. 3). The northeast (southwest-facing) wall of the pit is at the top of each of the plan maps. A) Level 1, about 25 to 30 cm (10–11 inches) below the local datum. Sediment zones were difficult to distinguish. The dominant material at this level was Zone A1, a very dark grayish brown (see text for Munsell color codes) sediment mixed with large amounts of heterogeneous gravel. In places Zone A1 material was also mixed with sediment of Zone C aspect. A small patch of yellowish red Zone B sediment was also recognized. “Rk” = rock fragment. B) Level 2, about 20 cm below Level 1. Significant amounts of heterogeneous gravel could be seen in much of the pit at this level, either by itself or mixed with other sediment. Zone A1 sediment here was dark brown material with considerable amounts of limestone debris and gravel. In addition, Zone A2 sediment, a very dark brown dense material lacking stones, could be recognized. Zone B sediment was light red with a high clay content (as indicated by feel), and Zone C was dusky red clay. Sediment layers at this level showed much intermixing.



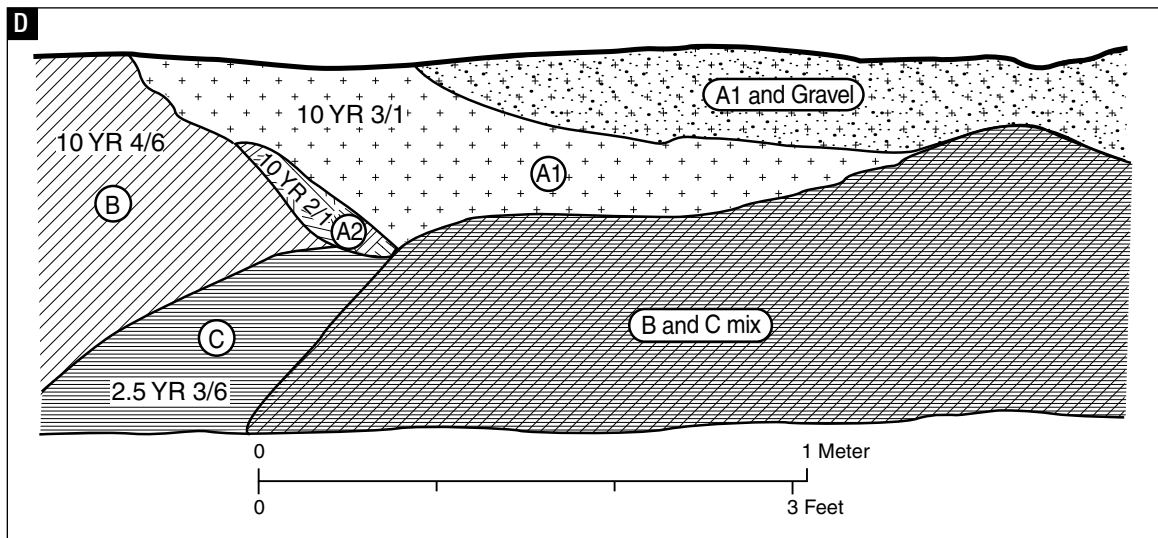
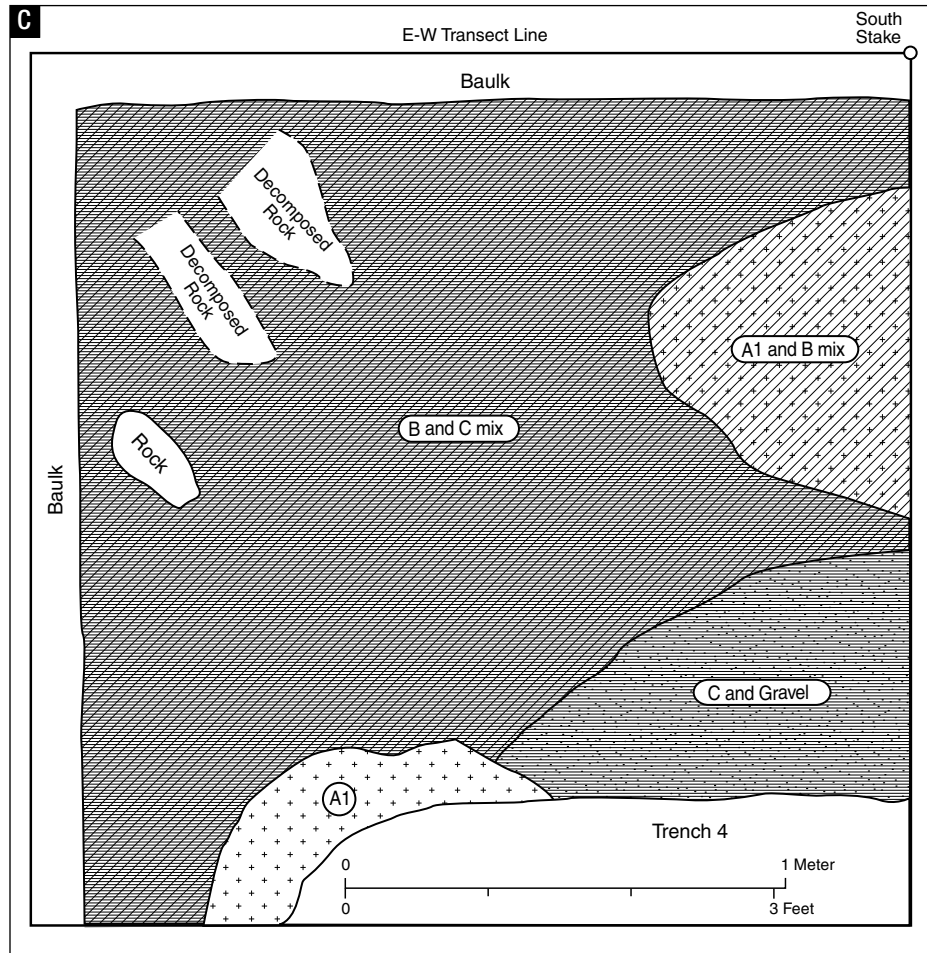


Figure 11 (cont.). C) Level 3, another 20 cm below Level 2. The dominant material at this level was a mixture of Zone B and C aspect. D) Profile 5 (fig. 5), northeast (southwest-facing) wall, showing the vertical distribution of sediments. In general, the typical downward sequence of Zone A/Zone B/Zone C could be seen, but not in a simple, horizontal fashion. Zone A1 was very dark gray sediment containing many pieces of limestone, and mixed at the top of the section with the heterogeneous gravel. Zone A2 consisted of black sediment devoid of rocks. Zone B was a clay-rich (as indicated by feel), dark yellowish brown sediment, and Zone C was dark red clay.

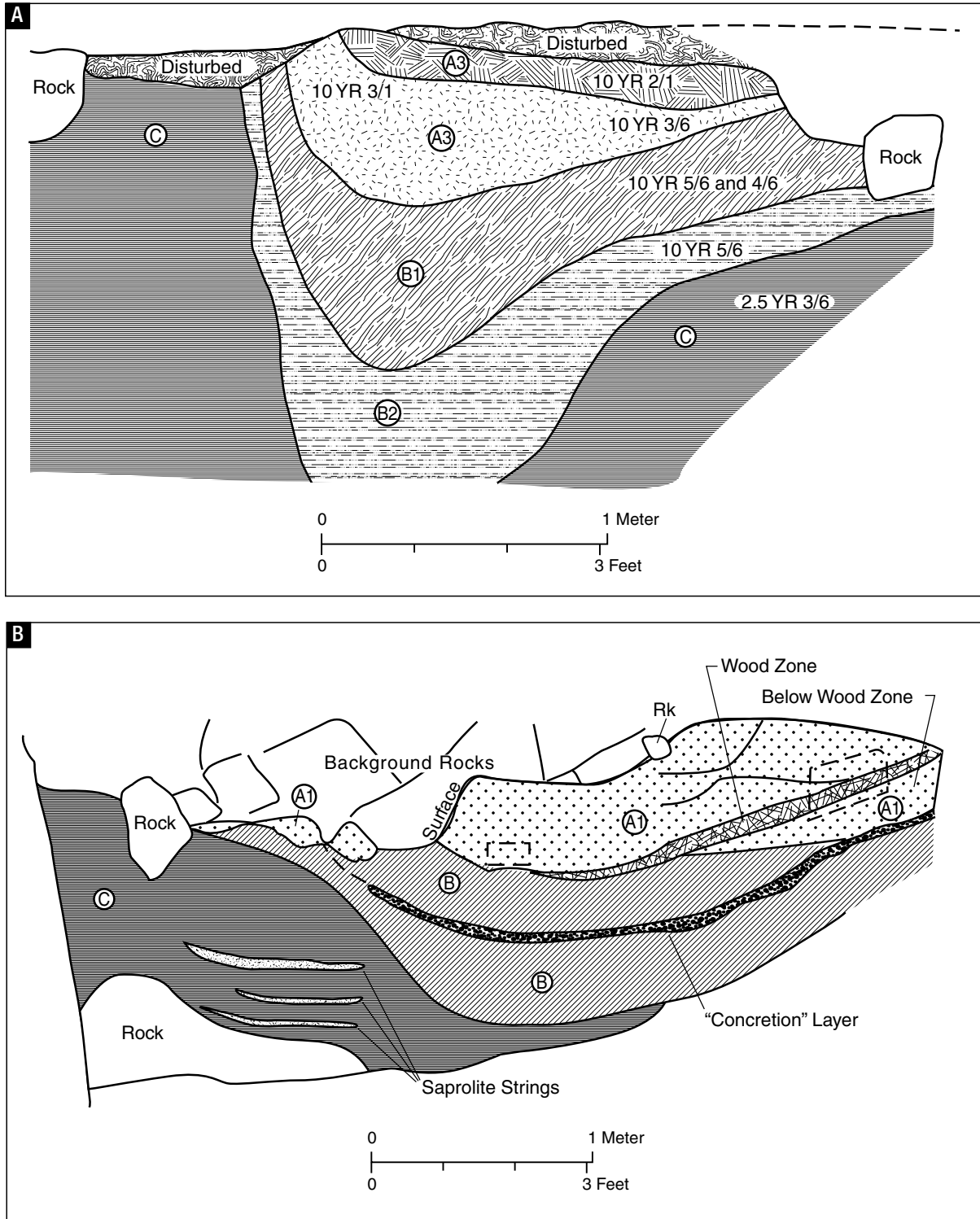


Figure 12. Illustrations showing features of the 2004 Southeast Trench (fig. 3). A) Profile 9, west (east-facing) wall profile of 2004 Trench 2 (fig. 5). Although Zones A, B (with A and B each divided into two subunits), and C were all present in their usual stratigraphic order (labeled by letter on the profile), they showed downward sagging (the degree of which increased with depth) like that seen in the 2003 Southwest Quadrant funnel (figs. 7C and 8). Significant amounts of the heterogeneous gravel were mixed in the B1 portion of Zone B sediments.

plant fossils observed. Below the wood layer, Zone A1 was a very dark gray (10 YR 3/1) to very dark grayish brown (10 YR 3/2) clay-silt mixture, again with numerous pieces of limestone.

Zone B was divided into two layers by a distinctive "concretion" layer. Zone B was a yellowish brown (10 YR 5/6) to dark yellowish brown (10 YR 4/6) sandy silt having a lower clay content than Zone A1. The portion of Zone B above the concretion layer contained angular pieces of cherty limestone and lenses of quartzite pebbles, many of them concentrated at the contact with the concretion layer. The concretion layer was a ca. 5-cm-thick (2-inch-thick), dark brown (7.5 YR 3/3) consolidated hardpan, probably of iron-rich material. Zone B below the concretion layer seemed to have a somewhat higher content of limestone fragments and quartzite pebbles than did the portion of this zone above the concretion layer. Zone C was dark red (2.5 YR 3/6) clay containing strings of saprolite; it terminated downward against limestone boulders.

Pit 14 (fig. 3) was another extension of Trench 2. It was dug working from Trench 2, and Zone A initially presented as a small cone of material about 75 cm thick. However, within a meter of Trench 2 the Zone A material in Pit 14 quickly thinned, as though about to play out, but then began to thicken to the northwest, in an area where the sediment had a markedly disturbed appearance and was very loose and easy to excavate. This portion of Pit 14 was renamed Pit 16, and fossiliferous sediment from it had not been completely removed when 2004 field work ended.

Trench 5 cut across the northwestern edge of what remained of the 2003 SW Quadrant Funnel. A profile of this feature as seen from Trench 5 was drawn (figs. 5, 7D, and 8B). This portion of the funnel preserved a small amount of Zone A material, surrounded on both sides by large amounts of Zone B and C sediment. Strings of saprolite were

present in Zone C. As in Trench 4 and other parts of the sinkhole, Zone C red clays were draped around the limestone boulders that defined the edges of the funnel. Again as in Trench 4, sheets of calcite crystals were distributed across portions of the limestone rocks. Sediment collected in the process of creating the 2004 profiles of the 2003 funnel were labeled "2003 funnel west wall scrapings" and "2003 funnel south wall scrapings."

On the basis of our 2004 excavations, it was possible to make a rough estimate of the size of the PCS pond at the level of the in situ sediments, based on the horizontal limits of Zone A sediment: at least 19 m (NW-SE) by 9.5 m (31 ft) (NE-SW). Of course, this does not necessarily mean that Zone A sediment formed simultaneously in all the places where it occurs; therefore, at any one time the pond could have been smaller.

2005 field season

Two main tasks were accomplished in the final year of excavation (figs. 4 and 13). Pit 16 was reexposed and extended, and Zone A sediment was removed from this pit until it played out. As best we could tell, no other significant areas of fossiliferous sediment were in the sinkhole.

A new dig area, Pit 17, was established on the northern periphery of the 2004 Excavation Plateau (fig. 4). As deeply as we could dig (fig. 13D), all that could be seen were limestone boulders chaotically dispersed within Zone C red clay.

We cleaned off all remaining Zone B and C sediment from above the limestone boulders in the Excavation Plateau (fig. 13B). Much of the eastern portion of this dig area was underlain by a single large limestone slab. Smaller limestone blocks lay on top of this large boulder; many of these were encrusted by patches of calcite crystals (fig. 13C).

Figure 12 (cont.). Illustrations showing features of the 2004 Southeast Trench (fig. 3). B) Profile 10 (fig. 5), north (south-facing) wall of 2004 Pit 13, and associated parts of Pit 15 and Trench 2. Sediment zones labeled by letter on profile. Rk = individual large rock. Zone A1 was recognized here, but was split into upper and lower portions by a layer of concentrated plant material (Wood Zone; figs. 10C, D). Most of this plant-rich layer was removed in pieces for processing in the laboratory; one sample (outlined by dashed lines) was collected as a single intact block. The rectangle denoted by dashed lines to the left of the wood zone indicates where a fairly complete pelvis of a medium-sized ungulate was collected. Zones B and C occurred in their usual order beneath Zone A1. Zone B was split into two portions by a 5-cm-thick hardpan of dark brown consolidated, concretionary material.

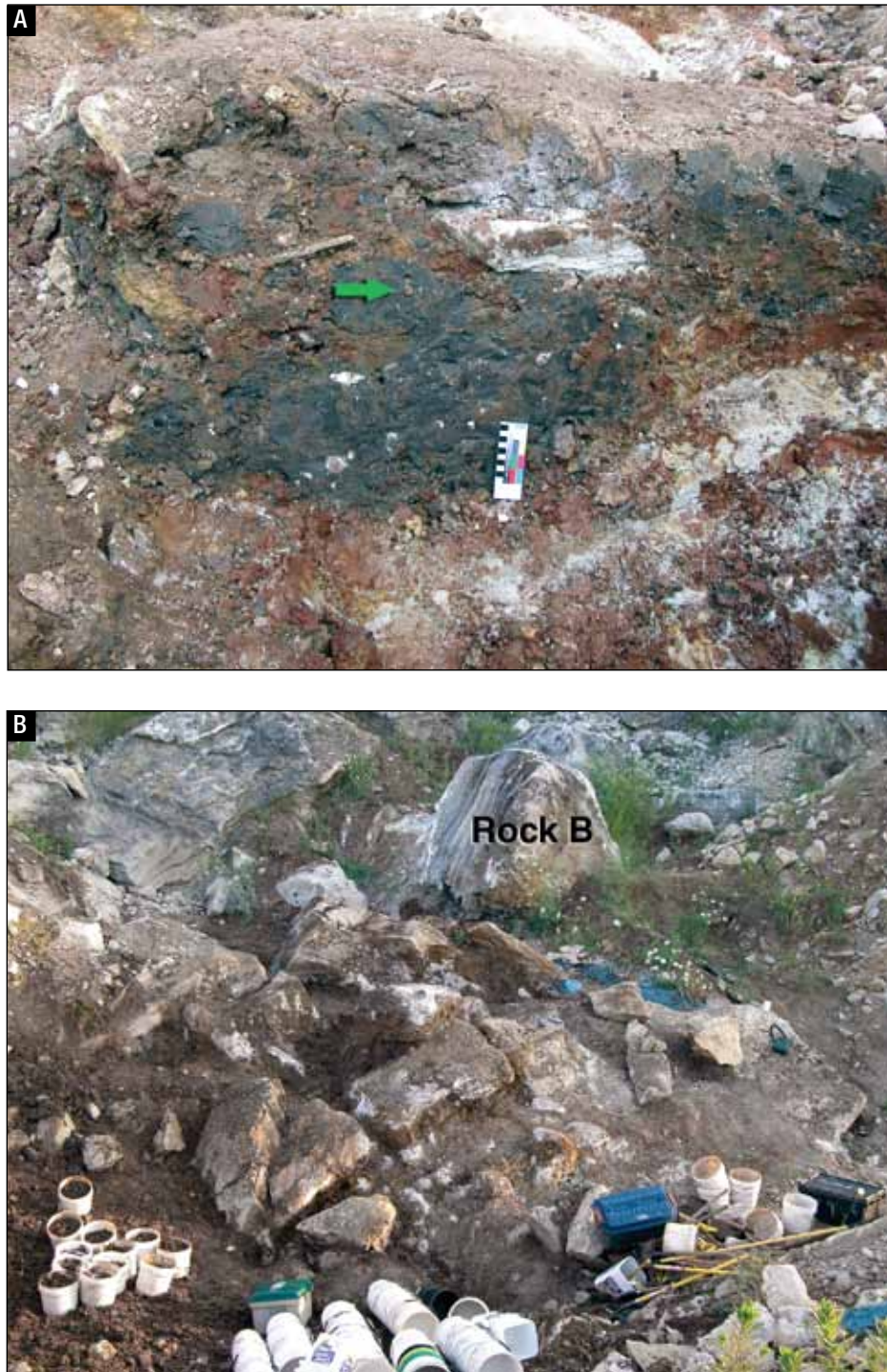


Figure 13. Photographs showing features of the 2005 excavations (fig. 4). A) Northwest (southeast-facing) wall of Pit 16. Note general pattern of dark Zone A sediment overlying red Zone C sediment, but with some intertonguing of the two sediment types (for example, in the area just beneath a flat rock seen in side view just left of center, where a tongue of Zone A material [arrow] pushes into Zone C material) to give a mottled appearance. Samples were collected from this exposure for pollen analysis. B) Exposure of large breakdown boulders that were beneath the 2004 Excavation Plateau. Landmark Rock B (fig. 2) is immediately beyond (above in the photograph) the boulders uncovered in 2005.



Figure 13 (cont.). Photographs showing features of the 2005 excavations (fig. 4). C) Large calcite crystals coating one of the exposed boulders. Similar crystal coats occurred on many limestone boulders in the sinkhole. D) South (north-facing) wall of Pit 17. This view shows that Zone C red clay and embedded limestone boulders occurred as deeply as we were able to dig.

Correlation across profiles

Vertical positions of the various wall profiles (fig. 14) were determined with respect to the top of Rock B (fig. 2). Elevation of the base of Zone A sediment varied as much as 2 m (6.5 ft) from one part of the sinkhole to another, often over short horizontal distances, associated with slumping or sagging of sediment between limestone boulders. The base of Zone B shows comparable variation in elevation.

GROUND PENETRATING RADAR SURVEYS

Prior to initiating site excavation in 2003, we made 12 GPR traverses on the exposed bedrock surface north and east of the sinkhole and 16 traverses within the sinkhole itself (fig. 15). Sites were georeferenced using a Trimble global positioning system (GPS) device. Cloth or plastic tapes were used to mark out lines or grids (metal instruments were eliminated or used only minimally because they reflect radar energy and yield spurious data). Ground penetrating radar lines were at irregular intervals. Grids of 10 by 10 meters (32 x 32 ft) have proved to be appropriate for such surveys, but because of the very uneven nature of the sinkhole, lines were run in families rather than in orthogonal grids. One grid pattern was run on the upper bedrock surface. Traverses ranged in length from 8 ft (2.4 m) to more than 300 ft (91 m).

Data were collected with a Sensors and Software Smart Cart using 250 MHz. Stacks of 16 pulses were sent downward for every 3 inches (7.6 cm) of horizontal travel and the times for waves reflected from underground features to return to the antennae were measured in nanoseconds. Travel times were converted to feet by using general velocity guidelines or by estimating wave velocities by matching parabola shapes. Radar strengths were plotted with distance from the traverse start in feet on the x-axis and travel time in feet of depth on the y-axis. The technique is very similar to that for seismic measurements, but uses much shorter wavelengths.

Field data were analyzed using Sensors and Software EKKO Mapper or PRO programs and plotted as cross sections. Signal saturation corrections were applied and root mean square amplitude was averaged to improve raw data. Because significant elevation changes did not occur, corrections for topography were not applied.

Depth of radar penetration was about 20 to 25 ft (6–7.5 m) in bedrock but much lower, generally less than 12 ft (3.6 m) deep, in sediments within the sinkhole (figs. 16 and 17). Clay-rich units limited penetration depths in many parts of the sinkhole, but bedrock units and even isolated rocks were easily seen. GPR data show many buried features in the limestone bedrock surrounding the sinkhole, including the dipping flank beds of the reef. A few cavities in the bedrock were also observed.

Within the sinkhole itself, obvious bedrock pieces, some quite large, were imaged. A few of these show rotation of the beds, implying that they fell into a void or were displaced by sediment movements after they fell. A number of shallow basins and some details of sediment fillings could also be seen. Overall, GPR imaging was consistent with features of sinkhole structure subsequently uncovered during our field excavations. The most interesting result of the GPR work was the discovery of other sediment-filled cave passages, supporting the hope that other sediment-filled (possibly fossiliferous) karst features can be found in the area.

SCREENING AND LABORATORY METHODS

Indiana State Museum screen-washing

Given limited resources of time and money, and our desire not to inconvenience the operators of the Pipe Creek Jr. Quarry any more than necessary, we needed to process large quantities of sediment quickly in the field. Once excavation began, buckets of Zones A and B sediment (and some Zone C sediment, although this turned out to be unproductive of fossils) were removed from the sinkhole each day and soaked in water as long as possible (usually at least overnight). Buckets of sediment were washed with hoses through a set of two stacked screens. The upper screen had a ¼-inch (6.35-mm) mesh, and the lower screen was fine fiberglass hardware cloth (about 1.2-mm mesh). Material concentrated in the upper screen (INSM coarse fraction) was picked on-site for obvious fossils. However, on-site washing did not completely disaggregate mud clumps. Consequently, some of the fossils assigned to the INSM coarse fraction in the field would actually have passed through the ¼-mesh screen had they not been stuck to clumps of clay that had not yet broken apart. This blurs the distinction between INSM coarse- and fine-fraction fossils.

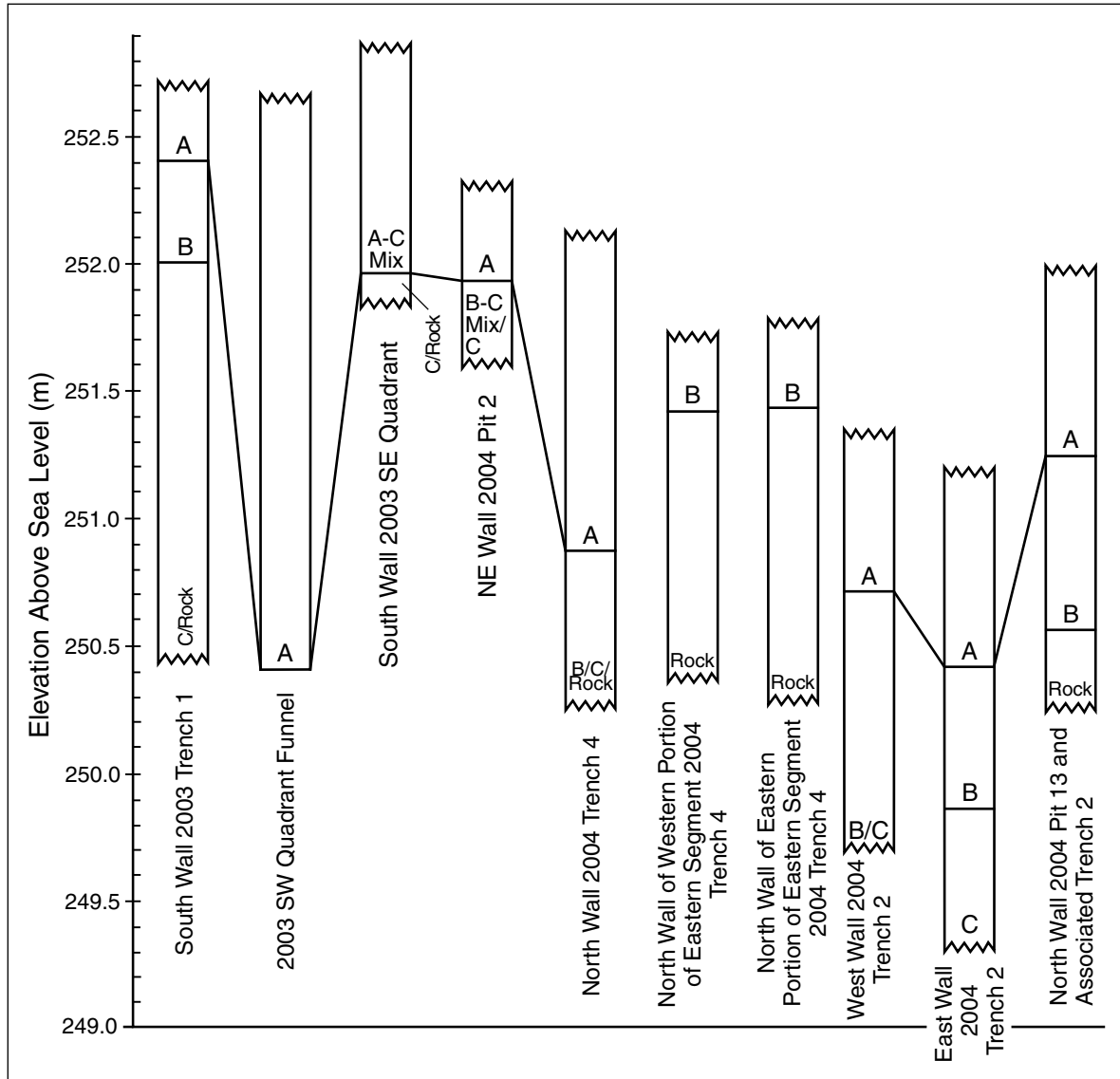


Figure 14. Illustration showing correlations across wall profiles. For each profile, the elevation of an individual profile datum at or near the top of the profile was measured with respect to the site datum, the top of Rock B (fig. 2), whose elevation was 254 m (833 ft) above sea level. The top, bottom, and selected intervals within each profile were then scaled with respect to the elevation of the profile's individual datum. Profiles are generalized here as rectangles (see preceding figures for their true geometry); although the top, bottom, and intervals within a profile are here indicated by horizontal squiggles or lines, these were not necessarily horizontal surfaces in the profile itself. The top of each profile as shown here represents the highest elevation of undisturbed material (not mixed by digging) within the profile, and is a man-made erosional surface indicated by a squiggly line. In most profiles the bottom of the profile is the lowest point to which we were able to dig; this, too, is an artificial level and so is drawn as another squiggly line. The lowest elevation at which Zone A or Zone B sediment (or both) was found in a profile is indicated by a horizontal line. The material encountered at the deepest elevation in a profile is identified by an abbreviation written immediately above the base of the profile; how much deeper than that elevation this or other sedimentary material extended is unknown. A = lowest elevation of Zone A material; A-C mix = lowest elevation of material of mixed Zone A and Zone C aspect; B = lowest elevation of Zone B material; C = Zone C red clay (in no profile did we reach the bottom of Zone C sediment); "Rock" indicates that limestone (probably breakdown boulder) was found at the deepest part of the profile (usually preventing further digging); B/C = both Zone B and Zone C found at the lowest elevation in the profile, but at different parts of the profile; B-C mix/C = both material of mixed Zone B and Zone C aspect and Zone C red clay found at the lowest elevation in the profile, but at different parts of the profile; B/C/Rock or C/Rock indicate that Zone B, Zone C, and limestone boulders, or Zone C and limestone boulders, occurred at the lowest elevation in the profile, but at different parts of the profile. Lines across profiles connect and compare the lowermost elevation of Zone A aspect sediment.

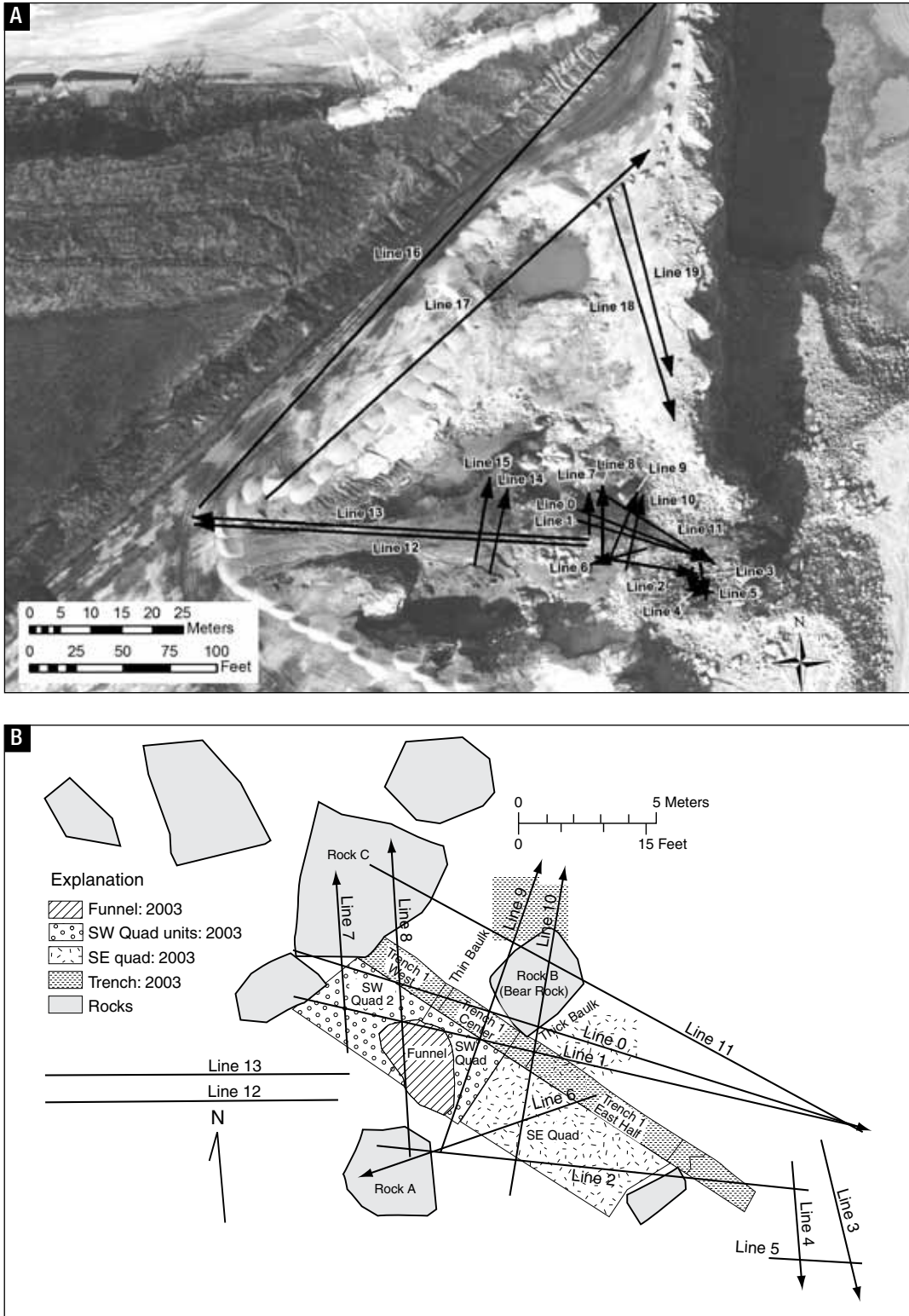


Figure 15. Locations of ground penetrating radar (GPR) traverses (lines) carried out prior to initiation of systematic excavation of the sinkhole sediments in 2003. Arrows point in the direction along which the lines were run. A) Aerial photograph. Lines 0–11 were traverses within the sinkhole itself; additional traverses were run to characterize bedrock features on the periphery of the sinkhole. B–D) Locations of traverses with respect to trenches and pits dug in 2003, 2004, and 2005. Although some traverses appear to go over boulders, in reality the traverses went around them.

After field picking, the residue of coarse fraction was bagged and taken back to the museum for later processing. Concentrate was later soaked once more, and again washed over coarse and fine screens. Material concentrated in the lower screen (INSM fine fraction) in the field was also bagged and later rewashed at the INSM over two layers of fine window screen. Concentrate was then picked in the lab using binocular microscopes at 10X magnification. Because this second washing passes sediment through double-stacked fine screen, material retained on the screen is a bit smaller than would be retained on a single fine screen.

The INSM screening technique allows large quantities of sediment to be washed very quickly in the field. It therefore maximizes sampling of diagnostic vertebrate skeletal elements and rare taxa. The trade-off is that it requires the sacrifice of any fos-

sils small enough to pass through fine window screen. These are generally not critical elements (for example, phalanges) of the vertebrate fauna. However, very small invertebrate or plant fossils are also lost.

The two INSM size fractions are distinguished mainly for ease in picking and sorting fossils. They do not permit quantitative taphonomic analysis in terms of proportions of vertebrate skeletal elements of different size. The INSM procedure has been described so that future workers on PCS fossils collected by this method will be aware of its strengths and weaknesses for characterizing the PCS paleobiota. Because of the INSM protocol's limitations for some kinds of analysis, a supplementary, more labor-intensive and time-consuming method of sediment washing was also employed.

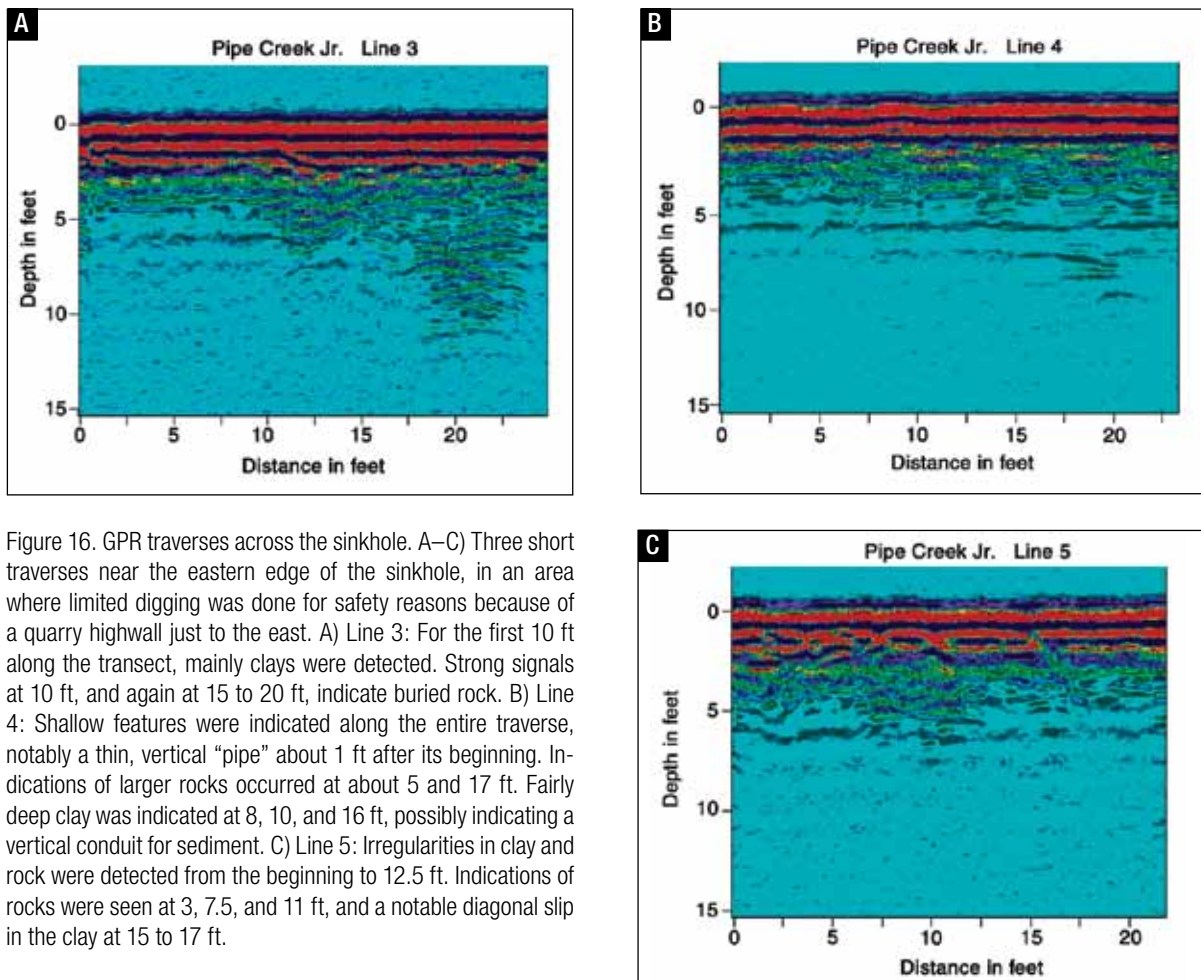


Figure 16. GPR traverses across the sinkhole. A–C) Three short traverses near the eastern edge of the sinkhole, in an area where limited digging was done for safety reasons because of a quarry highwall just to the east. A) Line 3: For the first 10 ft along the transect, mainly clays were detected. Strong signals at 10 ft, and again at 15 to 20 ft, indicate buried rock. B) Line 4: Shallow features were indicated along the entire traverse, notably a thin, vertical “pipe” about 1 ft after its beginning. Indications of larger rocks occurred at about 5 and 17 ft. Fairly deep clay was indicated at 8, 10, and 16 ft, possibly indicating a vertical conduit for sediment. C) Line 5: Irregularities in clay and rock were detected from the beginning to 12.5 ft. Indications of rocks were seen at 3, 7.5, and 11 ft, and a notable diagonal slip in the clay at 15 to 17 ft.

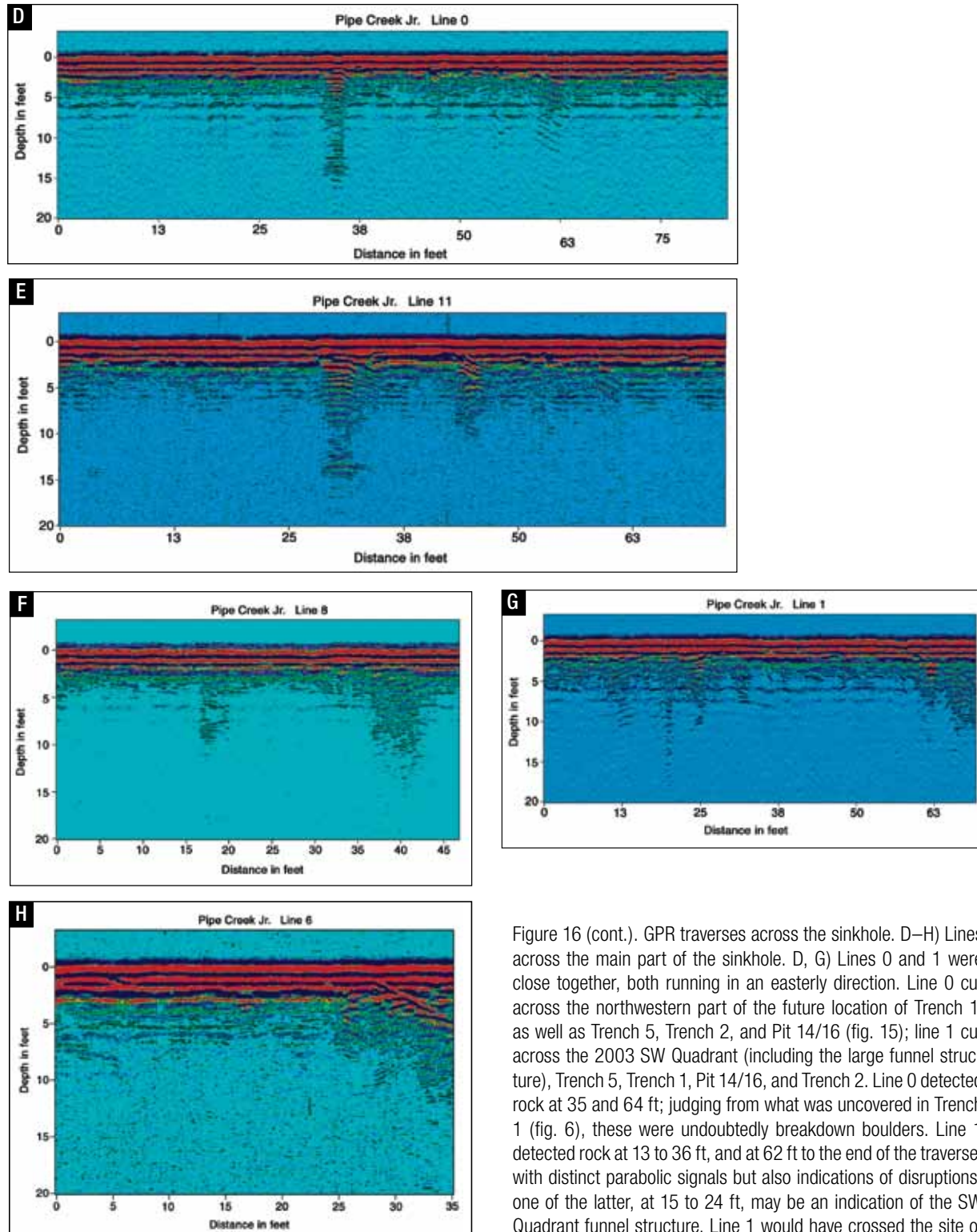


Figure 16 (cont.). GPR traverses across the sinkhole. D–H) Lines across the main part of the sinkhole. D, G) Lines 0 and 1 were close together, both running in an easterly direction. Line 0 cut across the northwestern part of the future location of Trench 1, as well as Trench 5, Trench 2, and Pit 14/16 (fig. 15); line 1 cut across the 2003 SW Quadrant (including the large funnel structure), Trench 5, Trench 1, Pit 14/16, and Trench 2. Line 0 detected rock at 35 and 64 ft; judging from what was uncovered in Trench 1 (fig. 6), these were undoubtedly breakdown boulders. Line 1 detected rock at 13 to 36 ft, and at 62 ft to the end of the traverse, with distinct parabolic signals but also indications of disruptions; one of the latter, at 15 to 24 ft, may be an indication of the SW Quadrant funnel structure. Line 1 would have crossed the site of Pit 14/16 and Trench 2 at about 40 to 60 ft, and a disruption of

the signal at 60 ft may correspond to the edge of Trench 2. E) Line 11 showed a strong rock signal at 27 ft, and indications of dipping or tilted rocks at 32, 42, and 60 ft. Line 11 would have crossed the future locations of Pit 14/16 and Trench 2 between 33 and 60 ft; F) Line 8 crossed the site of The SW Quadrant funnel at 9–17 ft; the strong signal at 17 ft on the traverse probably indicates a boulder on the periphery of the funnel. The strong signal between 30 and 45 ft may be associated with Rock C; H) Line 6 trended southwesterly from the site of Trench 1 across the 2003 SE Quadrant and the underlying 2004 Excavation Plateau. Details of bedding can be seen in the clay-rich sediments from 0 to 25 ft, after which rock signals become apparent as the line approaches landmark Rock A.

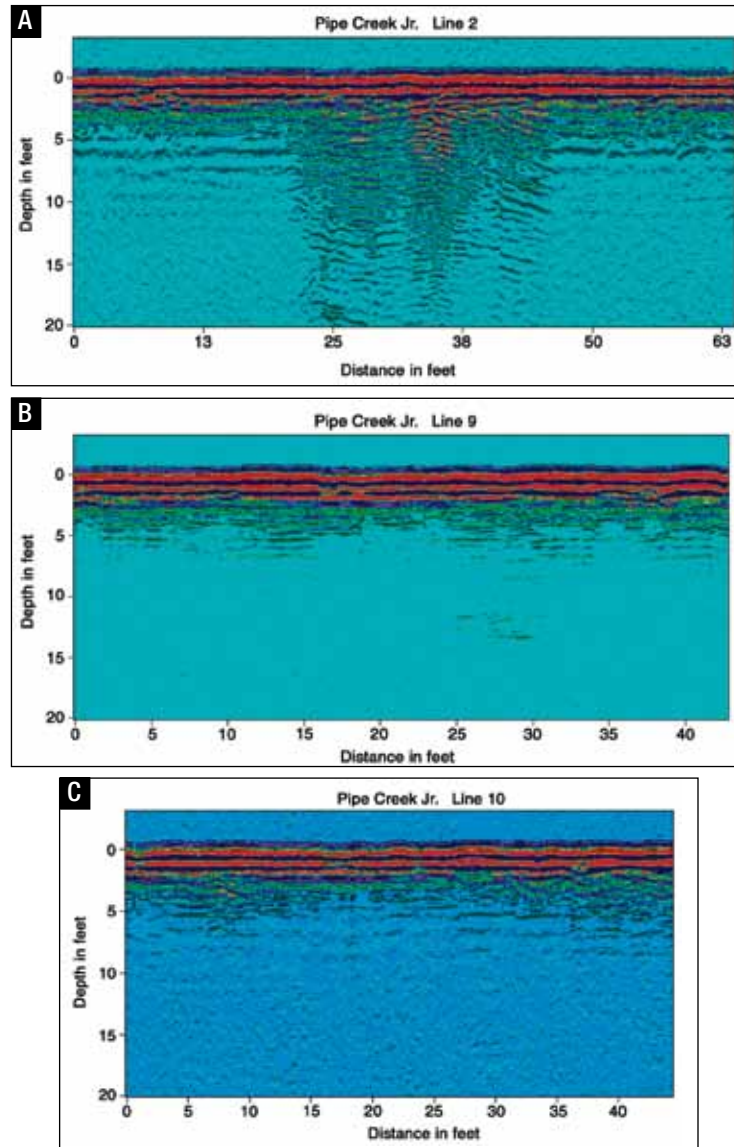


Figure 17. Additional GPR lines across the sinkhole, or over adjacent bedrock. A) Line 2 began at landmark Rock A and cut across the 2003 SE Quadrant and the underlying 2004 Excavation Plateau. Considerable bedrock was detected in the middle of the line, consistent with what was uncovered during digging through the Excavation Plateau (fig. 13B). B–C) Lines 9 and 10 moved northward across the 2003 SW and SE Quadrants, respectively, the Excavation Plateau beneath them, and Trench 1, and went around landmark Rock B (not directly over it, as shown in Figure 15). The two lines look rather similar; line 9 shows a prominent rock at its beginning (See fig. 15D), and line 10 shows disruptions over the first few feet that may be associated with boulder/clay boundaries in the 2004 Excavation Plateau; additional disruptions in line 10 occur at 20, 25, and 36 ft.

Indiana-Purdue University Fort Wayne screen-washing

Both prior to and during the INSM operations from 2003 through 2005, IPFW personnel collected large bags (generally weighing 20 to 50 pounds) of Zone A sediment from both the Spoil Pile and the remaining in situ deposits. These bags are (present tense is used to describe this procedure be-

cause it is on-going) air-dried for at least several months (given the time it takes to process them, most bags are not processed until a few years after collection).

Before processing, the aggregate dry contents of each bag are weighed; because of the large size of these samples, such weights are made on large scales to the nearest pound or 0.1 pound, and then

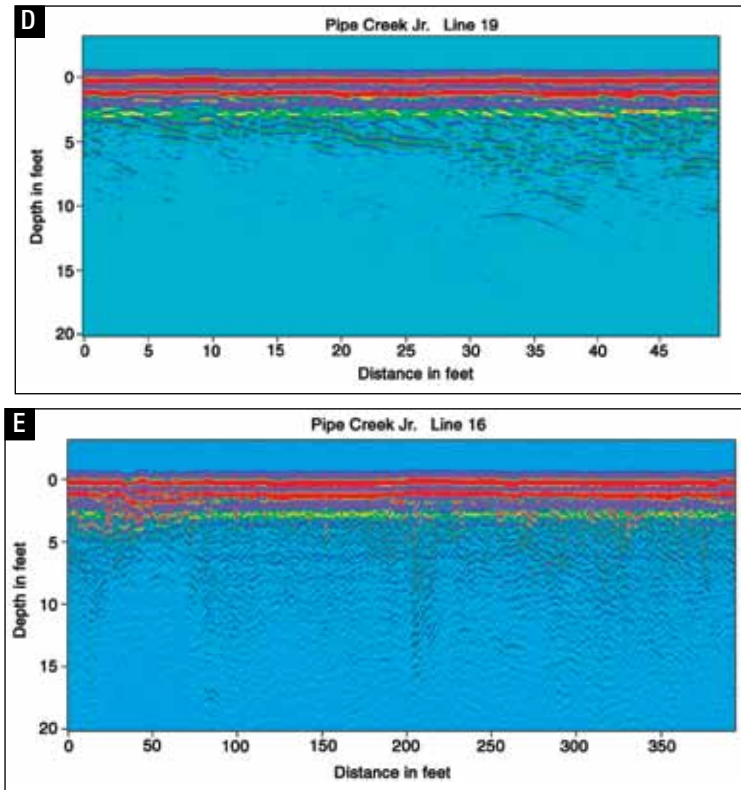


Figure 17 (cont.). Additional GPR lines across the sinkhole, or over adjacent bedrock. D–E) Traverses across the glacially polished bedrock surface adjacent to the sinkhole. D) Traverse 19 shows nicely dipping flank beds of the Paleozoic reef, with possible disruptions indicated by a parabolic feature at the end of the line. E) Line 16, a long traverse that began near the western margin of the sinkhole and headed to the northeast. A strong bedrock signal is reflected over most of the line, with disruptions at 100, 125, 260, 330, and 360 ft. The most interesting feature is a possible soft sediment-filled structure (filled cave passage?) at 30 to 70 ft.

converted to metric units. A volume of sediment roughly comparable to two human fists is removed from the bag and soaked at least overnight in a bucket of water to which about 2 tablespoons of baking soda have been added. The softened sediment and water are then washed through a stacked series of progressively finer U.S.A. Standard Testing Sieves. These routinely are 4-mm (#5; -2ϕ), 2-mm (#10; -1ϕ), 1-mm (#18; 0ϕ), and 0.5-mm (#35; 1ϕ) meshes. For many samples of Zone A sediment that were collected in situ in the sinkhole, 0.25-mm (#60; 2ϕ), 0.125-mm (#120; 3ϕ), and 0.063-mm (#230; 4ϕ) sieves are also used. Material concentrated on each sieve is dried overnight at 80°C or air-dried in the sun, and collected in a jar. This procedure is repeated until the entire bag of sediment has been processed, after which the total amount of material in each size fraction is weighed. The various concentrates are then picked or otherwise processed.

The finest sediment fractions are not directly weighed, but are routinely estimated by subtract-

ing from the total sediment dry weight the weights of material retained on the 4-mm through 0.5-mm fractions. Material passing through the 0.5-mm screen (the lower size limit of coarse sand) (Folk, 1980) is designated the routine fine fraction. For those samples processed still further, down through a 0.063-mm mesh screen (the lower limit of very fine sand), weight of the sub-sand size fraction (silt and clay-sized sediment) that passes through this screen is estimated by subtracting from the total sediment dry weight the weights of material retained on the 4-mm through 0.063-mm screens.

Although this protocol processes considerably smaller amounts of sediment at a time than INSM screen-washing in the field, it still involves a few to several hundred grams of sediment in a single batch. Given the large quantities of clay in PCS fossiliferous sediment, it is possible that the routine IPFW screen-washing uses too much sediment in any one run to allow thorough disaggregation of tiny mud lumps. As a check, one sample

(Pit 16 Zone A August 2005 Farlow Test Bag A) was washed in a series of batches, each of which weighed less than 100 g total dry weight, and the results compared with sediment from the same sample processed in the usual manner. As a second test of how well our standard protocol disaggregates sediment, samples of Zone A sediment were processed by a commercial testing laboratory (A & L Great Lakes Laboratory, Fort Wayne, Indiana), following ASTM protocol D422-63 (ASTM International, 2007).

The IPFW screen-washing protocol is designed to concentrate the vertebrate mesofauna and microfauna (bones of turtles, frogs, and snakes, and bones and teeth of small mammals). It therefore emphasizes the 4-mm, 2-mm, 1-mm, and 0.5-mm sediment fractions. Although the IPFW screen-washing procedure routinely retains fossils comparable in size to the lower limit of coarse sand (0.5 mm), and in some cases the lower limit of very fine sand (0.063 mm), any silt-sized and finer material is necessarily lost. However, limited samples of this finest sediment have been retained for future analysis, should this be warranted.

Sediment and fossil plant organic content, and sediment carbonate content determined by loss on ignition

Ecologists determining the organic content (= ash-free dry weight) of modern plant and animal tissues and geologists measuring the organic content of sediments use different protocols. Ecologists first dry modern samples at some temperature between 70 to 105°C (commonly 80°C) for at least 24 hours, and then ash the sample at 550°C for at least 3 hours, and often 12 to 18 hours (see Westlake, 1965; Likens and Bormann, 1970; Cummins and Wuycheck, 1971; Suberkropp and others, 1976; Carpenter and others, 1983; Delaney and others, 1996). The weight loss during ashing is the organic content. In contrast, Dean (1974) determined the organic content of sediment by first oven-drying a powdered sample at 90 to 100°C for one hour, and then ashing the sample at 550°C for another hour.

We determined the organic and carbonate content of Zone A bulk samples (excluding large clasts) and IPFW sediment size fraction concentrates by loss on ignition (LOI) at IPFW using three protocols (modified from Dean [1974] and procedures used by Farlow and Argast [2006]). In samples

used for LOI measurements of organic content of Zone A bulk sediment, large clasts (chert, limestone, quartz) and large pieces of fossil plant material were removed before processing.

Protocol 1: Samples were processed in batches of three replicates, and for some samples duplicate batches were run. Alumina crucibles were dried overnight at 110°C, cooled to room temperature in a desiccator, and weighed. About 6 grams of air-dried or oven-dried (at 80°C) sediment bulk sample or size concentrate sample (an attempt was made to homogenize the dried sediment size fraction by stirring prior to removing sample for grinding each batch) were weighed and finely ground, after which about a third of the sample was placed in each crucible. The crucibles with ground sample were then dried overnight at 110°C, cooled in a desiccator, and weighed; this step usually resulted in about a 1 percent decrease in sample dry weight over the air-dry or oven-dry at 80°C weight. Crucibles were then placed in a furnace set at 550°C and, once the furnace temperature returned to 550°C after having dropped while the furnace door was open, left in the furnace for 1 hour. Crucibles were then cooled to room temperature in a desiccator and reweighed. The difference in sample dry weights before and after ashing at 550°C was used to calculate the organic content as a percentage of sediment dry weight before ashing. Samples were then returned to the furnace, now set at 950°C, and once the furnace returned to that temperature, left in it for another hour. Samples were then cooled to room temperature in a desiccator and reweighed. The carbonate content of sediment was calculated as the loss in sediment dry weight between 550° and 950°C, and expressed as a percentage of sediment dry weight after ashing at 500°C.

Protocol 2: Same as protocol 1, except that: a) each sample weighed about 1 gram; b) ashing to determine organic content was done for 3 hours at 500°C; and c) combustion to determine carbonate content was done for 4 hours at 925°C. Replicates were done in batches of three or six.

Protocol 3: As in protocol 1, the organic content of dried samples was determined by weighing after the sample was ashed for 1 hour at 550°C. After that, samples were returned to the oven for another 2 hours at 500°C, and reweighed. Samples were then ashed for 1 hour at 950°C as in protocol 1. In some runs fewer replicates were done than in protocols 1 and 2 (often only one determination

per sample, depending on the amount of material available), and the dry weights of samples prior to LOI treatment varied between about 1 and 3 g.

In addition, determinations of the dry weight organic content of Zone A sediment were made by A & L Great Lakes Laboratories (Fort Wayne, Ind.), using ASTM protocol D2974-00 (ASTM International, 2000), which involves combusting samples at 440°C after previous drying at 105°C. Some of these determinations were done on bulk sediment, using all size fractions, and some were done on material retained on sieves of the various size fractions used in the laboratory's sediment size-frequency analyses.

LOI measurements of samples of PCS Zone A fossil plant material (wood, leaf and shoot fragments, seeds) were also made using Spoil Pile fossil plant samples (usually with dry weights of a gram or less) by all three of the protocols described above. For a few samples, after combusting plant material at 550°C for 1 hour, and 500°C for 2 hours by protocol 3, we returned the samples to the furnace for an overnight burn at 550°C (a procedure more like that used by plant ecologists). In some (but not all) fossil plant samples there was incomplete combustion of material after 1 hour at 550°C, with some of the black fossil plant material visibly not ashed. For such samples the additional 2 hours at 500°C under protocol 3 resulted in significant additional sample weight loss (and thus a higher LOI estimate of organic content). There was little (less than 1 percent) or no further loss of weight by ignition if fossil plant samples were burned overnight at 550°C after the additional 2 hours at 500°C under protocol 3. LOI-determined values of PCS fossil plant material organic content reported below reflect the additional 2 hours of combustion at 500°C under protocol 3, where those values are higher than obtained after the initial hour at 550°C.

For comparative purposes, we also did LOI determinations on leaf, twig, and bark samples of selected modern tree species, relatives of which occur in the PCS paleoflora (Farlow and others, 2001). Samples were collected in mid-October through early November 2007 (hardwoods) and mid-April 2008 (pine). Leaves and twigs that were collected for this work were still attached to the tree. Where possible, leaves were taken that had not yet changed to their autumn color; but otherwise, dead leaves that were still attached to the tree were used. Dead twigs were selected. Leaf samples were dried

at 110°C for at least 3 days prior to analysis, and bark and twig samples were dried at 110°C for at least a week before processing. Samples were then crushed and shredded to small pieces in a mortar and dried overnight at 110°C before processing by protocol 3. Sample dry weights in these analyses were a gram or less.

For a few samples we determined the LOI of PCS fossil plant and modern tree tissues using ashing protocols more like those used by ecologists. After the 2 hours at 500°C, some samples were returned to the furnace at 550°C for 6 or more (sometimes overnight) additional hours. One sample batch was dried at 80°C rather than the usual 110°C, and then ashed for 18 hours at 550°C. In contrast to some of the samples of PCS fossil wood, modern tree tissues combusted by protocol 3 showed little (less than 1 percent) or no difference between LOI determinations of organic content after the first hour at 550°C and after the additional 2 hours at 500°C. Additional burns of 6 hours or longer did not result in any significant further sample weight losses. A lower drying temperature of plant tissues prior to ashing did not affect measurement of organic content as a percentage of dry weight.

For comparative purposes we also did bulk LOI determinations for a sediment sample collected on the muddy bank of a modern tropical tidal creek (Chaguite Creek, Rio Tamarindo, Guanacaste Province, Costa Rica). The sediment was dark in color, and bits of black plant detritus could easily be seen.

We evaluated our LOI procedure using U.S. Geological Survey reference sample SDO-1 (Devonian Ohio Shale collected near Morehead, Kentucky). The "information value" mean weight percent of LOI of this sample is 21.7 percent with a standard deviation of 0.9 percent, and the mean water content is 1.21 percent with a standard deviation of 0.5 percent (Smith, 1991). Mean LOI less H₂O-moisture for this sample is (21.7 minus 1.2) or 20.5 percent. Six LOI measurements of the standard in our lab yielded a mean value of 19.2 percent (range 18.2–19.8 percent), about 6 percent less than mean LOI less H₂O- of the standard.

Sediment micromorphology

Oriented samples for thin sectioning were collected in 2005. These were dried and coated with

epoxy, after which thin sections were commercially prepared. The composition and fabric of thin sections were evaluated using an Olympus microscope with an EXPO fluorescence illumination system for detecting lignin (which excites under UV light) preserved in sediment.

Nodule petrography and stable isotope geochemistry

Sideritic nodules of varying size are ubiquitous to PCS Zone A sediments (fig. 18). A hand sample of nodule was impregnated with blue-dyed epoxide resin to clearly demarcate open pore spaces, slabbed by rock saw, and cut into a micropolished thin section for petrographic study. This sample was also analyzed for carbon and oxygen isotopes from the siderite.

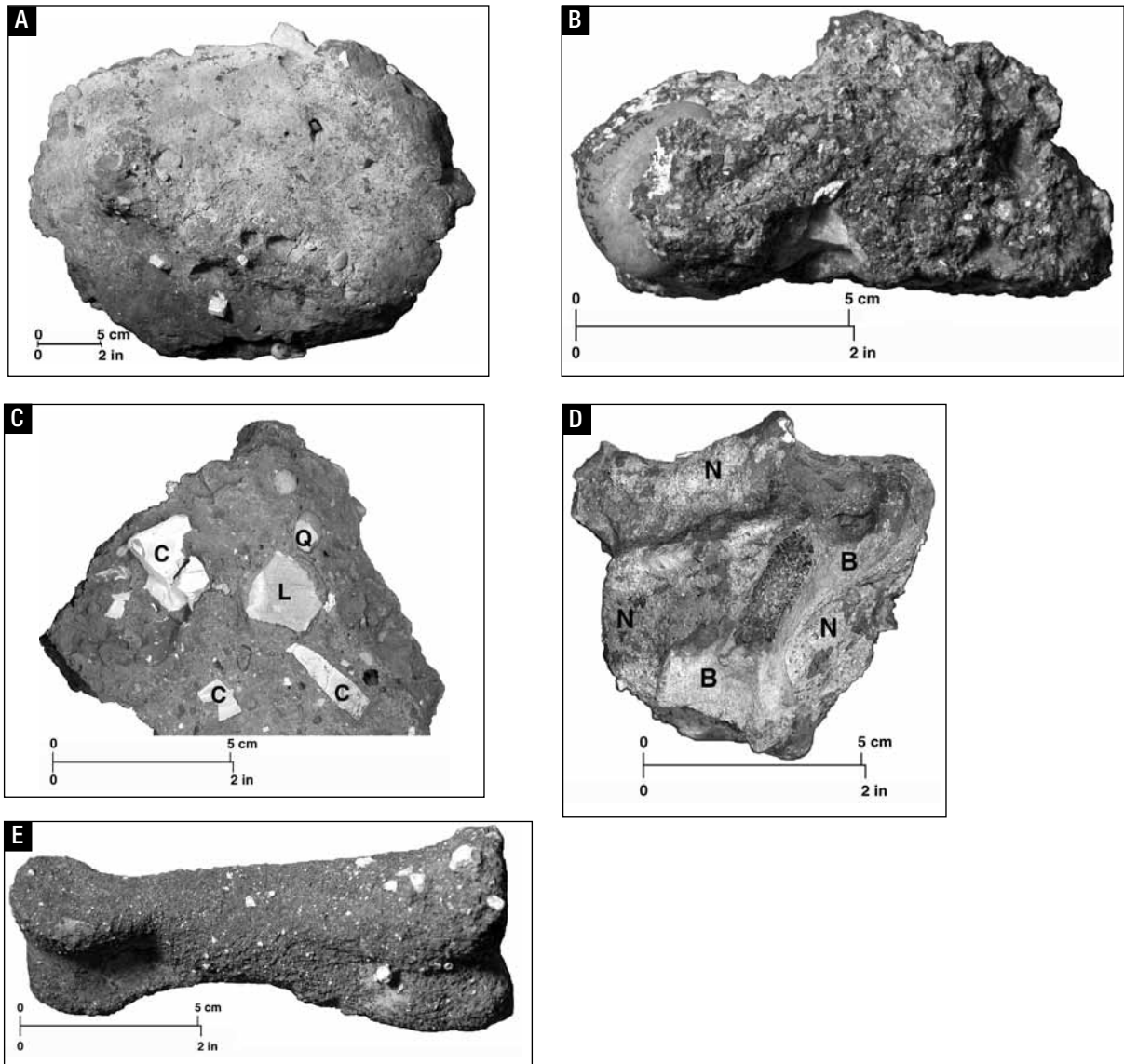


Figure 18. Photographs showing siderite nodules from Zone A. A) Unusually large nodule, probably from Spoil Pile material. B) Nodule from Spoil Pile partly enclosing large, rounded quartzite pebble (left end of nodule). C) Cut section through nodule, Southwest Quadrant Zone A/B mix, showing sections through angular clasts of chert (C) and limestone (L) and a rounded quartzite pebble (Q). D) Nodular material (N) partly surrounding fragmentary large vertebra (B = bone), Pit 3 Zone A/B mix June 17, 2004. E) Nodular material encrusting phalanx of large camel, probably from the Spoil Pile.

A polished thin slab from the thin section billet was microsampled by microscope-mounted microdrill assembly. Siderite powders of about 1 mg were vacuum-roasted at 200°C to remove volatile contaminants and were analyzed by a Finnigan Kiel device coupled to the inlet of a Finnigan MAT 252 stable isotope ratio mass spectrometer at the Paul H. Nelson Stable Isotope Laboratory in the Department of Geoscience at the University of Iowa. Analyses of interlaboratory carbonate standards indicate that the precision of this instrument is better than 0.1‰ for both carbon and oxygen isotopes.

RESULTS OF LABORATORY ANALYSES

Zone A sediment size distribution (IPFW samples)

To date we have wet-screened more than 500 kg of PCS Zone A fossiliferous sediment, representing both in situ and Spoil Pile material (Tables 1–3). Because of the possibility of mixing of Zone A fossiliferous sediment with other sediments in the Spoil Pile, data on sediment size distribution will be emphasized for in situ Zone A material.

Table 1. Summary breakdown of size distribution of Spoil Pile and of in situ fossiliferous sediment samples collected prior to June 2003, when systematic excavation of the sinkhole sediments was initiated

[Individual Spoil Pile sample total dry weights ranged from 12.2 to 29.3 kg, and the aggregate dry weight of sediment exceeded 500 kg. Individual in situ sample total dry weights ranged from 0.9 to 18.1 kg, and the aggregate dry weight of sediment exceeded 325 kg. Most or all of the in situ samples would have comprised Zone A material. Most Spoil Pile samples would also have mainly comprised Zone A material, but with a greater possibility of contamination by other sediments. Sediment fractions are analyzed in terms of the dry weight of material retained on standard testing sieves of specified mesh size; the 2-mm through 0.5-mm size fractions are those most likely to retain small vertebrate fossils. Dry weights are expressed as percentages of: (1) the combined 2-mm through 0.5-mm size fractions; and (2) the noncoarse fraction (material that passed through a 4-mm screen). In some samples analyzed early in the study, bone pieces and nodules containing bone were removed before the coarse fraction was weighed. Consequently the weight of the coarse fraction was slightly underestimated, and the weight of the noncoarse fraction overestimated. The fine fraction comprises sediment that passed through the 0.5-mm screen, and is estimated by subtracting the aggregate weight of all sediment retained on screens coarser than 0.5 mm from the total sediment dry weight. SD = standard deviation.]

Size fraction		Minimum	Maximum	Mean	Standard deviation	Number of samples
Spoil Pile samples						
2-mm fraction	(1)	23.7	39.6	30.05	4.08	29
	(2)	0.7	3.5	2.37	1.08	8
1-mm fraction	(1)	12.2	37.4	31.66	4.52	29
	(2)	1.0	3.6	2.29	0.89	8
0.5-mm fraction	(1)	24.7	51.3	38.29	5.33	29
	(2)	1.0	4.8	2.93	1.34	8
Fine fraction as % of noncoarse fraction		88.8	97.3	92.41	3.17	8
In situ sediment samples						
2-mm fraction	(1)	29.1	45.1	36.84	3.52	30
	(2)	0.6	9.7	4.63	2.58	22
1-mm fraction	(1)	19.5	44.8	31.26	3.74	30
	(2)	0.6	7.6	3.80	2.09	21
0.5-mm fraction	(1)	24.1	44.1	31.90	4.33	30
	(2)	0.7	7.3	3.80	1.83	22
Fine fraction as % of noncoarse fraction		75.4	98.1	87.98	6.41	21

Generally Zone A sediment is poorly sorted. Although the bulk of this material is very fine grained (Tables 1 and 2), a sample of Zone A material can include pebble-sized and even larger clasts, and bones of various sizes mixed within the fine-grained sediment.

Characterizing the size distribution of PCS Zone A fossiliferous sediments is complicated by the routine presence of the sideritic nodules (fig. 18) (Farlow and others, 2001; Farlow and Argast, 2006), which can range from as much as 210 mm in greatest dimension down at least to sand-grain size. The nod-

ules constitute exceptions to the otherwise unconsolidated nature of the fossiliferous deposit. Their presence in all size fractions collected in sieves means that the sediment size distribution based on weights of material in sieves unavoidably underestimates the proportion of fine-grained sediments in the prediagenetic deposit to an unknown degree.

Because of the predominance of mud in the PCS fossiliferous layer (see below), there was a tendency during screen-washing for mud to form tiny lumps that accumulated in the finer (particularly 1-mm and finer) sieves. We gently pressed mud lumps against the screen, and then directed

Table 2. Size distribution of in situ samples of fossiliferous sediment collected during Indiana State Museum excavations from 2003 through 2005

[Dry weights are expressed as percentages of: 1) the combined 2-mm through 0.5-mm size fractions; and 2) the noncoarse fraction (material that passed through a 4-mm screen). The fine fraction comprises sediment that passed through the 0.5-mm screen, and is estimated by subtracting the aggregate weight of all sediment retained on screens coarser than 0.5 mm from the total sediment dry weight.]

Source of sample	Total sample dry weight (kg)	Dry weight of noncoarse fraction (kg)	% of sample				
			2 mm	1 mm	0.5 mm	fine fraction	
SW Quadrant Zone A 6/20/03	9.72	8.32	(1)	32.0	30.9	37.1	-----
			(2)	1.7	1.7	2.0	94.5
	10.35	8.77	(1)	28.9	30.4	40.8	-----
			(2)	1.5	1.6	2.1	94.8
Pit 16 mixture of Zone A and B sediment 7/2/04	-----	-----	(1)	23.9	31.3	44.8	-----
	8.60	8.20	(1)	25.4	33.1	41.5	-----
			(2)	1.0	1.3	1.7	96.0
Pit 16 Zone A August 2005	13.10	11.97	(1)	25.7	35.8	38.5	-----
			(2)	1.4	1.9	2.1	94.6
	0.20	0.19	(1)	19.6	35.3	45.1	-----
			(2)	1.1	1.9	2.5	94.5
	0.16	0.15	(1)	25.5	36.3	38.2	-----
			(2)	1.7	2.4	2.6	93.3
	0.73	0.70	(1)	24.1	35.6	40.4	-----
			(2)	1.3	1.9	2.2	94.7
	0.19	0.18	(1)	22.3	38.4	39.3	-----
			(2)	1.4	2.3	2.4	93.9
	9.41	8.85	(1)	24.5	35.0	40.6	-----
			(2)	1.2	1.7	2.0	95.0
Pit 2 Zone A1 6/18/04	8.54	5.92	(1)	36.1	33.9	30.0	-----
			(2)	10.1	9.5	8.4	72.0
	5.81	3.37	(1)	36.3	33.7	30.0	-----
			(2)	16.3	15.2	13.5	55.0

Table 3. Breakdown of finer sediment fraction (as a percentage of the dry weight of the noncoarse fraction) for selected in situ fossiliferous samples

[Weight of the sub-sand fine fraction is estimated by subtracting the aggregate weight of all sediment size fractions coarser than 0.063 mm from the total sample dry weight.]

Sample	Dry weight of non-coarse fraction (kg)	% of noncoarse fraction			
		0.25 mm	0.125 mm	0.063 mm	<0.063 mm (sub-sand fine fraction)
3/4/97 spot sample	0.80	6.3	6.0	2.2	80.6
5/23/03 spot sample	3.87	3.8	2.4	1.1	89.6
SW Quadrant Zone A 6/20/03	8.32	5.1	3.4	2.2	83.8
	8.77	6.8	3.9	1.4	82.6
Pit 16 mixture of Zone A and B sediment 7/2/04	8.20	4.0	2.4	1.8	87.9
Pit 16 Zone A August 2005	11.97	4.1	2.5	1.3	86.8
	0.19	4.6	2.9	1.4	85.6
	0.15	3.9	2.2	0.7	86.5
	0.70	4.5	3.4	1.9	84.9
	0.18	4.1	2.6	1.3	85.9
	8.85	4.3	2.8	1.4	86.5
Pit 2 Zone A1 6/18/04	5.92	11.3	6.7	2.9	51.1
	3.37	17.6	11.6	5.4	20.3

streams of water against the squashed lumps until they disaggregated. However, for the finest sediment size fractions (0.25 mm and finer), our ability to break apart mud lumps was limited by our ability to see them. Consequently, the dry weights of these finer fractions may be overestimates, in which case the weight fractions of silt and clay-sized sediments would be underestimates.

The size of the sample processed did not affect the size-frequency distribution of sediment retained on screens. This can be seen by comparing the results of different samples of sediment from Pit 16 Zone A (Tables 2 and 3).

Dry weights of sediment size fractions generally include any vertebrate and invertebrate fossils. Bits of comminuted plant material are quite abundant in Zone A sediment, particularly in the finer size fractions (0.5–0.063 mm screen); in these finer fractions, the volume of presumed altered plant material is large enough to give the fraction a dark color (fig. 19). Dry weights of all sediment size fractions concentrated in sieves include this plant material.

The coarse fraction of Zone A sediment (material retained on a 4-mm mesh sieve) is composed mainly of angular, often corroded chunks of chert and less abundant pieces of limestone (including Silurian invertebrate fossils), both derived from erosion of bedrock surrounding the doline, as well as isolated pieces of calcite crystals, siderite nodules, rounded quartzite pebbles not of local origin, and occasionally other pebbles of heterogeneous lithology, as well as large vertebrate fossils (most commonly fragments of turtle or tortoise shell). The proportion of Zone A sediment composed of the coarse fraction is highly variable; it is generally 30 percent or less of the total dry weight of a sample, but makes up just under half the total sample dry weight of one of the atypical samples from Pit 2 Zone A1 (Table 2, fig. 20).

The 2-mm, 1-mm, and 0.5-mm fractions are usually subequal in weight (Tables 1 and 2). In most cases they are only a few percent of the total noncoarse fraction, but make up a much greater proportion of the samples from Pit 2 Zone A1 (Table 2). Sedi-

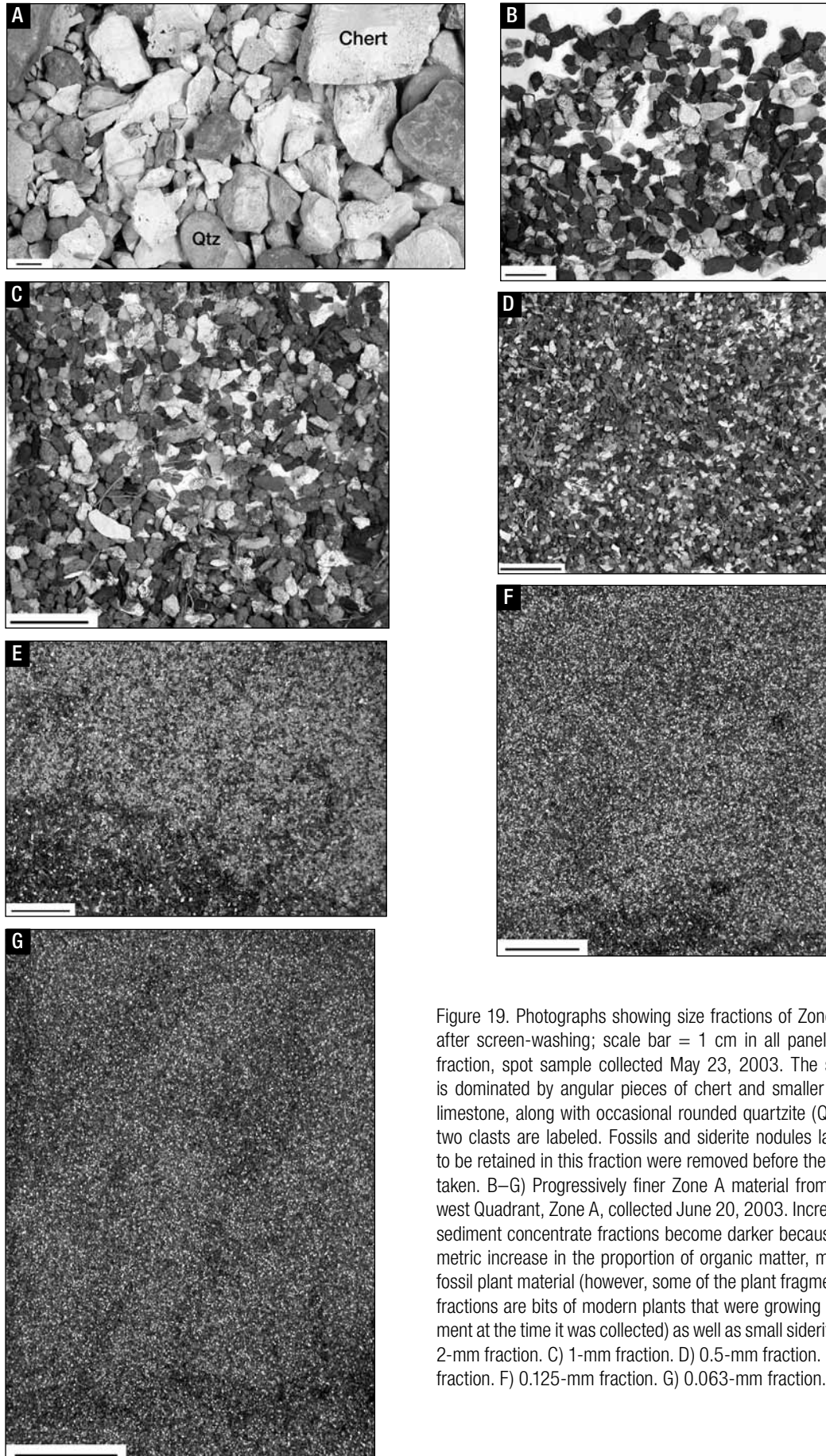


Figure 19. Photographs showing size fractions of Zone A material after screen-washing; scale bar = 1 cm in all panels. A) 4-mm fraction, spot sample collected May 23, 2003. The size fraction is dominated by angular pieces of chert and smaller amounts of limestone, along with occasional rounded quartzite (Qtz) pebbles; two clasts are labeled. Fossils and siderite nodules large enough to be retained in this fraction were removed before the picture was taken. B–G) Progressively finer Zone A material from the Southwest Quadrant, Zone A, collected June 20, 2003. Increasingly finer sediment concentrate fractions become darker because of a volumetric increase in the proportion of organic matter, mostly bits of fossil plant material (however, some of the plant fragments in these fractions are bits of modern plants that were growing on the sediment at the time it was collected) as well as small siderite pieces. B) 2-mm fraction. C) 1-mm fraction. D) 0.5-mm fraction. E) 0.25-mm fraction. F) 0.125-mm fraction. G) 0.063-mm fraction.

ment grains in these size fractions include smaller versions of the materials that compose the coarse fraction, but the sand-size fraction is dominated by quartz grains (see p. 41). Bones and teeth of rodents and other mammals, as well as snake vertebrae, fish bones, and especially frog bones are common in the 2-mm and 1-mm fractions, and smaller vertebrate bones (mostly fragments) also can be recognized in the 0.5-mm fraction. Steinkerns of small molluscs, along with seeds and charophyte gyrogonites, also occur in the 1-mm and 0.5-mm fractions; smaller size fractions have not yet been carefully examined for fossils.

Despite possible biases that could underestimate the weight of fine-grained sediments, the routine fine fraction (material passing through a 0.5-mm screen) generally constitutes at least 80 percent by dry weight of the noncoarse sediment fraction (Table 2), and in some samples makes up nearly all of it. A finer breakdown of this material (Table 3) shows medium sand to be slightly more abundant than fine sand, which, in turn, is more abundant than very fine sand. Although the boundaries be-

tween sand size categories differ slightly between our analyses and the more exacting ASTM analysis (Table 4), the latter yields a similar result. Both our analyses and the ASTM analysis show material finer than very fine sand to constitute 80 percent or more of the noncoarse sediment fraction. In most places in the sinkhole, Zone A sediments thus were a mud-rich diamicton (see Potter and others, 2005, p. 78). This suggests that the literally quick-and-dirty IPFW sieving protocol provides a good first approximation of the sediment size distribution.

Once again, however, the samples from Pit 2 Zone A1 are different, having much lower proportions of fine-grained sediment. Apart from the Pit 2 samples, Zone A fossiliferous sediments are essentially a clay with intermixed secondary amounts of coarser sediments.

IPFW sediment size distribution data provide an indication of the total amount of sinkhole sediment that was screened on-site during INSM fieldwork. The total dry weight of INSM fine fraction sediment after rewashing in the lab came to 890

Table 4. Sediment size distribution and organic content of Zone A fossiliferous sediment samples analyzed according to ASTM Protocols D422-63 and D2974

Sample size fraction	Sample fraction as a % of total noncoarse fraction dry weight					
	SW Quadrant Zone A 6/20/03	Pit 16 Zone A August 2005				
		Sample 1	Sample 2		Sample 3	
Noncoarse fraction	100.00	100.00	100.00	Organic content (% dry weight)	100.00	Organic content (% dry weight)
Very coarse sand (passes through 2-mm sieve; retained on 0.85- mm sieve)	2.03	3.17	3.12	46.0	3.90	43.8
Coarse sand (retained on 0.425-mm sieve)	2.16	2.81	3.62	17.2	4.46	18.7
Medium sand (retained on 0.25-mm sieve)	3.92	3.61	5.00	1.1	5.61	1.5
Fine sand (retained on 0.106-mm sieve)	3.85	3.12	4.51	2.3	4.61	< 0.1
Very fine sand (retained on 0.075-mm sieve)	0.95	0.64	0.98	0.1	0.99	0.8
Total silt (0.074-0.005 mm)	34.1	32.6	32.8	-----	30.4	-----
Total clay (< 0.005 mm)	53.0	54.0	50.0	-----	50.0	-----

Table 5 (opposite page). Organic content of Pipe Creek Sinkhole Zone A bulk samples and sediment size fractions as determined by loss on ignition (LOI)

[Comparative data are also reported for a muddy, organic-rich sediment from a tropical estuarine tidal creek (Chaguite Creek, Costa Rica). See text for details of the different LOI protocols. Organic content is reported as mean (range) when there was more than one sample in a batch. Each line within a sample/size fraction category represents a different batch of replicates; the number of determinations for each sample in a batch ranged from one to six. Comparison of separate lines for a particular sample and size fraction categories indicates variability between/among different batches. For protocol 3 as applied to sediment size fractions the first value is based on weight loss after one hour at 550°C, and the value in parentheses is based on weight loss after an additional two hours at 500°C. For protocol 3 with bulk samples only the higher of the two determinations (1 hour at 550°C vs. 1 hour at 500°C plus 2 additional hours at 500°C) of organic content is reported; there was <1 percent difference between the two values.]

kg for sediment collected during 2003, 1,856 kg in 2004, and 219 kg in 2005, for a total of 2,965 kg. The INSM fine fraction would be roughly equivalent to the combined IPFW 2-mm and 1-mm fractions, which together make up about 3 to 4 percent by weight of the noncoarse fraction of typical Zone A sediment. This suggests that the total dry weight of noncoarse sediment washed in the field may have exceeded 75,000 kg.

Zone A organic and carbonate content

LOI estimates of organic content of bulk Zone A sediment were made at IPFW for three samples (Table 5): a spot sample collected in September 1997, a sample from SW Quadrant Zone A (collected on June 20, 2003), and a sample from Pit 16 Zone A (collected August 2005). These yielded organic content estimates of 7 to 8 percent, 6 to 7 percent, and 8 to 10 percent sediment dry weight respectively.

Three bulk samples of Zone A sediment from Pit 16 had overall organic contents of 7.9, 8.5, and 9.2 percent of sediment dry weight as determined by the commercial lab. A sample of Zone A material from the 2003 SW Quadrant had a bulk organic content of 5.2 percent of sediment dry weight by the same protocol. There was thus reasonable agreement for Zone A bulk sediment organic content between the two labs. LOI determinations of bulk sediment organic content for the modern tropical mudflat were half-again to twice the values obtained for PCS Zone A sediment by the same protocol (Table 5).

However, depending on type, clay minerals lose water at temperatures above 105°C (for example, Brindley and Brown, 1980). The ASTM protocol for determining sediment organic matter content involves combustion at 440°C after drying at 105°C. Because the Zone A bulk samples contain expandable clays, it is reasonable to assume that the concentration of organic matter is somewhat less than the values reported here. In any case, the

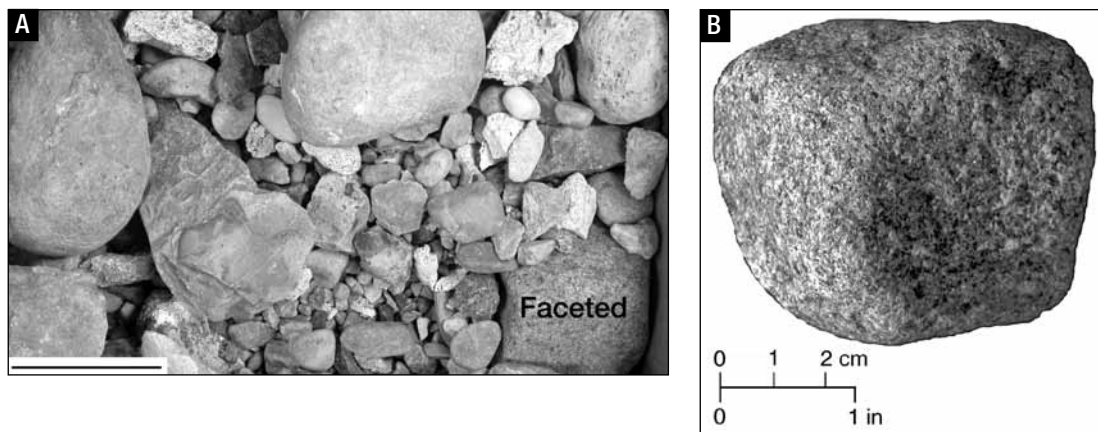


Figure 20. Photographs showing coarse (4-mm) fraction, Pit 2 Zone A1, June 18, 2004. A) Portion of the entire sample of the size fraction; scale bar = 5 cm. In addition to typical Zone A clasts, this sample includes rounded and sometimes faceted cobbles of a variety of lithologies. B) Faceted cobble of igneous rock (visible in the lower right-hand corner of panel A).

Sample	Size fraction	Protocol	Organic content (% dry weight)	Number of samples in batch
September 1997 Zone A spot sample	Bulk sample	3	7.83 (7.78–7.88)	2
		3	7.05 (6.99–7.11)	2
SW Quadrant Zone A 6/20/03	Bulk sample	3	6.86 (6.83–6.89)	2
		3	6.65 (6.45–6.84)	2
Pit 16 Zone A August 2005	Bulk sample	3	9.95 (9.89–10.0)	2
		3	8.10 (8.01–8.18)	3
SW Quadrant Zone A 6/20/03	2 mm	1	7.27 (6.79–7.69)	3
Pit 16 Zone A August 2005	2 mm	1	8.17 (8.00–8.31)	3
		3	6.15 (6.15)	1
SW Quadrant Zone A 6/20/03	1 mm	1	9.00 (8.28–9.88)	3
Pit 16 Zone A August 2005	1 mm	1	11.5 (9.90–13.4)	3
			7.69 (7.45–8.00)	3
		2	8.77 (8.36–9.08)	6
			3	5.51 (5.63)
		4.74 (4.62)		1
		5.22 (5.26)	1	
SW Quadrant Zone A 6/20/03	0.5 mm	1	6.25 (6.21–6.33)	3
Pit 16 Zone A August 2005	0.5 mm	1	7.77 (7.36–8.09)	3
			3	5.70 (5.79)
		3.80 (3.67)		1
		4.05 (4.07)	1	
SW Quadrant Zone A 6/20/03	0.25 mm	1	3.85 (3.79–3.94)	3
Pit 16 Zone A August 2005	0.25 mm	1	2.73 (2.66–2.83)	3
			3	3.69 (3.78)
		3.18 (3.23)		1
		3.31 (3.21–3.40) (3.40 [3.30–3.50])	2	
SW Quadrant Zone A 6/20/03	0.125 mm	1	5.39 (5.16–5.60)	3
Pit 16 Zone A August 2005	0.125 mm	1	3.19 (3.12–3.31)	3
			3	4.84 (4.88)
		3.53 (3.54)		1
SW Quadrant Zone A 6/20/03	0.063 mm	1	7.13 (7.02–7.19)	3
			7.74 (7.22–8.01)	3
		2	7.73 (7.59–7.81)	3
Pit 16 Zone A August 2005	0.063 mm	1	8.50 (8.38–8.63)	3
			3	9.71 (9.79)
		8.81 (8.96)		1
Chaguite Creek, Rio Tamarindo, Guanacaste Province, Costa Rica	Bulk sample	3	13.4 (13.2–13.6)	6

organic content was high enough to have an impact on the color (fig. 19) of the fine fraction.

Because of the possibility that water loss from clay sediments inflates the LOI values, we measured the LOI-determined organic content of Zone A sand-size fraction concentrates as proxies for Zone A organic content. The organic content of Zone A sediment size fraction concentrates retained after IPFW screen-washing obviously does not duplicate the organic content of Zone A bulk sediments. However, such determinations do allow comparison of the organic content of comparable sediment size fractions in different parts of the sinkhole, and between PCS Zone A sediment size fractions and those that future workers may determine for other fossiliferous deposits. The organic content of Zone A sediment-size-fraction concentrates determined by LOI was between 3 to 15 percent of oven-dry weight (Table 5). There was little difference among values obtained by different LOI protocols. Values across size fractions from the same overall Zone A sample (SW Quadrant 6/20/03 or Pit 16, August 2005) were much the same, but the significance of this is questionable, given likely comminuting of plant fragments during screen-washing. More interestingly, values for the same size fraction of the two samples differed little. Weighted organic contents (% dry weight) from the IPFW 2-mm through 0.063-mm size fractions for each sample can be calculated as the sum of values of the organic content (% dry weight) of each size fraction multiplied by that size fraction's proportional representation in the aggregate weight of the 2-mm through 0.063-mm size fractions, and are 5 to 6 percent for both the SW Quadrant and the Pit 16 Zone A samples.

Pit 16 Zone A size fraction concentrates processed by the commercial lab had considerably higher organic contents of the coarser than the finer size fractions (Table 4). This may corroborate the inference that IPFW screen-washing breaks plant materials into small bits. However, the weighted organic content across the Pit 16 Zone A sediment size fractions processed by the commercial lab was about 14 percent of oven-dry weight, more than twice the value obtained from IPFW samples from Pit 16 Zone A. The samples processed by the commercial lab were considerably smaller (a few hundred grams) than those processed at IPFW (Table 2); a likely explanation for the higher organic content of Pit 16 samples processed by the lab is that these came from a part of the overall Pit 16 Zone

A sample that had a higher concentration of fossil plant material and larger pieces of that plant material than typical for all Pit 16 Zone A sediments in aggregate. The presence of distinct organic accumulations, like the wood zone of 2004 Pit 13 (fig. 10D), indicates that the organic content of localized samples of sediment from different parts of the sinkhole could be fairly heterogeneous. Such small-scale variability in sediment organic content is likely eliminated in comparisons of large samples, as seen in the similar values obtained for Pit 16 and the SW Quadrant Zone A samples processed at IPFW.

All (or nearly all) sediment organic determinations are probably overestimates to some extent, owing to contamination by roots of modern plants that were growing in the sinkhole at the time our systematic excavations began in 2003. However, based on our visual assessment of the relative abundance of fossil fragments as opposed to clearly modern plant fragments in the sediment size fractions, we believe this overestimation to be minor.

Organic contents of PCS fossil plant materials determined by LOI (Table 6) were about 88 to 90 percent of oven-dry weights (ash contents of about 10 to 12 percent). Modern leaf, twig, and bark samples of tree genera that also occur in the PCS paleoflora yield LOI estimates of organic content of 84 to 98 percent (Table 7); modern wood has an ash content of only 0.4 to 2 percent dry weight (Misra and others, 1993; Miller, 1999). Modern aquatic macrophytes generally have an ash content of 5 to 25 percent dry weight (Westlake, 1965; Květ and others, 1998). These values differ only slightly from our results for PCS fossil plant material, suggesting that PCS plant fossils have retained most of their refractory organic constituents (presumably cellulose, hemicellulose, and lignin) (see Webster and Benfield, 1986).

The LOI-estimated carbonate content of the sand-sized PCS Zone A sediment was consistently higher for the 2005 Pit 16 sample than the 2003 SW Quadrant sample in all size fractions (Table 8). The 1-mm and 0.5-mm size fractions had substantially higher carbonate fractions than other size fractions, reaching values of 20 to 30 percent of the total weight of the sediment remaining after ashing to remove organic material. Carbonates thus made up at most about a quarter of the Zone A sand-sized fraction by weight in the samples we analyzed.

Table 6. Loss on ignition (LOI) determinations of organic content of fossil plant material from Pipe Creek Sinkhole Zone A fossiliferous sediment

Sample	Organic content (% dry weight)	Number of samples in batch
Wood fragments	88.5 (88.3–88.6)	3
	87.8 (87.5–88.1)	2
	90.4 (90.3–90.5)	2
Mixed plant fragments (wood, seeds, shoots/leaves)	87.9 (87.7–88.1)	6
	88.8 (88.4–89.1)	4
	87.7 (87.7–87.7)	2
	87.1 (86.7–87.5)	2
	86.4 (85.9–87.6)	5
Mixed plant fragments (excluding obvious wood)	88.8	1
	87.9 (87.6–88.3)	2
<i>Carya</i> pericarp	82.8	1

Sediment micromorphology and organic content

Zone A: In thin section (fig. 21), Zone A sediment is characterized by its dark, low-chroma (gleyed) color. This color primarily relates to the large amounts of organic matter present. The organic matter occurs in clasts of varying size, including large, >2 mm oblate disks that are usually aligned with highly macerated silt and presumably clay size components. Interestingly, most of the organic matter does not become excited under UV light, which indicates that the wood is altered, with lignin having been replaced by minerals such as iron-manganese (Fe/Mn) (fig. 21F), which likely indicates that our LOI determinations of sediment organic content somewhat underestimate the prediagenetic organic content. Another distinguishing characteristic of Zone A sediment is the large amount of well-rounded, coarse to fine sand-sized clasts composed of dominantly monocrystalline quartz, although some angular polycrystalline quartz and chert and other grains occur in low abundance.

The Zone A fabric appears to have quasi-laminated structure defined by variations in either grain size or organic matter, but the laminae are irregular, varying in size from a few millimeters to several centimeters, and in some cases these layers change thickness in a wedge shape across the width of the thin section (fig. 21B). The fabric is also characterized by abundant rounded clasts of reworked material of silt to pebble size; the reworked grains are supported by a matrix having the same composition (fig. 21A).

Zone A has large amounts of Fe/Mn globules and staining, as well as framboidal pyrite, but also contains small amounts of primary FeOOH accumulations; there seem to be FeOOH grains that were likely transported along with the other reworked peds. Although the unit includes very small amounts of illuviated clay (fig. 21E), it appears to have remained in reducing conditions with poor drainage throughout most of its history. There are some burrows with pendant coatings (fig. 21D), but no clear signs of rooting existed within this unit. Interestingly, there was one nodule composed of micritic carbonate that may either represent growth from precipitation of carbonate out of solution (fig. 21C), or alternatively a reworked lithoclast transported from the watershed into the sinkhole.

Zone C: This unit is dominantly composed of clastic or diagenetic sediment (or both) in the clay size fraction. The red sediment also includes large amounts of carbonate material and the carbonate fraction includes clasts derived from local bedrock as well as what appear to be calcite nodules that precipitated from CaCO_3 in solution. This unit also includes very rare fine silt-sized grains of quartz.

Zone C has two different fabric types (fig. 22). The first consists of large (average about 1 mm) cylindrical to blocky intraclasts that appear to represent reworked mudballs that are supported by interlaced angular clay matrix with the same composition as the intraclasts (fig. 22D). In addition, there is illuviated clay through the fabric; interestingly, some of

Table 7. Loss on ignition (LOI) determinations of organic content of tissues from modern tree species congeneric with some of the Pipe Creek Sinkhole fossil plant species

[Multiple determinations of some samples were done to assess analytical precision of ashing procedures.]

Species	Tissue	Organic content (% dry weight)	Number of samples in batch
<i>Fagus grandifolia</i> (American beech)	Leaves	95.1 (94.8–95.8)	3
	Twigs	92.6 (91.2–94.2)	3
	Bark	90.5 (90.2–91.1)	3
<i>Salix amygdaloides</i> (peachleaf willow)	Leaves	94.9 (94.7–95.1)	3
	Twigs	97.2 (95.9–99.1)	3
	Bark	84.0 (83.8–84.4)	3
<i>Platanus occidentalis</i> (sycamore)	Leaves	91.3 (91.2–91.3)	3
		89.9 (89.8–90.0)	3
		89.9 (89.9–90.0)	2
		89.9 (89.8–90.0)	5
		90.4 (90.3–90.5)*	3
	Twigs	96.2 (95.6–96.9)	3
Bark	91.2 (91.2–91.3)	3	
<i>Populus deltoides</i> (eastern cottonwood)	Leaves	86.5 (86.2–86.7)	3
	Twigs	92.5 (91.5–93.7)	3
	Bark	90.3 (89.8–90.6)	3
<i>Acer saccharum</i> (sugar maple)	Leaves	91.3 (91.0–91.6)	3
	Twigs	93.7 (93.0–94.4)	3
	Bark	86.3 (85.8–86.9)	3
<i>Carya glabra</i> (pignut hickory)	Leaves	92.2 (92.1–92.3)	3
	Twigs	93.0 (92.5–93.8)	3
	Bark	90.9 (90.5–91.2)	3
<i>Pinus strobus</i> (white pine)	Needles	97.3 (97.3–97.4)	6
		98.3 (97.7–98.8)	6
	Bark	97.3 (97.3–97.3) [†]	4
		97.0 (96.9–97.1)	5
		96.2 (96.1–96.3)	2

*Sample dried at 80°C rather than 110°C, and combusted overnight at 550°C.

[†]Sample dried at 110°C and combusted overnight at 500°C.

this translocated clay is yellow and appears identical to Zone B material (see p. 45) (fig. 22E). The second fabric type is a more homogeneous mixture of typical Zone C red clay and yellow clay of Zone B aspect, giving it an overall red/brown color in hand sample and thin section analysis. This second, homogeneous Zone C sediment has abundant root traces (with framboidal pyrite overprint-

ing the infilled root structures) (fig. 22A), whereas the first fabric type shows no evidence of rooting.

Other features of Zone C include abundant Fe/Mn staining, nodules, FeOOH staining, and illuviated clay, which suggest that the sediments experienced periods of reducing conditions as well as oxidizing conditions with free drainage. Little organic mat-

Table 8. Carbonate content of Pipe Creek Sinkhole Zone A sediment size fraction concentrates as determined by LOI

[See text for details of the different LOI protocols. Each line within a sample represents a different batch of replicates; the number of determinations for each sample in a batch ranged from one to six.]

Sample	Size fraction	Protocol	Carbonate content (% ashed dry weight; mean [range])	No. of samples in batch
SW Quadrant Zone A 6/20/03	2 mm	1	4.07 (3.83–4.25)	3
Pit 16 Zone A August 2005	2 mm	1	11.7 (11.6–11.9)	3
		3	11.7	1
SW Quadrant Zone A 6/20/03	1 mm	1	8.71 (7.83–9.31)	3
Pit 16 Zone A August 2005	1 mm	1	23.2 (22.8–23.8)	3
			23.8 (23.7–23.8)	3
		2	23.0 (22.7–23.3)	6
		3	18.1	1
			28.5	1
25.6	1			
SW Quadrant Zone A 6/20/03	0.5 mm	1	7.85 (7.70–8.07)	3
Pit 16 Zone A August 2005	0.5 mm	1	21.8 (21.6–21.9)	3
		3	16.0	1
			25.8	1
			26.5	1
SW Quadrant Zone A 6/20/03	0.25 mm	1	3.23 (3.11–3.37)	3
Pit 16 Zone A August 2005	0.25 mm	1	6.68 (6.65–6.72)	3
		3	7.36	1
			8.18	1
			8.66 (8.60–8.73)	2
SW Quadrant Zone A 6/20/03	0.125 mm	1	3.92 (3.85–3.40)	3
Pit 16 Zone A August 2005	0.125 mm	1	6.32 (6.29–6.33)	3
		3	5.38	1
			8.93	1
SW Quadrant Zone A 6/20/03	0.063 mm	1	6.07 (5.85–6.36)	3
			6.51 (6.22–7.01)	3
		2	6.80 (6.74–6.89)	3
Pit 16 Zone A August 2005	0.063 mm	1	11.2 (11.6–11.8)	3
		3	9.29	1
			9.21	1

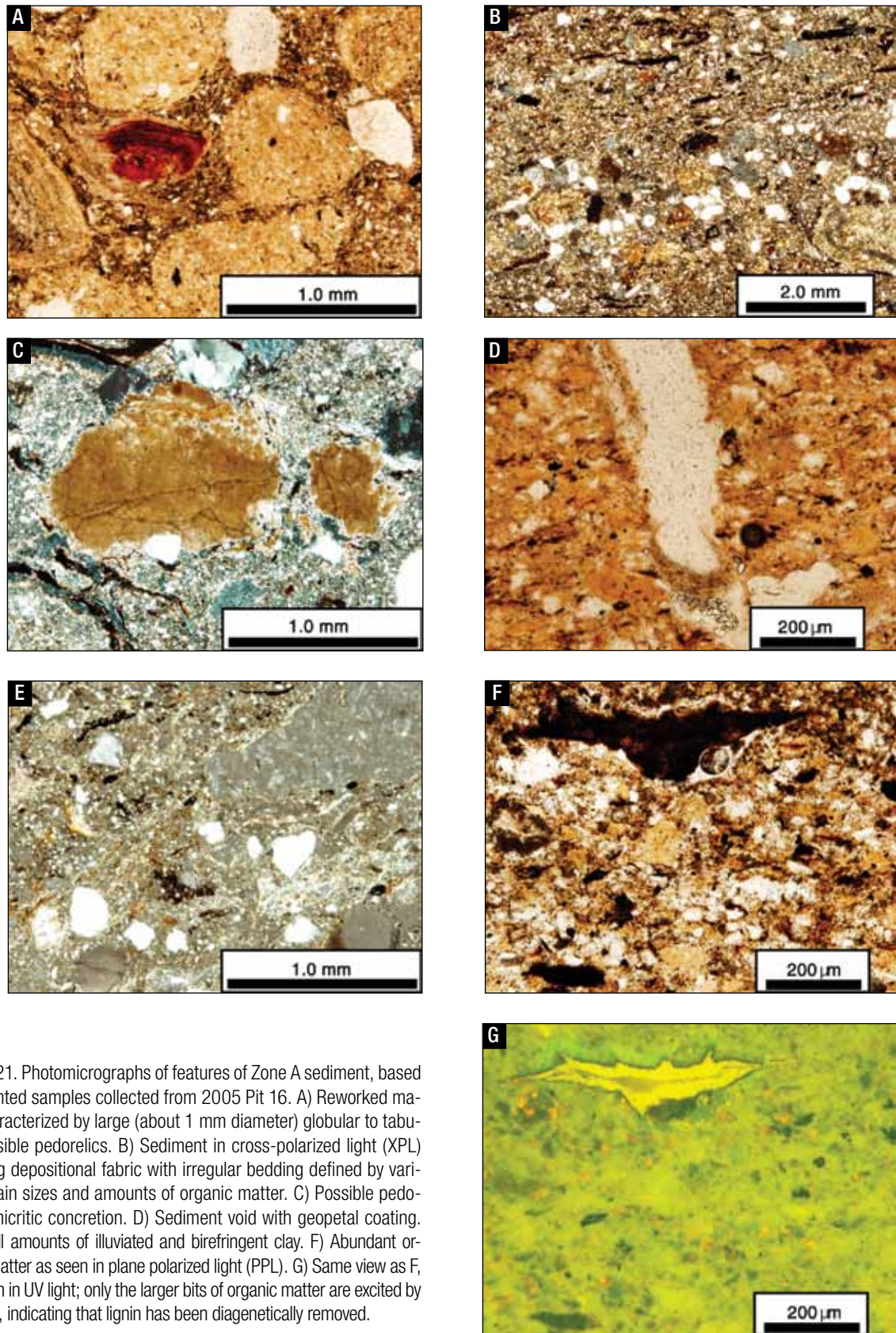


Figure 21. Photomicrographs of features of Zone A sediment, based on oriented samples collected from 2005 Pit 16. A) Reworked matrix characterized by large (about 1 mm diameter) globular to tabular possible pedorelics. B) Sediment in cross-polarized light (XPL) showing depositional fabric with irregular bedding defined by variable grain sizes and amounts of organic matter. C) Possible pedogenic micritic concretion. D) Sediment void with geopetal coating. E) Small amounts of illuviated and birefringent clay. F) Abundant organic matter as seen in plane polarized light (PPL). G) Same view as F, but seen in UV light; only the larger bits of organic matter are excited by UV light, indicating that lignin has been diagenetically removed.

ter is preserved within this unit, but there are infilled voids composed of high amounts of calcite, yellow-colored illuviated clay, and Fe/Mn, which appear to have been vertical flow paths that collected translocated material.

Zone B: This yellowish unit (fig. 23) is similar to Zone C in being composed almost exclusively of clay-size sediment. There are, however, slight amounts of carbonate material precipitated from solution and clasts derived from the host rock, but the carbonate appears to be a smaller component as compared to Zone C (although this observation could be an artifact of sampling). Zone B unit seems to have slightly more quartz silt grains in the matrix, but this clastic fraction remains a small component of the total sediment fabric.

The Zone B fabric is much more homogenous than that of Zone C and lacks the intraclasts and interlaced angular clay orientations observed within the red unit. Portions of Zone B sediment were deposited in a linear (beddinglike) pattern that strongly suggests that these sediments were water-lain (fig. 23B). Interestingly, there are areas along the transition between Zones B and C with intraclasts that are half red and half yellow, indicating that the yellow color results from alteration of the red sediment (fig. 22E). Furthermore, roots are common where this mixing occurs. Zone B also shows angular cracks that seem to have functioned as transportation conduits for water, resulting in the formation of dark hypocoatings and, in some cases, illuviated clay in association with these voids. This indicates that this unit was freely drained at some time during its history.

Zone B sediments also contain abundant Fe/Mn and silt-sized framboidal pyrite grains that overprint root structures; this feature in combination with the FeOOH staining indicate that these sediments were alternately oxidized and reduced (fig. 23A). The abundant root traces are cryptic in hand samples and under magnification, unless viewed in cross-polarized light to reveal their birefringent clay infillings or observed under UV light to expose the small amount of organic debris that remains in the structure (fig. 23F). Zone B also has burrows (fig. 23C) that may be infilled with clay and lignin.

Siderite morphology and geochemistry

Nodule morphology: The siderite cement in PCS nodules occurs in two distinct morphologies. The dominant morphology comprises homogeneous masses of equant microcrystalline siderite with crystal dimensions of a few tens of microns (fig. 24A, B). Cemented masses of siderite with this morphology engulf all components of the deposit, including vertebrate bone, quartz sand, mudstone intraclasts, pisolites with clay coatings on mudstone intraclasts (fig. 24C, D), and limestone clasts from the local Silurian bedrock. The microcrystalline siderite is very dark brown with inclusions of the hosting fine-grained sediment, probably mainly clay minerals. This siderite morphology is very similar to that described from reducing hydromorphic paleosols in the Cretaceous Nanushuk Formation of North Slope, Alaska (Ufnar and others, 2004a).

A secondary morphology of siderite is as void-filling spherulites. These crystalline aggregates display sweeping pseudo-uniaxial cross-extinction patterns under cross-polarized light (fig. 24F), and have larger dimensions than the microcrystalline siderite crystals, with diameters of several hundreds of microns (fig. 24E, F). They are also free of inclusions, suggesting that they filled open space in the sediment as void-filling cements. In pedogenic contexts, this siderite morphology has been referred to as sphaerosiderite, and it has been widely described from paleosols in coal-bearing sedimentary strata (McCarthy and Flint, 1998; Driese and Ober, 2005; Ufnar and others, 2005). Sphaerosiderite has also been noted as a minor morphologic component in the hydromorphic paleosols of the Cretaceous Nanushuk Formation (Ufnar and others, 2004a).

Carbon and oxygen isotopic geochemistry: Carbon and oxygen isotopic values from the PCS nodule hand sample plot within a very narrow range, with $\delta^{13}\text{C}$ values ranging between -11.2 to -10.2‰ Vienna Pee Dee Belemnite standard (VPDB), and $\delta^{18}\text{O}$ values ranging between -2.6 to -2.1‰ VPDB (fig. 25). The invariant $\delta^{18}\text{O}$ values, and the slightly larger range of $\delta^{13}\text{C}$ values indicates that these data are arrayed along a meteoric sphaerosiderite line (or MSL; in the sense of Ludwigson and others, 1998) having a $\delta^{18}\text{O}$ value of $-2.4 \pm 0.1\%$ VPDB. This term refers to a diagenetic trend specific to freshwater siderites that records the formation of

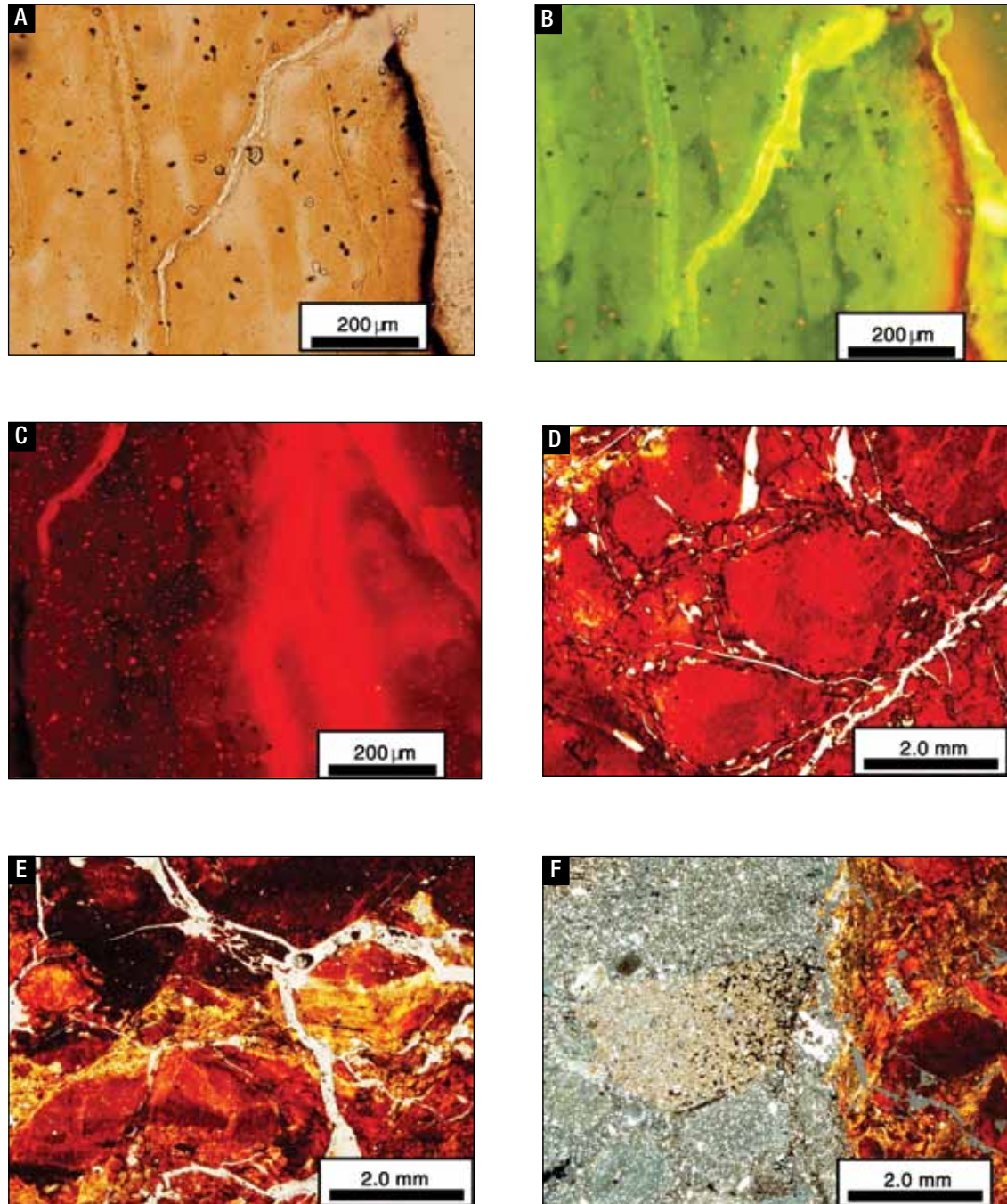


Figure 22. Photomicrographs of features of Zone C sediment. A) Homogeneous red/brown depositional fabric of the sediment seen in plane polarized light, but with a cryptic root structure. B) Same as A, but in UV-NB (narrow blue cube filter) light, which makes the root structure more readily visible. C) A different, larger root structure seen in UV-TR (Texas Red filter) light. D) One of the typical Zone C sediment fabrics: Very coarse, sand-sized pedoclasts are supported in a matrix composed of the same material, but of silty-clay size. E) Area of illuviated yellow clay cutting across large pedoclasts. Note apparent alteration of pedoclast color from red to yellow. F) Sharp contact between red Zone C material (right) and black Zone A material (left) in a section that may show soft sediment deformation, with injection of a plume of Zone A material into Zone C (see fig. 13A).

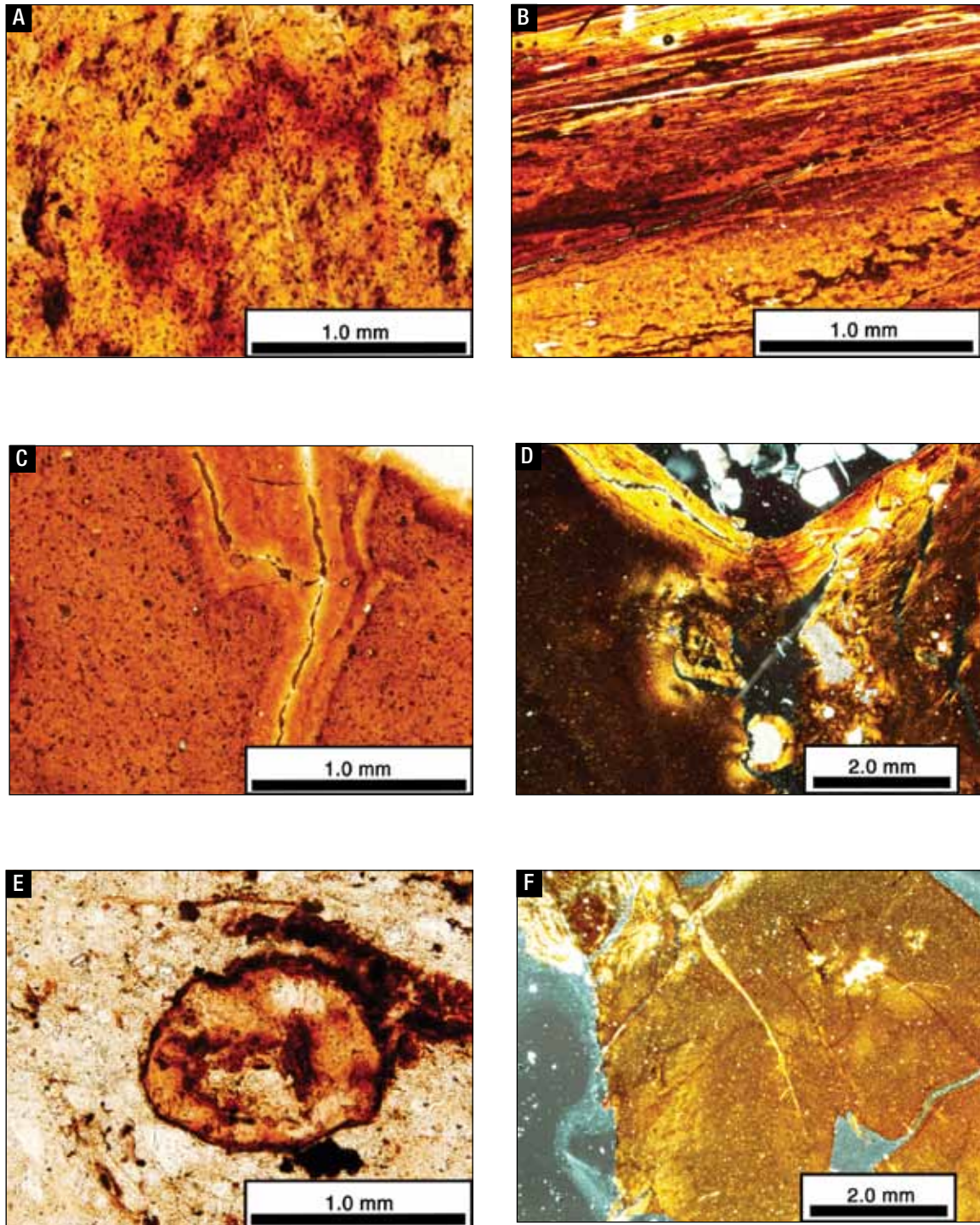


Figure 23. Photomicrographs of features of Zone B sediment. A) Fine-grained, homogeneous matrix fabric stained with Fe/Mn that has also formed globular structures. B) Laminar alignment of clays at a submillimeter scale. C) Structure showing evidence of burrowing and backfilling; note lack of Fe/Mn within the infilling, suggesting that backfilling occurred under oxidizing conditions. D) Meniscus geopetal pendant coating of a void in cross-polarized light that likely transmitted water vertically through Zone B. E) Cross section through a root structure coated with Fe/Mn. F) Well-developed root structure in cross-polarized light, with microhairs extending from the root structure and backfilling of illuviated clay.

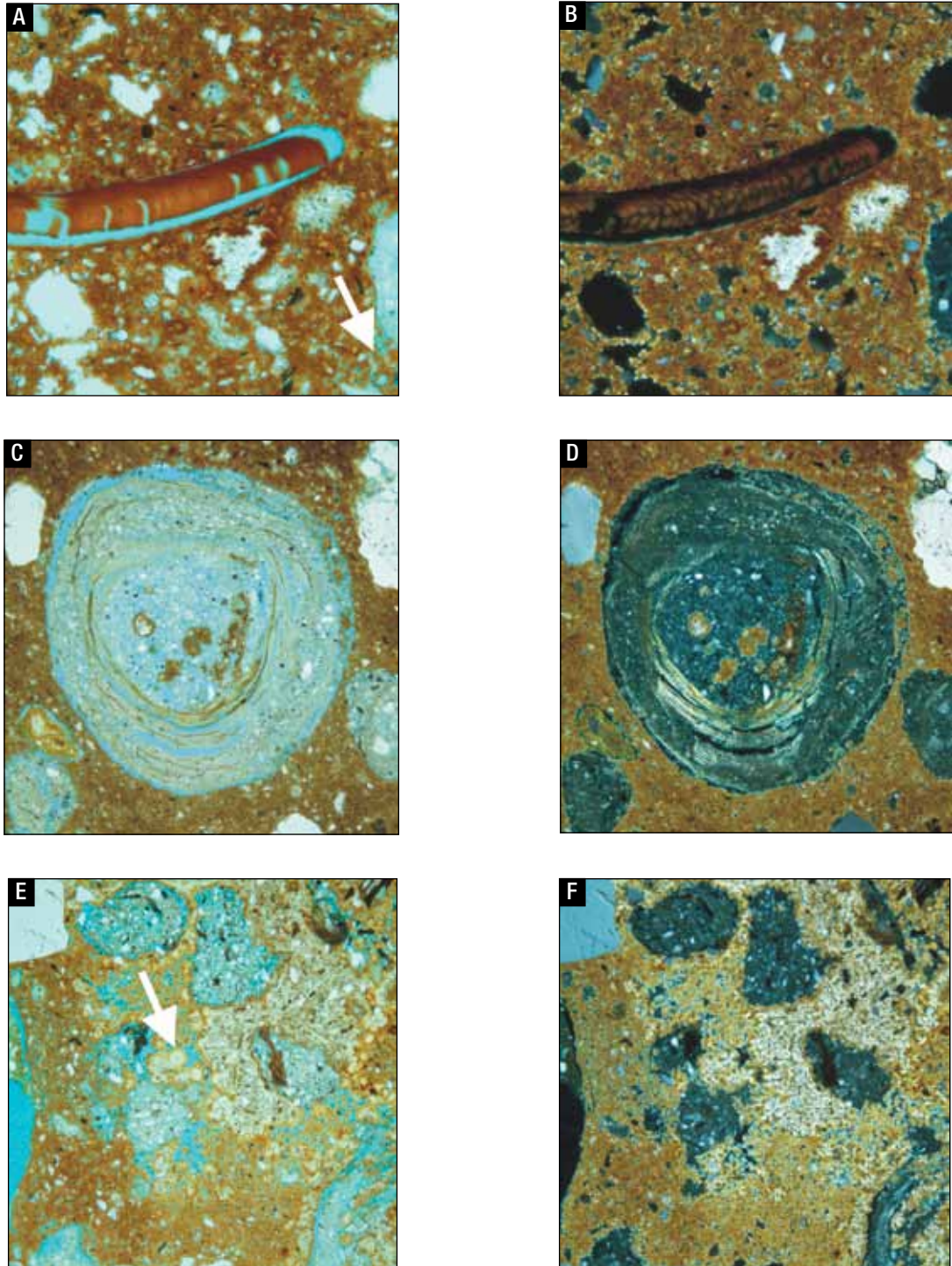


Figure 24. Photomicrographs of siderite morphologies from Pipe Creek Sinkhole Zone A nodules. A) Microcrystalline siderite engulfing a phosphatic vertebrate fossil, quartz sand and silt grains, and siliclastic mudstone intraclasts. White arrow points to single anhedral siderite crystal a few tens of microns in diameter. Pore space is filled by blue-dyed epoxide resin. PPL (plane polarized light); field of view is 0.62 mm. B) Same field of view in XPL (cross polarized light). C) Pisolite of laminated birefringent clay coating a siliclastic mudstone intraclast. Birefringent brown siderite overprints part of the mudstone intraclast and laminated coating. PPL; field of view 1.25 mm. D) Same field of view in XPL. E) Clear siderite spherulites (white arrow) engulfing siliclastic mudstone intraclasts, surrounded by darker, more inclusion-rich microcrystalline siderite cements. PPL; field of view 6.24 mm. F) Same field of view in XPL. Note pseudo-uniaxial cross extinction patterns in spherulites.

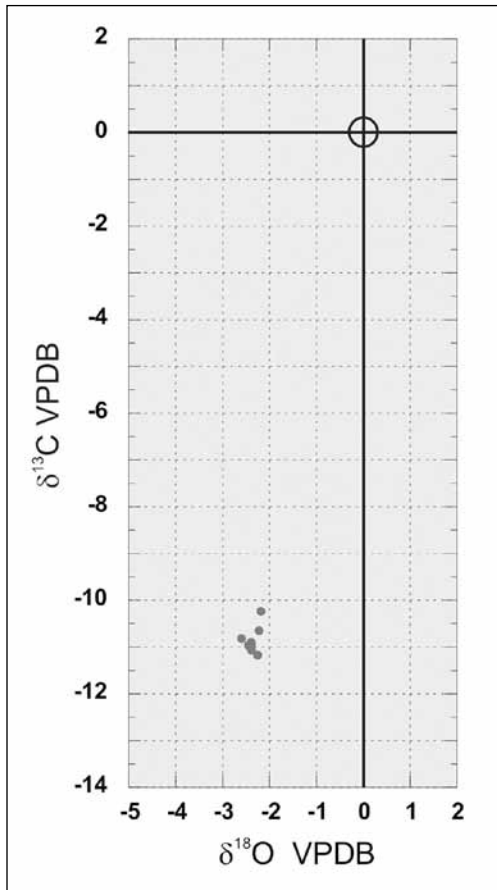


Figure 25. Carbon and oxygen isotope plot from Pipe Creek Sinkhole Zone A siderites. Values are in per mil deviations from the Vienna Peedee Belemnite (VPDB) carbonate standard. The data are arrayed along a meteoric sphaerosiderite line trend with a $\delta^{18}\text{O} = -2.4 \pm 0.1$ per mil VPDB.

authigenic siderite in shallow reducing groundwater below the sediment-water interface. The MSL value integrates the time-averaged $\delta^{18}\text{O}$ value of infiltrating groundwater, and the mean annual temperature of the near-surface sediments (Ludvigson and others, 1998). MSL values have been used in paleohydrologic and paleoclimatic reconstructions to estimate the time-averaged $\delta^{18}\text{O}$ values of paleoprecipitation (Ufnar and others, 2002, 2004b). MSL values determined from specific stratigraphic intervals in the PCS deposit, when integrated with $\delta^{18}\text{O}$ values from coeval paleohydrologic proxies from aquatic vertebrate materials in the deposit, have the potential to yield mineral-pair paleotemperature estimates.

DISCUSSION

Age and history of the Pipe Creek Sinkhole

To a first approximation, the disposition of sedimentary beds that remained in situ in the sinkhole was very simple: fossiliferous, organic-rich, dark-colored Zone A sediment overlay sparsely fossiliferous, brown Zone B sediments, which in turn overlay unfossiliferous red Zone C clay. Zone C clay overlay, surrounded, and coated numerous limestone boulders. Many limestone boulders have large patches of multigeneration calcite crystals on their surfaces.

Because we were unable, using either heavy machinery or human labor, to reach bedrock at the bottom of the sinkhole, we do not know how far beneath the surface Zone C extends. Consequently, we cannot say whether the PCS originated as a collapse or a subsidence doline (White, 1988), although we suspect the former. In any case, the chaotically arranged limestone boulders found in Zone C and even overlying sediments are probably breakdown from the creation of the sinkhole.

At some point in the early history of the Pipe Creek Sinkhole, perhaps more than once, prior to its actually becoming a doline, we think that what would become the PCS was a water-filled cave passage. Our reason for this inference is the presence of large solution grooves in limestone bedrock parallel to bedding, which can be seen both on one of the remaining walls of the sinkhole and on some of the breakdown boulders within the doline (fig. 7D). We have seen similar solution sculpturing in the walls of modern caves. The calcite crystals lining many of the breakdown boulders may also have formed, at least in part, while the cave was filled with water:

"Some caves flooded with calcite-supersaturated water...have crystal linings...Conditions under which crystal-lined caves can develop are very restricted. The water must become highly supersaturated to develop large massive crystals and yet must be sufficiently free of impurities to allow individual calcite crystals to develop without interruption" (White, 1988, p. 257).

However, the PCS calcite crystals show several generations of growth, implying a complex history of development that may reflect changes in paleoclimatic conditions over the long life of the sinkhole.

Along with breakdown boulders, Zone C red clays were the first sediments to be deposited in the sinkhole, and very likely in the cave from which it developed. Red clays are commonly associated with karst (see McGrain, 1947; Deike, 1960; Hall, 1976; Olson and others, 1980; Young, 1986; Mizota and others, 1988; Moresi and Mongelli, 1988; Durn and others, 2001; Tsatskin and Gendler, 2002; Durn, 2003; Foster and others, 2004; Merino and Bannerjee, 2008) and the origin of such clays, whether as residuum from the limestones themselves, as a product of chemical weathering of nearby rocks other than the limestones, or as a material that itself creates the karst with which it is associated, has been much debated.

While some of the Zone C clays may be autochthonous to the sinkhole, we suspect that the bulk of this unit represents products of chemical weathering outside the doline itself (Argast and Farlow, this volume) that were transported into the sinkhole, in large part while it was still a cave. The general rarity of clasts larger than silt (other than pieces of limestone and isolated calcite crystals) and organic matter in Zone C suggest that the site was largely closed to the surface during much of the deposition of this unit. The depositional fabric of much of Zone C is composed of abundant reworked material having the same composition as the rest of the unit. Because the reworked clasts would have been vulnerable to destruction during transport, they likely originated on the landscape very near the site of the cave. On a larger scale, evidence for transport of the red clay can be seen in the association of saprolitic strings with Zone C; in some cases the strings showed complicated swirls, suggesting transport in a mudflow.

Zone B material is similar to Zone C red clay in mineralogy. Fossils do occur here, but not commonly, and as in Zone C there is little organic matter. Unlike Zone C, Zone B clay does not have reworked pedoclasts, but does show fine laminae, suggesting deposition by water. The abundance of root structures, burrows, and illuviated clay with meniscae indicate that Zone B underwent subaerial exposure and at least modest pedogenesis, and the occurrence of portions of Zone C that were partially altered from red to yellow suggests that Zone B represents the end product of alteration of Zone C clay. All this suggests that Zone B was a soil (Shunk and others, 2009), and that by the time of its deposition the sinkhole was open to sunlight, making plant growth possible.

Zone A clays are mineralogically like those of Zones B and C (Argast and Farlow, this volume), but Zone A is characterized by large numbers of plant fossils and thus large amounts of organic matter, and a higher (but still low) content of coarse clastic sediments. The dark gleyed color of Zone A, the presence of large amounts of Fe/Mn and framboidal pyrite in the sediment, the common occurrence of siderite both in nodules and as permineralizing material in fossil bone (Farlow and Argast, 2006), and stable isotope geochemistry indicate waterlogged, alkaline, stagnant (reducing) conditions within Zone A sediments (see Coleman and Roberts, 2000; Retallack, 2001; as well as Shunk and others, 2006, for laminated organic-rich lacustrine sediments at the Gray Fossil Site), and the abundant fossils of wetland and aquatic plants and animals in the paleobiota (Farlow and others, 2001) further suggest that Zone A sediments accumulated in a wetland that at one or more times was a pond. As with Zone C clays, Zone A fabric shows signs of reworked pedoclasts. Consequently much Zone A material represents continued input of fine-grained sediment from the surrounding landscape. Although laminations consistent with sediment deposition in water can be seen in places, for the most part Zone A is poorly sorted. Continued colluvial input as mudflows may account for this (see Vallance and Scott, 1997; Potter and others, 2005); another possibility is bioturbation by large animals as they waded through the pond.

Unfortunately, as seen in several of our sections, the downward Zone A/Zone B/Zone C sequence is not always uniform or straightforward. In several places we observed downward sagging of sinkhole sediments into downward drainage conduits between breakdown boulders (for example, figs. 6, 7C, 8, 9A, and 10B), either under their own weight (possibly in response to dissolution of underlying limestone?) or that of overlying sediments (or even Pleistocene glaciers?). The interpretation of these features seems rather straightforward.

More complicated is the fact that the downward vertical sequence of Zone A/Zone B/Zone C is not what is invariably seen in the doline. In some places Zone B is absent, and Zone A directly overlies Zone C, or Zones A and C interpenetrate each other (figs. 13A and 22F). In several sections, observed sediments seem to be mixtures of the three zones. Conceivably these observations could also be related to bioturbation, or soft-sediment deformation because of a heavy overburden, or perhaps very

localized (centimeter- to meter-scale) variation in environmental conditions during sediment deposition or diagenesis (see Potter and others, 2005).

The most puzzling field observation is the mixing in places of the atypical, lithologically heterogeneous gravels with typical sinkhole sediment, particularly where such mixtures seem to be in proper stratigraphic sequence (figs. 11 and 12A). Such mixing does not invariably occur in our sediment sections, but seems to typify only some of them. Note, for example, the roughly order-of-magnitude greater amount of coarse clastic material in Zone A sediments from Pit 2 Zone A1 than Zone A sediments from other parts of the sinkhole (Table 2).

The origin of the heterogeneous pebbles is uncertain. Some of them appear to be faceted (fig. 20B), so one possibility is that they are glacial in origin. If the heterogeneous pebbles (and associated sand) are of glacial origin, then the fact that they occur intermixed with typical Zone A sediments suggests the possibility that the biostratigraphically determined late Miocene or early Pliocene age of the PCS mammalian fauna (Farlow and others, 2001; Martin and others, 2002; Bell and others, 2004) notwithstanding, the fossiliferous deposit, is in fact of Pleistocene (presumably interglacial) age. We think this highly unlikely. Had there been a significant input of glacial sediment at the time Zones A, B, and C were deposited, we would have expected to see a substantial component of quartz in the clay mineralogy of these units, as rock flour.

Most of the heterogeneous gravels are well rounded, so an alternative hypothesis is that they are of fluvial origin. The rounded quartzite pebbles (some of which are quite large) that are so common in Zone A sediment are unlike anything seen in the local bedrock, and so had to have been transported into the state from a considerable distance away by a large river(s). Rivers big enough to do this might also have collected other kinds of large, exotic clasts from distant external sources.

Whatever their nature, the heterogeneous gravels, unlike the ubiquitous quartzite pebbles, probably postdate typical Zone A sediments. We have sectioned many of the sideritic nodules that are so common in Zone A. Although we frequently find the quartzite pebbles and pieces of locally derived bedrock, as well as plant and vertebrate fossils, in such sections through the nodules (just as they abundantly co-occur in unconsolidated Zone A

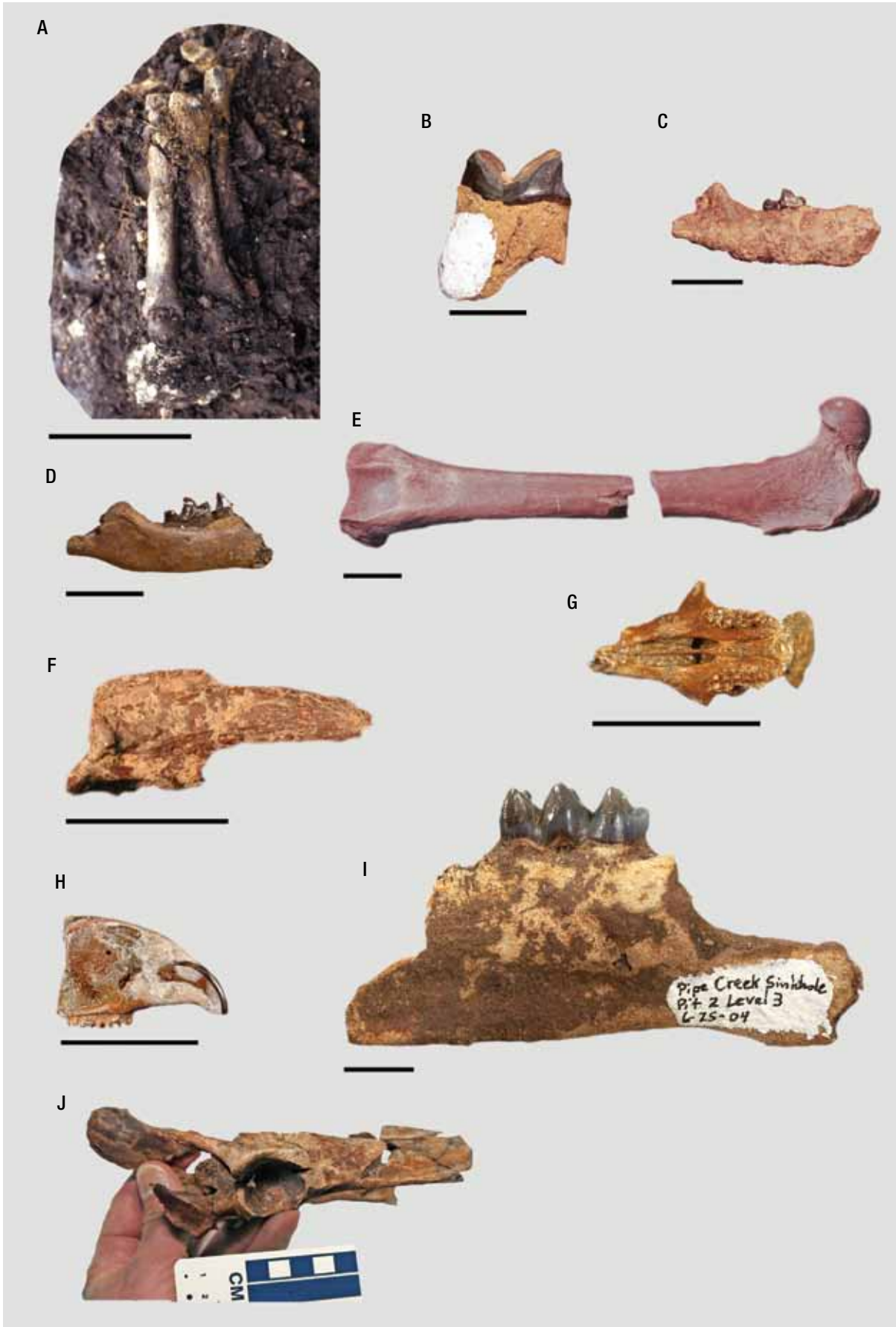
sediment), we have never found any of the heterogeneous gravels in the nodules.

An admittedly ad hoc hypothesis to account for intermixing in some places of the younger heterogeneous gravels and sand with typical Zone A sediments is that the former were deposited immediately adjacent to, as well as above, the pond sediments (possibly even cutting across the latter). If a doline drainage conduit were to develop beneath the spot where the typical Zone A sediments and the heterogeneous gravels were in immediate contact, then if they slowly sagged into the conduit they might mix in a manner like that seen in the west wall of 2004 Trench 2 (fig. 12A). Regardless of whether this specific hypothesis accounts for our field observations, postdepositional disturbance of microstratigraphic sequences in caves and sinkholes is not unusual (Sutcliffe and others, 1976).

The likelihood that the heterogeneous gravels postdate typical Zone A, B, and C sediments raises the possibility that fossils of later age, even as late as Pleistocene, could similarly have been mixed with older taxa through reworking of the latter. However, the chemical similarity of preservation of the vertebrate fossils (Farlow and Argast, 2006), and the routine occurrence of typical PCS plant and animal fossils within the siderite nodules, together suggest that the paleobiota represents a single rather than a temporally mixed assemblage.

Our confidence in our interpretation of the age of the fossil assemblage as late Hemphillian (Farlow and others, 2001; Martin and others, 2002) or possibly early Blancan (Bell and others, 2004), without any later addition of Pleistocene forms, is bolstered by the fact that new mammalian taxa confirmed or discovered during the present phase of the project (fig. 26) are consistent with a late Neogene age. The skunk *Buisonictis* ranges throughout the Pliocene (Baskin, 1998). *Felis* (or *Lynx*) *rexroadensis* ranges from Late Hemphillian through Blancan (Martin, 1998). The stratigraphic range of the beaver *Dipoides* is Hemphillian-Blancan (Korth, 1994). The hare *Hypolagus* ranges from the Barstovian through the Blancan in North America (Dawson and others, 2008).

Even so, the co-occurrence of some of the rodent taxa (*Ogmodontomys*, *Symmetrodontomys*, *Pliophenacomys*, and *Geomys*) with the rhinoceros *Teleoceras* is unusual (Martin and others, 2002; Bell and others, 2004). Although it is unlikely that there is mixing of Neogene and Pleistocene taxa in the



PCS fauna, at present we cannot exclude the possibility of mixing of late Hemphillian with early Blancan taxa, even though, as indicated above, we think it more likely that we are dealing with a single fauna. The temporal difference between classic late Hemphillian and early Blancan faunas would be short enough that it would not be astonishing if some mammalian taxa characteristic of the two intervals had actually coexisted in a fauna from a previously unsampled region of late Neogene North America. Our interpretation that the PCS vertebrate assemblage is not a temporally mixed fauna could be tested by comparing the rare earth element signatures of bones of different mammalian taxa in the PCS assemblage for consistency (see Trueman and Benton, 1997; Trueman, 1999, 2007; Trueman and others, 2006; MacFadden and others, 2007; Suarez and others, 2007), but that is beyond the scope of the present paper.

Anthony and Granger (2004, 2006) dated the inception of cave systems along the Cumberland Plateau at 5 to 6 Ma. This is close enough to our estimated age of the PCS to suggest that creation of our doline may have been part of events affecting much of eastern North America.

Paleoenvironmental and taphonomic interpretations

Taphonomic interpretations of the PCS paleobiota are necessarily preliminary, pending detailed description of the various components of the flora and fauna. However, several generalizations seem warranted.

PCS plant macrofossils and palynomorphs include both aquatic/wetland and nonwetland taxa (Farrow and others, 2001; Shunk and others, 2009). The palynomorph assemblage is dominated by pine, freshwater algae, and hickory, and considerably lesser amounts of nonaquatic herbaceous plants;

pollen typical of dense forests is conspicuously absent (Shunk and others, 2009).

Aquatic/wetland plant taxa presumably were members of the biological community that lived in or on the margins of the pond or wetland (or both) in which Zone A sediments accumulated. Macrofossil fragments of non-wetland taxa, such as trees, could have been carried into the sinkhole from the surrounding environment by the same processes that we hypothesize to be responsible for transport of isolated vertebrate bones into the doline. However, dense concentrations of plant material like that of the 2004 Pit 13 wood layer (fig. 10D) seem more likely to have accumulated directly in situ in the pond, because they are not thoroughly intermixed with inorganic sediment. If not growing in the sinkhole wetland, such plants presumably grew immediately nearby.

Decomposition of dead vascular plants in freshwater environments begins soon after such debris falls into the water (Webster and Benfield, 1986). Leaves lose significant amounts of soluble organic substances within a day, and are quickly attacked by aquatic fungi and bacteria. Microbial attack softens leaves, making them more susceptible to mechanical disintegration, and microbial processing of leaves makes them more attractive to leaf-shredding benthic invertebrates. Woody tissues break down much more slowly than leaves, and so are considerably more likely to be preserved as fossils.

Large quantities of wood and other plant detritus accumulating in the PCS pond presumably lowered oxygen levels in Zone A sediments, contributing to their own preservation in those water-logged sediments by retarding microbial activity (Retallack, 2001). The circumstances of preservation of plant fossils in Zone A sediments would have been similar to what occurs in modern poorly drained backswamp deposits of the Mississippi River:

Figure 26 (opposite page). Photographs showing samples of new fossil mammal specimens found during field and laboratory work, 2003–present. Scale bar = 1 cm except where otherwise indicated. A) Foot of the canid *Borophagus* preserved in partial articulation, Balk of Zone A material between SW Quadrant and SW Quadrant 2, 2003. B) Carnassial tooth of a felid, probably *Felis* cf. *F. rexroadensis* found in SW Quadrant Zone A1 Balk, 2003. C–D) Partial mandibles of the skunk *Buisnictis* from: C) SE Trench, Zone A Disturbed, 2004; D) Spoil Pile. Specimens in A–D identified by S. Tucker (written commun., 2006). E) Femur (SW Quadrant Zone A1 Balk, 2003) of a badger. F) Ungual phalanx (SW Quadrant Zone A, 2003) of a badger (not necessarily the same individual as in E). G) Palatal view; and H) right lateral view of an upper muzzle of the mouse *Symmetrodontomys daamsi* (a species presently known only from Pipe Creek Sinkhole, and described on the basis of less complete material by Martin and others, 2002), SE Trench, West Wall Scrapings, 2004. I) Partial peccary mandible, Pit 2, Level 2, 2004. J) Partial pelvis of a medium-sized ?ungulate (?deer), Pit 15, Zone A1 above the wood layer, 2004. Scale bar marked off in 1-cm increments.

“deposits laid down under such conditions generally consist of highly organic black clays with occasional thin laminations of silt introduced by floods. Woody peat beds are usually intercalated randomly throughout the sequence, but rarely attain considerable thickness. Large wood fragments and laminations consisting of compressed leaves, twigs and seeds are common.... Upon burial, free oxygen is quickly exhausted but anaerobic bacteria continue the work of destruction and modification. Water stagnation however, results in more rapid concentration of the humic derivatives and high toxicity soon develops and decay is arrested. A high rate of organic accumulation leads to arresting decomposition at a very shallow depth in the accumulating deposit and large portions of the original organic fraction survive to be preserved...it can generally be stated that the floral remains represent the local vegetation growing in such an environment” (Coleman and Roberts, 2000, p. 60).

The muddy sediments from Chaguite Creek in Costa Rica (Table 5) indicate that the sediment organic content in such settings can be a sizeable fraction of sediment dry weight.

Poorly drained backswamp deposits of the modern Mississippi River are similar to PCS Zone A sediment in a second way, in the relative abundance of some microfloral constituents. Charophytes are common in both and diatoms uncommon or absent in both (Coleman and Roberts, 2000; Farlow and others, 2001).

If low oxygen levels characterized pond water and sediment pore water, the abundance of benthic detritivores may have been reduced, further increasing the chances of preservation of plant remains. At least occasional periods of stagnant water in the PCS pond (Shunk and others, 2009) might explain the absence or rarity of large molluscs in the PCS paleofauna (Farlow and others, 2001), yet another feature in which Zone A sediments are similar to poorly drained backswamp deposits of the modern Mississippi River (Coleman and Roberts, 2000). Unlike the latter, however, the PCS ostracode assemblage was fairly diverse (Farlow and others, 2001).

Stable carbon isotope ratios of PCS wood suggest that the trees were growing under slightly water-stressed conditions, an interpretation reinforced

by the presence of burned plant fragments in Zone A sediment (Shunk and others, 2009). Combined with the composition of the palynoflora (Shunk and others, 2009), and some of the vertebrate taxa (Farlow and others, 2001), these observations suggest that the paleocommunity around the PCS was an open woodland or savanna situation as opposed to a closed canopy forest (Farlow and others, 2001; Shunk and others, 2009).

The dominance of aquatic and wetland taxa in the PCS small vertebrate assemblage suggests that it is composed mostly of animals that lived in or close to the presumed PCS pond. Although they obviously have no vertebrate taxa in common with the PCS, Late Cretaceous (Judith River and Two Medicine Formations of Montana) floodplain pond vertebrate microfossil assemblages are likewise dominated by small bones of both aquatic and terrestrial forms. The Late Cretaceous microvertebrates are disarticulated, dissociated, and dispersed through an organic-rich sedimentary layer (Rogers and Kidwell, 2007). Because most PCS microvertebrate and mesovertebrate specimens (for example, frogs, snakes, small mammals) were collected by screen-washing, the degree of articulation and completeness of individual skeletons is unknown. However, the PCS bonebed definitely resembles the far older Late Cretaceous pond bonebeds in occurring in organic-rich sediments. Unlike most vertebrate microsites, however (Eberth and others, 2007), the PCS microvertebrate assemblage probably accumulated *in situ* rather than as a transported assemblage.

From the standpoint of vertebrate taphonomy, PCS Zone A can be characterized as a bonebed, because it is a localized concentration of vertebrate hard parts (Behrensmeier, 2007; Rogers and Kidwell, 2007). Eberth and others (2007) characterized the PCS vertebrate assemblage as a mixed (in the sense of including significant numbers of both vertebrate macrofossils and microfossils), multitaxic, multidominant (in the sense that two or more taxa constitute 50 percent or more of the specimens, in terms of number of identifiable specimens or minimum number of individuals) bonebed. Although a quantitative analysis of the relative abundance of PCS vertebrate specimens cannot be done until all Zone A samples have been screened, and all bones identified (which will likely take many years), our impression is that the PCS bonebed will turn out to be better characterized (following the classification of Eberth and others, 2007) as a microfossil-



Figure 27. Reconstruction of the Pipe Creek Sinkhole. A rhinoceros (*Teleoceras*) confronts a pack of canids (*Borophagus*) feeding on the carcass of a peccary, while a bear (*Plionarctos*) lazily watches the drama, and frightened turtles and a frog scramble into the water for safety. Painting by paleoartist Karen Carr; used by permission of the Indiana State Museum.

sil (where 75 percent or more of identifiable bones are less than 5 cm in maximum dimension), multitaxic but monodominant bonebed (with leopard frogs likely making up 50 percent or more of vertebrate specimens). This would make the PCS an unusual vertebrate microsite; probably because most microsites represent transported rather than autochthonous bone accumulations, they are generally high-diversity assemblages composed of hydraulically similar bones, with no one taxon dominating the assemblage (Eberth and others, 2007). The PCS is also unusual in being a wetland accumulation whose vertebrate fossils are not dominated by macrofossil bone elements (Eberth and others, 2007). Whether the vertebrate microfossil assemblage is primarily attritional as opposed to catastrophic (see Henrici and Fiorillo, 1993) is not yet known.

Fossils of PCS large mammals were often big enough to be noticed during excavation of in situ sediments from 2003 through 2005. With few exceptions (fig. 26A), large mammal specimens are single, isolated bones. This indicates that large mammals in the PCS probably were not victims of a catastrophic depositional event(s) that quickly buried intact carcasses (see Brinkman and others, 2007; Rogers and Kidwell, 2007). How the large mammal bones were attritionally introduced into the sinkhole is uncertain. The PCS pond might have been a water source for large animals living in a moderately dry environment (see Therrien and Fastovsky, 2000; Greb and others, 2006; Shunk and others, 2009), some of which may then have died in and around the pond (fig. 27). Alternatively, bones of large mammals may have been swept from nearby on the landscape into the sinkhole by one or more fine-grained debris-flow events of the kind hypothesized to account (at least in part) for the poor sorting of Zone A fossiliferous sediments (see Rogers, 2005); bones may have accumulated in a debris cone(s) in the sinkhole before being reworked into the pond itself (Shunk and others, 2009). Once buried in the waterlogged, stagnant, slightly alkaline Zone A deposits of the PCS pond, vertebrate bones were in an ideal environment for preservation (Farlow and Argast, 2006).

ACKNOWLEDGMENTS

We thank Irving Materials, Inc., for making the Pipe Creek Sinkhole site available to us, and for

considerable assistance with the details of our project; without their cooperation, this study would not have been possible. In particular, we thank Jon Havens, Ron Lewis, Rick Lucas, and Ray Rich. We also thank Indiana State Museum staff and volunteers from around the state of Indiana for helping us in the field, and volunteers at the Indiana State Museum (under the supervision of Gerhard Gennrich), and students at Indiana-Purdue University Fort Wayne, for their efforts in processing sediment. Too many persons contributed in these ways to name individually, but their efforts were greatly appreciated. Two IPFW students in particular, Tamra Reece and Hope Sheets, were involved in both laboratory and field work throughout the project. Anne Argast, Ben Dattilo, Solomon Isorho, Jack Sunderman, and Tony Swinehart provided helpful discussion throughout this study. Kim Sowder and James Whitcraft assisted in the preparation of artwork. We dedicate this paper to Ernest Lundelius, Jr., for his many contributions to the study of cave-related vertebrate paleontology. This research was supported by NSF Grant 0207182-EAR to James Farlow.

REFERENCES

- Andrews, P., 1990, Owls, caves and fossils—predation, preservation, and accumulation of small mammal bones in caves, with an analysis of the Pleistocene cave faunas from Westbury-sub-Mendip, Somerset, UK: Chicago, University of Chicago Press, 231 p.
- Anthony, D. M., and Granger, D. E., 2004, A late Tertiary origin for multilevel caves along the western escarpment of the Cumberland Plateau, Tennessee and Kentucky, established by cosmogenic ²⁶Al and ¹⁰Be: *Journal of Cave and Karst Studies*, v. 66, no. 2, p. 46–55.
- Anthony, D. M., and Granger, D. E., 2006, Five million years of Appalachian landscape evolution preserved in cave sediments, *in* Harmon, R. S., and Wicks, C., eds., *Perspectives on karst geomorphology, hydrology, and geochemistry—a tribute volume to Derek C. Ford and William B. White*: Geological Society of America Special Paper 404, p. 39–50.
- Argast, A., and Farlow, J. O., this volume. Interstratified kaolinite-smectite from a terra rossa in the Pipe Creek Sinkhole, northern Indiana.
- ASTM International, 2000, Standard test methods for moisture, ash, and organic matter of peat and other organic soils: West Conshohocken, Penn., Protocol D2974-00, 4 p.

- ASTM International, 2007, Standard test method for particle-size analysis of soils: West Conshohocken, Penn., Protocol D422-63, 8 p.
- Baskin, J. A., 1998, Mustelidae, in Janis, C. M., Scott, K. M., and Jacobs, L. L., eds., Evolution of Tertiary mammals of North America, v. I—Terrestrial carnivores, ungulates, and ungulatelike mammals: Cambridge, U.K., Cambridge University Press, p. 152–173.
- Bechtel, T. D., Hojdila, J. L., Baughman, S. H., II, DeMayo, T., and Doheny, E., 2005, Relost and found—detection of a paleontologically, historically, cinematically, and environmentally important solution feature in the carbonate belt of southeastern Pennsylvania: *The Leading Edge*, v. 24, no. 5, p. 537–540.
- Behrensmeyer, A. K., 2007, Bonebeds through time, in Rogers, R. R., Eberth, D. A., and Fiorillo, A. R., eds., Bonebeds—genesis, analysis, and paleobiological significance: Chicago, University of Chicago Press, p. 65–101.
- Bell, C. J., Lundelius, E. L., Jr., Barnosky, A. D., Graham, R. W., Lindsay, E. H., Ruez, D. R., Jr., Semken, H. A., Jr., Webb, S. D., and Zakrewski, R. J., 2004, The Blancan, Irvingtonian, and Rancholabrean mammal ages, in Woodburne, M. O., ed., Late Cretaceous and Cenozoic mammals of North America: New York, Columbia University Press, p. 232–314.
- Brindley, G. W., and Brown, G., eds., 1980, Crystal structures of clay minerals and their X-ray identification: London, Mineralogical Society, 495 p.
- Brinkman, D. R., Eberth, D. A., and Currie, P. J., 2007, From bonebeds to paleobiology—applications of bonebed data, in Rogers, R. R., Eberth, D. A., and Fiorillo, A. R., eds., Bonebeds—genesis, analysis, and paleobiological significance: Chicago, University of Chicago Press, p. 221–263.
- Bush, A. M., Kowalewski, M., Hoffmeister, A. P., Bambach, R. K., and Daley, G. M., 2007, Potential paleoecologic biases from size-filtering of fossils—strategies for sieving: *Palaios*, v. 22, no. 6, p. 612–622.
- Carpenter, J., Odum, W. E., and Mills, A., 1983, Leaf litter decomposition in a reservoir affected by acid mine drainage: *Oikos*, v. 41, no. 2, p. 165–172.
- Cifelli, R. L., ed., 1996, Techniques for recovery and preparation of microvertebrate fossils: Oklahoma Geological Survey Special Publication 96-4, 36 p.
- Coleman, J. M., and Roberts, H. H., 2000, The Mississippi River delta-depositional system guidebook: Baton Rouge, La., Coastal Studies Institute, Louisiana State University, 122 p.
- Cummins, K. W., and Wycheck, J. C., 1971, Caloric equivalents for investigations in ecological energetics: *Internationale Vereinigung für Theoretische und Angewandte Limnologie Mitteilung* 18, 158 p.
- Dawson, M. R., Farlow, J. O., and Argast, A., 2008, *Hypolagus* (Mammalia, Lagomorpha, Leporidae) from the Pipe Creek Sinkhole, Late Neogene, Grant County, Indiana, in Farley, G. H., and Choate, J. R., eds., Unlocking the unknown—papers honoring Dr. Richard J. Zakrzewski: Hays, Kansas, Fort Hays State University, p. 5–10.
- Dean, W. E., Jr., 1974, Determination of carbonate and organic matter in calcareous sediments and sedimentary rocks by loss on ignition: comparison with other methods: *Journal of Sedimentary Petrology*, v. 44, no. 1, p. 242–248.
- Deike, G. H., III, 1960, X-ray analysis of some Missouri cave clays: *Missouri Speleology*, v. 2, no. 1, p. 9–11.
- Delaney, M. T., Fernandez, I. J., Simmons, J. A., and Briggs, R. D., 1996, Red maple and white pine litter quality—initial changes with decomposition: University of Maine, Orono, Maine Agricultural and Forest Experiment Station Technical Bulletin 162, 19 p.
- Devaney, K., Wilkinson, B. H., and Van Der Voo, R., 1986, Deposition and compaction of carbonate clinothems—the Silurian Pipe Creek Junior Complex of east-central Indiana: *Geological Society of America Bulletin*, v. 97, no. 11, p. 1,367–1,381.
- Driese, S. G., and Ober, E. G., 2005, Paleopedologic and paleohydrologic records of precipitation seasonality from early Pennsylvanian “underclay” paleosols, U.S.A.: *Journal of Sedimentary Research*, v. 75, no. 6, p. 997–1,010.
- Durn, G., 2003, Terra rossa in the Mediterranean region—parent materials, composition, and origin: *Geologia Croatica*, v. 56, no. 1, p. 83–100.
- Durn, G., Slovenic, D., and Čović, M., 2001, Distribution of iron and manganese in terra rossa from Istria and its genetic implications: *Geologia Croatica*, v. 54, no. 1, p. 27–36.
- Eberth, D. A., Shannon, M., and Noland, B. G., 2007, A bonebeds database—classification, biases, and patterns of occurrence, in Rogers, R. R., Eberth, D. A., and Fiorillo, A. R., eds., Bonebeds—genesis, analysis, and paleobiological significance: Chicago, University of Chicago Press, p. 103–219.
- Farlow, J. O., and Argast, A., 2006, Preservation of fossil bone from the Pipe Creek Sinkhole (late Neogene, Grant County, Indiana, U.S.A.): *Journal of the Paleontological Society of Korea*, v. 22, no. 1, p. 51–75.
- Farlow, J. O., Chin, K., Argast, A., and Poppy, S., 2010, Coprolites from the Pipe Creek Sinkhole (Late Neogene, Grant County, Indiana, U.S.A.): *Journal of Vertebrate Paleontology*, v. 30, no. 3, p. 959–969.
- Farlow, J. O., Sunderman, J. A., Havens, J. J., Swinehart, A. L., Holman, J. A., Richards, R. L., Miller, N. G., Martin, R. A., Hunt, R. M., Jr., Storrs, G. W., Curry, B. B., Fluegeman, R. H., Dawson, M. R., and Flint, M.

- E. T., 2001, The Pipe Creek Sinkhole biota, a diverse late Tertiary continental fossil assemblage from Grant County, Indiana: *American Midland Naturalist*, v. 145, no. 2, p. 367–378.
- Folk, R. L., 1980, *Petrology of sedimentary rocks*: Austin, Tex., Hemphill Publishing Company, 184 p.
- Foster, J., Chittleborough, D. J., and Barovich, K., 2004, Genesis of a terra rossa soil over marble and the influence of a neighbouring texture contrast soil at Delamere, South Australia, *in* SuperSoil 2004, 3rd Australian New Zealand Soils Conference, University of Sydney, Australia, p. 1–8.
- George, C. O., Lundelius, E. L., Jr., and Meissner, L., eds., 2007, Late Quaternary cave sites of central Texas: Field trip guidebook, Society of Vertebrate Paleontology 67th Annual Meeting, Austin, Tex., 48 p.
- Greb, S. F., DiMichele, W. A., and Gastaldo, R. A., 2006, Evolution and importance of wetlands in earth history, *in* Greb, S. F., and DiMichele, W. A., eds., *Wetlands through time*: Geological Society of America Special Paper 399, p. 1–40.
- Hall, R. D., 1976, Stratigraphy and origin of surficial deposits in sinkholes in south-central Indiana: *Geology*, v. 4, no. 8, p. 507–509.
- Henrici, A. C., and Fiorillo, A. R., 1993, Catastrophic death assemblage of *Chelomophrynus bayi* (Anura, Rhinophrynidae) from the Middle Eocene Wagon Bed Formation of central Wyoming: *Journal of Paleontology*, v. 67, no. 6, p. 1,016–1,026.
- Hulbert, R. C., Jr., ed., 2001, *The fossil vertebrates of Florida*: Gainesville, University of Florida Press, 350 p.
- Janis, C. M., Scott, K. M., and Jacobs, L. L., eds., 1998, *Evolution of Tertiary mammals of North America*; v. 1, *Terrestrial carnivores, ungulates, and ungulatelike mammals*: Cambridge, U.K., Cambridge University Press, 691 p.
- Korth, W. W., 1994, *The Tertiary record of rodents in North America*: New York, Plenum Press, 319 p.
- Kowalewski, M., and Hoffmeister, A. P., 2003, Sieves and fossils—effects of mesh size on paleontological patterns: *Palaios*, v. 18, no. 4–5, p. 460–469.
- Kvet, J., Westlake, D. F., Dykyjova, D., Marshall, E. J. P., and Ondok, J. P., 1998, Primary production in wetlands, *in* Westlake, D. F., Kvet, J., and Szczepanski, A., eds., *The production ecology of wetlands*: Cambridge, U.K., Cambridge University Press, p. 78–168.
- Latham, A. G., 1999, Cave breccias and archaeological sites: *Cave Archaeology and Palaeontology Research Archive* (electronic journal) no. 1. [Available at <<http://capra.group.shef.ac.uk>>, date accessed, June 23, 2009.]
- Lehmann, P. J., and Simo, A., 1988, Depositional facies and diagenesis of the Pipe Creek Jr. Reef, Silurian, Great Lakes region, *in* Geldsetzer, H. H. J., James, N. P., and Tebutt, G. E., eds., *Reefs—Canada and adjacent areas*: Canadian Society of Petroleum Geologists, Memoir 13, p. 319–329.
- Likens, G. E., and Bormann, F. H., 1970, Chemical analyses of plant tissues from the Hubbard Brook Ecosystem in New Hampshire: *Yale University School of Forestry Bulletin* 79, 25 p.
- Ludvigson, G. A., Gonzalez, L. A., Metzger, R. A., Witzke, B. J., Brenner, R. L., Murillo, A. P., and White, T. S., 1998, Meteoric sphaerosiderite lines and their use for paleohydrology and paleoclimatology: *Geology*, v. 26, no. 11, p. 1,039–1,042.
- Lundelius, E. L., Jr., 2006, Cave site contributions to vertebrate history: *Alcheringa Special Issue* 1, p. 195–210.
- MacFadden, B. J., Labs-Hochstein, J., Hulbert, R. C., Jr., and Baskin, J. A., 2007, Revised age of the late Neogene terror bird (*Titanis*) in North America during the Great American interchange: *Geology*, v. 35, no. 2, p. 123–126.
- Martin, L. D., 1998, Felidae, *in* Janis, C. M., Scott, K. M., and Jacobs, L. L., eds., *Evolution of Tertiary mammals of North America*, v. I—*Terrestrial carnivores, ungulates, and ungulatelike mammals*: Cambridge, U.K., Cambridge University Press, p. 236–242.
- Martin, R. A., Goodwin, H. T., and Farlow, J. O., 2002, Late Tertiary (late Hemphillian) rodents from the Pipe Creek Sinkhole, Grant County, Indiana: *Journal of Vertebrate Paleontology*, v. 22, no. 1, p. 137–151.
- McCarthy, P. J., and Plint, A. G., 1998, Recognition of interfluvial sequence boundaries—integrating paleopedology and sequence stratigraphy: *Geology*, v. 26, no. 5, p. 387–390.
- McGrain, P., 1947, An example of lapies in the Indiana karst region: *Proceedings of the Indiana Academy of Science*, v. 57, p. 148–152.
- McKenna, M. C., Bleefeld, A. R., and Mellett, J. S., 1994, Microvertebrate collecting—large-scale wet sieving for fossil microvertebrates in the field, *in* Leiggi, P., and May, P., eds., *Vertebrate paleontological techniques*: Cambridge, U.K., Cambridge University Press, p. 93–111.
- Merino, E., and Banerjee, A., 2008, Terra rossa genesis, implications for karst, and eolian dust; a geodynamic thread: *Journal of Geology*, v. 116, no. 1, p. 62–75.
- Miller, R. B., 1999, Structure of wood, *in* Forest Products Laboratory, *Wood handbook—wood as an engineering material*: U.S. Department of Agriculture, Forest Service, General Technical Report FPL-GTR-113, p. 2-1–2-4.
- Misra, M. K., Ragland, K. W., and Baker, A. J., 1993, Wood ash composition as a function of furnace temperature: *Biomass and Bioenergy*, v. 4, no. 2, p. 103–116.
- Mizota, C., Kusakabe, M., and Noto, M., 1988, Eolian contribution to soil development on Cretaceous lime-

- stones in Greece as evidenced by oxygen isotope composition of quartz: *Geochemical Journal*, v. 22, no. 1, p. 41–46.
- Moresi, M., and Mongelli, G., 1988, The relation between the terra rossa and the carbonate-free residue of the underlying limestones and dolostones in Apulia, Italy: *Clay Minerals*, v. 23, no. 4, p. 439–446.
- Moriarty, K. C., McCulloch, M. T., Wells, R. T., and McDowell, M. C., 2000, Mid-Pleistocene cave fills, mega-faunal remains and climate change at Naracoorte, South Australia—towards a predictive model using U-Th dating of speleothems: *Palaeogeography, Palaeoclimatology, Palaeoecology*, v. 159, nos. 1/2, p. 113–143.
- Olson, C. G., Ruhe, R. V., and Mausbach, M. J., 1980, The terra rossa limestone contact phenomena in karst, southern Indiana: *Soil Science Society of America Journal*, v. 44, no. 5, p. 1,075–1,079.
- Pinsak, A. P., and Shaver, R. H., 1964, The Silurian formations of northern Indiana: *Indiana Geological Survey Bulletin* 32, 87 p.
- Potter, P. E., Maynard, J. B., and Depetris, P. J., 2005, *Mud and mudstones—introduction and overview*: Berlin, Springer, 297 p.
- Prothero, D. R., 2005, *The evolution of North American rhinoceroses*: Cambridge, U.K., Cambridge University Press, 218 p.
- Prothero, D. R., 2006, *After the dinosaurs—the age of mammals*: Bloomington, Ind., Indiana University Press, 362 p.
- Reed, E. H., 2006, *In situ* taphonomic investigation of Pleistocene large mammal bone deposits from The Ossuaries, Victoria Fossil Cave, Naracoorte, South Australia: *Helictite*, v. 39, no. 1, p. 5–15.
- Retallack, G. J., 2001, *Soils of the past—an introduction to paleopedology* (second edition): Oxford, U.K., Blackwell Science, 404 p.
- Richards, R. L., 2007, The history and status of karst vertebrate paleobiology in Indiana, *in* Atz, A., ed., *Back underground in Indiana—a guidebook for the 2007 National Convention of the National Speleological Society*: Marengo, Ind., 462 p.
- Rogers, R. R., 2005, Fine-grained debris flows and extraordinary vertebrate burials in the Late Cretaceous of Madagascar: *Geology*, v. 33, no. 4, p. 297–300.
- Rogers, R. R., and Kidwell, S. M., 2007, A conceptual framework for the genesis and analysis of vertebrate skeletal concentrations, *in* Rogers, R. R., Eberth, D. A., and Fiorillo, A. R., eds., *Bonebeds—genesis, analysis, and paleobiological significance*: Chicago, University of Chicago Press, p.1–63.
- Sankey, J. T., and Baszio, S., eds., 2008, *Vertebrate microfaunal assemblages—their role in paleoecology and paleobiogeography*: Bloomington, Ind., Indiana University Press, 278 p.
- Schubert, B. W., Mead, J. I., and Graham, R. W., eds., 2003, *Ice Age cave faunas of North America*: Bloomington, Ind., Indiana University Press, 299 p.
- Shaver, R. H., Burger, A. M., Gates, G. R., Gray, H. H., Hutchison, H. C., Keller, S. J., Patton, J. B., Rexroad, C. B., Smith, N. M., Wayne, W. J., and Wier, C. E., 1970, *Compendium of rock-unit stratigraphy in Indiana*: Indiana Geological Survey Bulletin 43, 229 p.
- Shaver, R. H., and Sunderman, J. A., 1982, Silurian reefs at Delphi and Pipe Creek Jr. Quarry, Indiana, with emphasis on the question of deep vs. shallow water: *Field Trip 5, North-Central Section, Geological Society of America*, West Lafayette, Ind., Purdue University, 39 p.
- Shaver, R. H., and Sunderman, J. A., 1989, Silurian seascapes—water depth, clinothems, reef geometry, and other motifs—a critical review of the Silurian reef model: *Geological Society of America Bulletin*, v. 101, no. 7, p. 939–951.
- Shaver, R. H., Sunderman, J. A., Mikulic, D. G., Kluessendorf, J., McGovney, J. E. E., and Pray, L. C., 1983, Silurian reef and interreef strata as responses to cyclical succession of environments, southern Great Lakes area (Field Trip 12), *in* Shaver, R. H., and Sunderman, J. A., eds., *Field trips in midwestern geology*: Geological Society of America, Indiana Geological Survey and Indiana University Department of Geology, p. 141–196.
- Shunk, A. J., Driese, S. G., and Clark, G. M., 2006, Latest Miocene to earliest Pliocene sedimentation and climate record derived from paleosinkhole fill deposits, Gray Fossil Site, northeastern Tennessee, U.S.A.: *Palaeogeography, Palaeoclimatology, Palaeoecology*, v. 231, no. 3–4, p. 265–278.
- Shunk, A. J., Driese, S. G., Farlow, J. O., Zavada, M. S., and Zobia, M. K., 2009, Late Neogene paleoclimate and paleoenvironment reconstructions from the Pipe Creek Sinkhole, Indiana, USA: *Palaeogeography, Palaeoclimatology, Palaeoecology*, v. 274, no. 3–4, p. 173–184.
- Simo, J. A., and Lehmann, P. J., 2000, Diagenetic history of Pipe Creek Jr. Reef, Silurian, north-central Indiana, U.S.A.: *Journal of Sedimentary Research*, v. 70, no. 4, p. 937–951.
- Smith, D. B., 1991, Devonian Ohio Shale, SDO-1: U.S. Geological Survey Certificate of Analysis, 3 p. [Available at U.S. Geological Survey Web site, <http://minerals.cr.usgs.gov/geo_chem_stand/ohioshale.html>, date accessed, Aug. 27, 2009.]
- Suarez, C. A., Suarez, M. B., Terry, D. O., Jr., and Grandstaff, D. E., 2007, Rare earth element geochemistry and taphonomy of the Early Cretaceous Crystal

- Geyser Dinosaur Quarry, east-central Utah: *Palaios*, v. 22, no. 5, p. 500–512.
- Suberkropp, K., Godshalk, G. L., and Klug, M. J., 1976, Changes in the chemical composition of leaves during processing in a woodland stream: *Ecology*, v. 57, no. 4, p. 720–727.
- Sunderman, J. A., Farlow, J. O., and Havens, J. J., 1998, Tertiary sediments and fossils from the northern Indiana Pipe Creek Jr. sinkhole site: 32nd Annual Meeting, North-Central Section, Geological Society of America Abstracts and Program, p. 74.
- Sunderman, J. A., and Mathews, G. W., eds., 1975, Silurian reef and interreef environments: Field Trip Guidebook, Great Lakes Section, Society of Economic Paleontologists and Mineralogists, Fort Wayne, Ind., 94 p.
- Sutcliffe, A. J., Bramwell, D., King, A., and Walker, M., 1976, Cave palaeontology and archaeology, in Ford, T. D., and Cullingford, C. H. D., eds., *The science of speleology*: London, U.K., Academic Press, p. 495–549.
- Therrien, F., and Fastovsky, D. E., 2000, Paleoenvironments of early theropods, Chinle Formation (Late Triassic), Petrified Forest National Park, Arizona: *Palaios*, v. 15, no. 3, p. 194–211.
- Trueman, C. N., 1999, Rare earth element geochemistry and taphonomy of terrestrial vertebrate assemblages: *Palaios*, v. 14, no. 6, p. 555–568.
- Trueman, C. N., 2007, Trace element geochemistry of bonebeds, in Rogers, R. R., Eberth, D. A., and Fiorillo, A. R., eds., *Bonebeds—genesis, analysis, and paleobiological significance*: Chicago, University of Chicago Press, p. 397–435.
- Trueman, C. N., Behrensmeyer, A. K., Potts, R., and Tuross, N., 2006, High-resolution records of location and stratigraphic provenance from the rare earth element composition of fossil bones: *Geochimica et Cosmochimica Acta*, v. 70, no. 17, p. 4,343–4,355.
- Trueman, C. N., and Benton, M. J., 1997, A geochemical method to trace the taphonomic history of reworked bones in sedimentary settings: *Geology*, v. 25, no. 3, p. 263–266.
- Tsatskin, T., and Gendler, T. S., 2002, Further notes on terra rossa and related soils near Kfar Hahores Archaeological Site, Israel: *Options Méditerranéennes, Série A*, no. 50, p. 109–120.
- Ufnar, D. F., González, L. A., Ludvigson, G. A., Brenner, R. L., and Witzke, B. J., 2002, The mid-Cretaceous water bearer—isotope mass balance quantification of the Albian hydrologic cycle: *Palaeogeography, Palaeoclimatology, Palaeoecology*, v. 188, no. 1–2, p. 51–71.
- Ufnar, D. F., Ludvigson, G. A., González, L. A., Brenner, R. L., Witzke, B. J., 2004a, High latitude meteoric $\delta^{18}\text{O}$ compositions—paleosol siderite in the Middle Cretaceous Nanushuk Formation, North Slope, Alaska: *Geological Society of America Bulletin*, v. 116, no. 3/4, p. 463–473.
- Ufnar, D. F., González, L. A., Ludvigson, G. A., Brenner, R. L., and Witzke, B. J., 2004b, Evidence for increased latent heat transport during the Cretaceous (Albian) greenhouse warming: *Geology*, v. 32, no. 12, p. 1,049–1,052.
- Ufnar, D. F., González, L. A., Ludvigson, G. A., Brenner, R. L., Witzke, B. J., and Leckie, D., 2005, Reconstructing a mid-Cretaceous landscape from paleosols in western Canada: *Journal of Sedimentary Research*, v. 75, no. 6, p. 984–996.
- Vallance, J. W., and Scott, K. M., 1997, The Osceola mudflow from Mount Ranier—sedimentology and hazard implications of a huge clay-rich debris flow: *Geological Society of America Bulletin*, v. 109, no. 2, p. 143–163.
- Wallace, S. C., and Wang, X., 2004, Two new carnivores from an unusual late Tertiary forest biota in eastern North America: *Nature*, v. 431, no. 7008, p. 556–559.
- Webster, J. R., and Benfield, E. F., 1986, Vascular plant breakdown in freshwater ecosystems: *Annual Review of Ecology and Systematics*, v. 17, p. 567–594.
- Westlake, D. F., 1965, Some basic data for investigations of the productivity of aquatic macrophytes: *Memorie dell'Instituto Italiano di Idrobiologia dott, Marco De Marchi*, v. 18, p. 229–248.
- White, W. B., 1988, *Geomorphology and hydrology of karst terrains*: Oxford, U.K., Oxford University Press, 464 p.
- Woodburne, M. O., ed., 2004, *Late Cretaceous and Cenozoic mammals of North America*: New York, Columbia University Press, 391 p.
- Worthy, T. H., and Holdaway, R. N., 2002, *The lost world of the moa—prehistoric life of New Zealand*: Bloomington, Ind., Indiana University Press, 718 p.
- Young, K., 1986, The Pleistocene terra rossa of central Texas, in Abbott, P. L., and Woodruff, C. M., Jr., eds., *The Balcones Escarpment—geology, hydrology, ecology and social development in central Texas*: Geological Society of America Annual Meeting, San Antonio, p. 63–70.

Interstratified Kaolinite-Smectite from a Sediment Derived from Terra Rossa in the Pipe Creek Sinkhole, Indiana

By Anne Argast and James O. Farlow

ABSTRACT

Interstratified kaolinite-smectite occurs in sediments preserved in the Pipe Creek Sinkhole, Grant County, Indiana. These sediments are from terra rossa and associated materials developed originally in close proximity to the sinkhole that developed during the Mio-Pliocene in Silurian limestones. The presence of kaolinite-smectite in this time and place is suggestive of a Mediterranean-type climate circa 5 million years ago in the North American midcontinent.

This is the third published description of interstratified kaolinite-smectite in sediments developed on or near a limestone, thus suggesting that a relationship may exist between terra rossa and the conditions necessary to develop interstratified kaolinite-smectite.

The kaolinite-smectite at Pipe Creek Sinkhole is randomly interstratified and consists of 70 percent kaolinite layers. Though widely distributed at the sinkhole, the kaolinite-smectite is limited to only the finest grain sizes. Discrete kaolinite also occurs at the sinkhole, but not in the same grain sizes as the interstratified mineral.

Heating causes a gradual shift in the position of the $d_{001/002}$ peak. Up to about 400°C the d-spacing changes that happened because of heating can be partially restored through rehydration. Above about 450°C the d-spacing collapse is permanent. A statistically correlated relationship exists between temperature and the amount of shift in the position of the $d_{001/002}$ peak.

Calcium is the dominant exchange cation on the naturally occurring clay. Saturation with other ions does not induce permanent change in the kaolinite-smectite chemistry or interstratification.

INTRODUCTION

Interstratified kaolinite-smectite (KS) was first described in acid clays from Japan (Sudo and Hayashi, 1956). Since then, at least 45 accounts of KS occurrences were published, and it is possible that KS has been previously misidentified as “poorly crystallized kaolinite,” beidellite, and other minerals (Hughes and others, 1993; Cuadros and others, 1994).

Kaolinite-smectite is most commonly described from soils, paleosols, and other environments strongly affected by weathering. This is especially common for soils developed on basalts and other mafic rocks (Herbillion and others, 1981; Buhmann and Grubb, 1991; Corti and others, 1998; Righi and others, 1999; Proust and others, 2006; Thanachit and others, 2006), though KS from soils developed on andesite (Wilson and Cradwick, 1972), and even on tills and Quaternary alluvium (Yerima and others, 1985; Aleta and others, 1999; Grimley and others, 2003) are also reported. A study by Proust and others (2006) interestingly demonstrates the influence of microenvironments within individual crystals on the potential for development of an interstratified mineral.

Kaolinite-smectite clays also develop in soils and sediments containing, or in association with, limestone, chalk, and calcareous fossils (Schultz and others, 1971; Brindley and others, 1983; Amouric and Olives, 1998; Lynch 2000). Experiments by Środoń (1980) suggest that the formation of KS is favored by the presence of calcium ions (Ca^{2+}) in solution.

There is one description of kaolinite-smectite developed in Pennsylvanian underclays of the Illinois Basin (Hughes and others, 1987). This occurrence, developed on a shaly source, was made possible by plants and ground water that acted to extract potassium ions (K^+), magnesium ions (Mg^{2+}), and silica from the system.

Soil KS commonly, but not always, forms under tropical and subtropical conditions, and the presence of KS is not by itself a reliable climatic indicator. Fisher and Ryan (2006) suggest that all kaolinite produced by the weathering of smectite passes through a KS intermediary phase. Slope and drainage are important in determining whether KS or noninterstratified kaolinite persists in the system (Herbillion and others, 1981; Yerima and others, 1985; Hughes and others, 1993; Righi and others, 1999), probably because slope and drainage affect

the removal rate of base cations. For example, Delvaux and Herbillion (1995) describe a weathering sequence of smectite to KS to kaolinite with a concomitant decrease in soil exchangeable magnesium (Mg) and total Mg content, finding that KS is favored by well-drained environments.

KS is also reported from a few hydrothermal systems (Wiewióra, 1973; Cuadros and Dudek, 2006; Dudek and others, 2006) and has been synthesized under hydrothermal conditions in the laboratory (Środoń 1980; Delvaux and others, 1989). However, Patrier and others (2003), while describing surficial clay assemblages in proximity to geothermal activity in the French West Indies, found that KS occurred only in areas unaffected by hydrothermal waters.

KS (probably formed in a paleosol) has been observed to persist to depths up to 9,000 ft in a Gulf Coast well (Calvert and Pevear, 1983). Despite its burial depth, there is no illite interstratified with the KS in this core sample, suggesting that the interlayer environment of KS is sufficiently different from the interlayer environment of interstratified illite/smectite to prevent fixation of potassium.

There are related minerals that differ in either the 1:1 or the 2:1 component. (Phyllosilicates are constructed, in part, from tetrahedral sheets with cations in tetrahedral coordination, and octahedral sheets with cations in octahedral coordination. 1:1 and 2:1 describe the ratio of the tetrahedral and octahedral sheets in a particular phyllosilicate. Kaolinite is an example of a 1:1 phyllosilicate; smectite is an example of a 2:1 phyllosilicate.) For example, both interstratified kaolinite/vermiculite and interstratified halloysite/smectite have been identified (Wada and Kakuto, 1983; Cho and Mermut, 1992; Nurcholis and Tokashiki, 1998; Aspandiar and Eggleton, 2002). Even for smectitic varieties, Hughes and others (1993) preferred the term “mixed-layered kaolinite/expandables” because the expandable 2:1 phase is not always smectite in a strict sense. It should be remembered that 1:1/2:1 interlayered clays may occupy a range of points in a wide compositional continuum.

Środoń (1980) and Brindley and others (1983) have each commented on a discrepancy in the estimated number of kaolinite layers in a kaolinite-smectite based upon chemical and X-ray diffraction data. In both cases the chemical data indicate fewer kaolinite layers than the X-ray data. Środoń (1980) attrib-

uted this to “unreacted smectite” though Brindley and others (1983) found no evidence for this.

Nearly all examples of interstratified kaolinite-smectite are randomly ordered. A sample from the suspended sediment load of the Parana River in Argentina is, however, reported to have $R = 1$ ordering (Bertolino and others, 1991) as is a sample from a part of the Triassic Taylorsville Basin in Virginia that was affected by “late hot reactive water” (Thomas, 1989). In addition, kaolinite-smectite from the Argiles Plastiques Formation of the Paris Basin was found having localized $R = 1$ and $R = 2$ ordering (Amouric and Olives, 1998).

With very few exceptions (Wiewióra, 1972; Sakharov and Drits, 1973), smectite is the presumed precursor for kaolinite-smectite. In one scenario, the tetrahedral sheet of the smectite is stripped to produce kaolinitic patches that evolve into KS (Dudek and others, 2006). This may be combined with a secondary process that intercalates a neoformed kaolinite layer into the smectite (Amouric and Olives, 1998). It is also possible that smectite layers are completely dissolved and kaolinite crystallized in the smectite interlayers (Środoń 1980; Righi and others, 1999). Środoń (1999) provides an expanded review of possible mechanisms for the development of an interstratified kaolinite-smectite phase.

This report describes a newly recognized occurrence of interstratified kaolinite-smectite from the Pipe Creek Sinkhole (PCS) of northern Indiana (Farlow and others, 2001). A detailed account of the sedimentary units found at Pipe Creek Sinkhole is provided by Farlow and others (this volume). The sinkhole developed during the latest Miocene or earliest Pliocene in limestone reef rocks of Silurian age. Although most of the sinkhole’s preglacial sedimentary fill was removed by quarrying prior to scientific study, enough in situ sediment remained to allow characterization of sinkhole microstratigraphy. Sinkhole sediments are largely unconsolidated. The uppermost in situ preglacial sediment layer (Zone A) is a poorly sorted, fossiliferous, organic-rich deposit containing reworked limestone and chert lithoclasts, well-rounded quartzite pebbles, and abundant sideritic nodules. Beneath Zone A is a yellow-brown, sparsely fossiliferous layer (Zone B) containing root structures and burrows. Beneath Zone B is an unfossiliferous sediment (Zone C) containing abundant limestone clasts of varying size likely derived from a terra rossa and transported into a cave before the sink-

hole developed. Kaolinite-smectite is found abundantly in all three zones.

Clay minerals are often found in cave deposits. For example, kaolinite, dickite, and hydrated halloysite (among other clay minerals) occur in caves of the Guadalupe Mountains (Polyak and Güven, 2000). This, however, is the first description of an interstratified kaolinite-smectite from a cave and the third description of KS from or in close association with a terra rossa. Lynch (2000), in an abstract, describes KS in a terra rossa from the Pleistocene of central Texas where it developed in marls of the Edwards Formation, which also contain illite, kaolinite, and ordered illite-smectite. Schultz and others (1971) describe kaolinite-smectite in close association with a terra rossa from the Yucatán Peninsula of Mexico. That occurrence developed in marine limestones of Eocene age.

Terra rossa is a red soil developed over limestone or dolostone bedrock, commonly in areas of Mediterranean climate (for example, Boero and others, 1992). A terra rossa is thought to develop when insoluble components derived from autochthonous and allochthonous sources are concentrated as the parent limestone or dolostone dissolves (Boero and Schwertmann, 1989; Durn, 2003). Merino (2005), working from an idea first proposed by Maliva and Siever (1988), suggests a pressure-solution process causes clay calcite forms “intracrystalline microstylolites,” driven by a pressure solution process. We have no preference, but note that Merino’s model produces acid whereas the conventional model implies reactive solutions near neutral pH (Durn, 2003).

METHODS

Representative samples of 10 to 20 g were obtained from Zones A, B, and C at the Pipe Creek Sinkhole. These were dispersed in deionized water without using a dispersing agent, treated with an ultrasonic disaggregator, and sized into $<0.08\text{-}\mu\text{m}$, $<0.10\text{-}\mu\text{m}$, $0.1\text{-}0.2\text{-}\mu\text{m}$, $0.2\text{-}1\text{-}\mu\text{m}$, $1\text{-}2\text{-}\mu\text{m}$, and $2\text{-}5\text{-}\mu\text{m}$ fractions through a combination of gravitational settling and centrifugation. Generally, three to five cycles of washing, disaggregation, and settling/centrifugation were required to get adequate dispersal. The sample from Zone C was easiest to disperse at the finer sizes, and a far greater quantity of very fine clay was produced from Zone C than was produced for Zones A and B. Because of

this, and to simplify the study, the majority of analyses dealt with samples recovered from Zone C.

X-ray diffraction patterns were prepared using a Philips APD3520/PW1710 diffractometer equipped with a graphite monochromator and theta-compensating slit set to open early at low angles. Oriented samples were scanned from 2 to 43° 2 θ , 200 steps/deg, 1 sec/step, using copper (Cu) radiation at 40 kV and 30 mA. Random scans were run from 2 to 70° 2 θ . All data were smoothed using a 15-pt weighted moving average. Low-angle scans of the glycolated, heated, and rehydrated samples were repeated at faster scan rates to check if the samples had changed during the time it took to complete a slow scan.

Oriented mounts for X-ray diffraction (XRD) were prepared using the filter transfer method of Drevier (1973). Mounts in each size fraction were saturated with calcium using a chloride solution drawn through the filter paper. Selected samples were also prepared using sodium (Na), potassium (K), or magnesium (Mg) as the exchange ion. One set of samples was first saturated with calcium (Ca) and then resaturated with another cation before drying.

Some Ca-saturated samples were glycolated at 60°C for a minimum of 24 hours. Another set of samples was subjected to heat treatments (50°C steps, 1 hour each step) from 100°C to 500°C. At each step, the sample was scanned by XRD, rehydrated overnight at 100 percent relative humidity, and rescanned by XRD.

A portion of the Ca-saturated, <0.10- μm fraction of Zone C was prepared using a side-loaded mount and scanned from 10 to 80° 2 θ . A second portion was prepared with admixed fluorite and scanned from 55° to 65° 2 θ at 200 steps/deg, 5 sec/step, a range that includes the clay 060 peak and the fluorite 311 peak, which was used as an internal standard.

Filter papers used for the preparation of XRD slides were retained for chemical analysis by energy-dispersive X-ray spectroscopy (EDX). Rectangular sections were cut from the filters, glued to aluminum stubs, and coated with carbon. These were analyzed using a Kevex Sigma System EDX spectrometer running Quasar software. The EDX was mounted on an ISI DS 130 scanning electron microscope operated at 18.3 kiloelectron volts (KeV). The samples could not be polished, but did present

a reasonably uniform surface for analysis. Results were processed using a standardless method, with oxygen determined by stoichiometry assuming iron is present as iron oxide (Fe₂O₃). We generally expect results to be reproducible to within about 1 percent relative to the amount present. Duplicates of five samples were prepared and are reported in Table 1 as replicates to provide an indicator of analytic precision. Chlorine (Cl) was checked in all EDX spectra to be sure that analyzed Mg, Ca, Na, and K were not present as precipitated salt left behind by inadequate washing of the exchange solutions. Additional information about EDX precision and accuracy is available (Argast, 2002).

RESULTS

Evidence for interstratified kaolinite-smectite

Kaolinite-smectite is identified by diagnostic shifts of the 001/002 peak towards smaller diffraction angles when samples are heated to 375°C or treated with ethylene glycol (Moore and Reynolds, 1997). The shift on heating occurs because the smectite 001 peak collapses to approximately 9° 2 θ upon dehydration, pulling the KS 001/002 towards lower angles relative to the air-dried sample. Figure 1 shows the air-dried, glycolated, and 375°C patterns for the Ca-saturated <0.08- μm fraction from Zone C. Shown for comparison is the theoretical pattern produced in Newmod (Reynolds and Reynolds, 1996) for an ethylene glycol-solvated R0 kaolinite (0.75)/smectite. The patterns show characteristic shifts from 7.64 Å for the air-dried sample to 7.85 Å for the glycolated sample and 8.02 Å for the heated sample. There is also high correspondence between the Newmod calculation and the experimental data. The results indicate the presence of interstratified kaolinite-smectite in the sediments from the PCS.

Moore and Reynolds (1997) provide data to calculate the percent kaolinite layers based upon the difference in the positions of the 001/002 and 002/005 KS peaks. Based upon this calculation, the KS from the PCS has about 70 percent kaolinite layers and is R0 kaolinite (0.70)/smectite. There is no indication of a superlattice that would suggest an ordered structure.

The clay mineralogy of Zones A, B, and C is essentially the same. This was determined by compar-

Table 1. Chemical composition (wt. %) of selected samples used for X-ray diffraction*

ID	O	Si	Al	Fe	Mg	Ca	Na	K
<0.1 μm , Zones A, B and C								
A(unex) ^{†‡}	48.2	25.5	18.1	4.08	0.86	1.31		1.16
B(unex)	48.0	25.2	117.1	6.51	0.96	1.00		1.29
C(unex)	47.8	24.6	17.5	6.69	0.95	0.95	0.23	1.28
A(Ca) [§]	48.5	25.5	18.4	4.40	0.53	1.23		1.29
B(Ca)	47.9	25.0	17.3	6.41	0.84	1.24		1.30
C(Ca)	47.7	24.5	17.4	7.44	0.50	1.27		1.26
<0.08 μm , Zone C								
(unex)	48.3	25.3	17.9	5.37	0.92	1.10		1.10
(unex)r ^{**}	48.4	25.4	18.1	5.06	0.91	0.90	0.11	1.09
(Ca)	48.3	25.4	18.0	5.15	0.70	1.35		1.10
(Ca)r	48.3	25.5	17.9	5.22	0.65	1.26		1.19
(Na)	48.4	25.4	17.9	5.33	0.73		1.24	0.99
(Na)r	48.4	25.5	18.0	5.18	0.64		1.21	1.08
(K)	47.8	25.1	17.9	5.14	0.70			3.41
(K)r	47.8	25.1	17.8	5.05	0.75			3.50
(Mg)	48.7	25.5	18.3	4.85	1.58			1.07
(Mg)r	48.7	25.7	18.1	4.89	1.49			1.05
(NaCa)	48.5	25.6	18.0	4.93	0.70	1.25		1.10
(KCa)	48.4	25.4	18.0	5.08	0.74	1.26		1.15
(MgCa)	48.3	25.5	17.9	4.90	0.80	1.29	0.16	1.18

*Determined by X-ray spectroscopy. Results are calculated on an H-free basis and summed to 100 percent.

[†]The first letter indicates the zone. Symbols in parentheses indicate exchanged cation; unex = unexchanged sample, NaCa = sample first exchanged with Na and then re-exchanged with Ca, and so on.

[‡]Sample also contains 0.75 percent S.

[§]Sample also contains 0.20 percent Ti.

**Samples labelled "r" are replicates.

ing the XRD patterns of the <0.1- μm fraction of the three zones (fig. 2). In each case, the fine fraction is dominated by KS with associated goethite and a combination of smectite, illite, and mixed-layer illite/smectite. Hematite is not present at detectable concentrations. Similar correspondence occurs in other size fractions. Results from Zone C are a good proxy for sediment found elsewhere in the sinkhole, though Zone A does have obviously higher concentrations of organic matter. The clay from Zone C

was easier to disperse at the finest sizes. Subsequent analysis concentrates on Zone C.

Mineralogy in different size fractions

There is a systematic change in the mineralogy when moving from one size fraction to another (fig. 3). As already described, KS with subordinate illite, illite/smectite, and goethite occur in

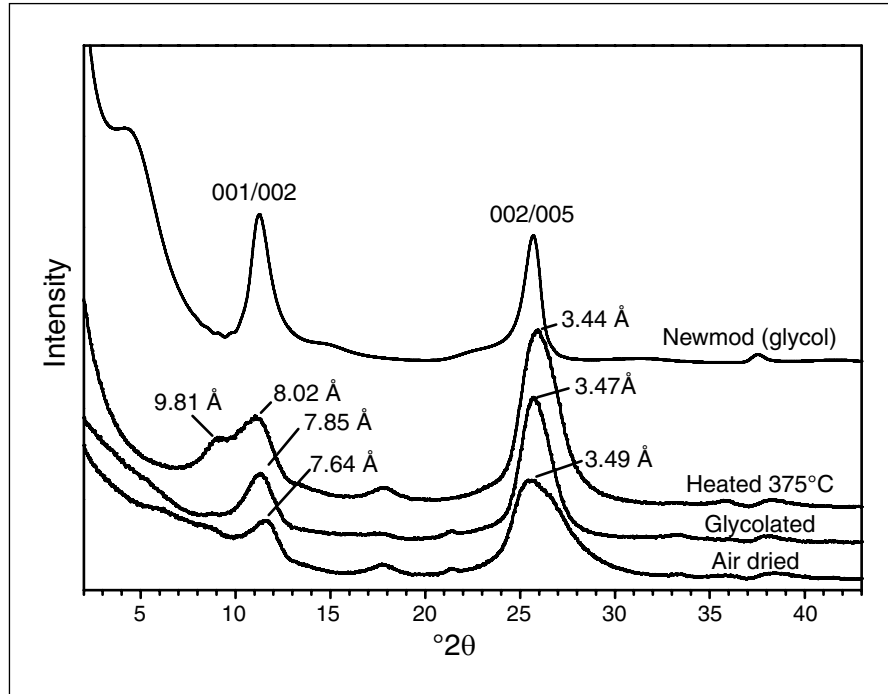


Figure 1. X-ray diffraction patterns for air-dried, glycolated, and heated samples from the $<0.08 \mu\text{m}$ fraction (all Ca-saturated) from Zone C in the Pipe Creek Sinkhole. Experimental data are shown compared to theoretical data produced by the Newmod computer program. The data indicate the presence of an interstratified kaolinite-smectite (labeled 001/002 and 002/005) in the Pipe Creek sediments.

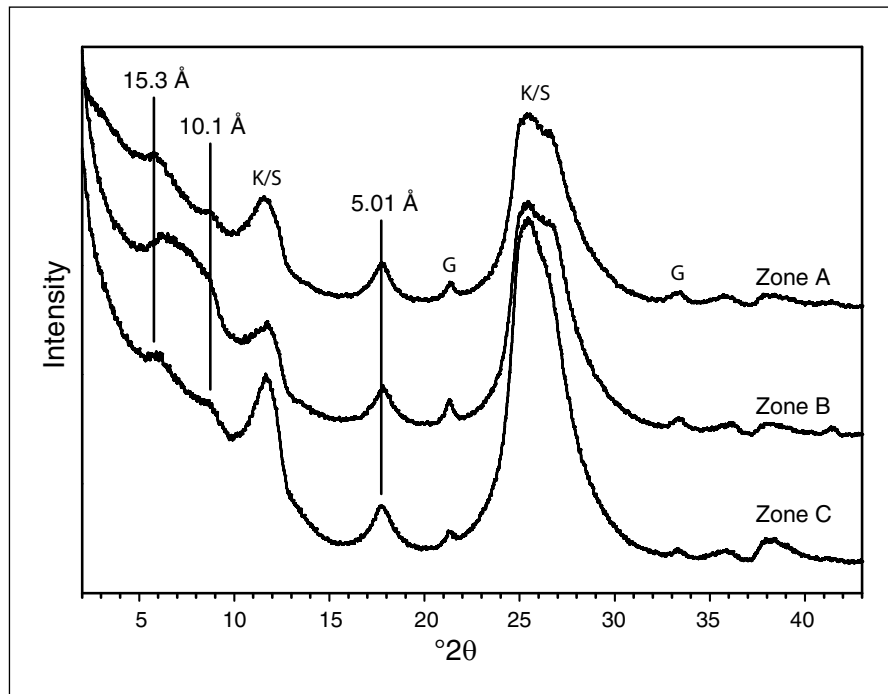


Figure 2. X-ray diffraction patterns for the $<0.1\text{-}\mu\text{m}$ fraction (Ca-saturated, air-dried) from Zones A, B, and C. K/S = interstratified kaolinite-smectite; G = goethite. Selected d-spacings corresponding to peaks because of smectite, illite, or mixed layer illite/smectite are also indicated.

the <0.08- μm and <0.1- μm sizes. Kaolinite is either very rare or absent in the size fractions that contain interstratified KS.

Interstratified KS is rare or absent in the 0.1- to 0.2- μm and 0.2- to 1- μm fractions. Kaolinite is common, and discrete illite, illite/smectite, and goethite also occur throughout the 0.1- to 1- μm size range. Very minor quartz occurs at the coarse end of the range.

Quartz is dominant in the 1- to 2- μm and 2- to 5- μm fractions. Goethite and discrete illite are also present, but there is little or no mixed layer illite/smectite. Minor calcite is present in the coarsest size.

The presence of illite as opposed to halloysite (10 Å) in the 1- to 2- μm and 2- to 5- μm fractions was confirmed by obtaining a diffraction pattern after heating to 110°C for several hours, a procedure that collapses a 10 Å halloysite peak (Brindley, 1980). The possible presence of halloysite (7 Å) is not, however, so easy to dismiss. Peaks at 12.38° 2 θ (7.15 Å), 19.91° 2 θ (4.46 Å), 24.92° 2 θ (3.57 Å), and 34.97° 2 θ (2.57 Å) are consistent with either hallo-

ysite or kaolinite. Curiously the peaks at 19.91° 2 θ and 34.97° 2 θ are present in the 1- to 2- μm and 2- to 5- μm fractions, but not in the kaolinite-bearing 0.1- to 0.2- μm and 0.2- to 1- μm fractions. This suggests that the 7 Å phase in the coarser fractions is in fact halloysite (7 Å). Examination by scanning electron microscopy did not reveal anything having a morphology characteristic of tubular halloysite. Halloysite (7 Å) may be present, but it is not confirmed.

Effect of heating

The XRD pattern of interstratified kaolinite-smectite is changed by modest increases in temperature. Collapse of the structure occurs gradually as the temperature is increased, with clear evidence of partial collapse at temperatures as low as 150°C (fig. 4) where the $d_{001/002}$ peak was measured at 7.78 Å and the $d_{002/005}$ peak was measured at 3.50 Å. The maximum shift was observed at 400°C with $d_{001/002}$ at 8.06 Å and $d_{002/005}$ at 3.40 Å. Collapse is complete and the KS peaks disappear because of the dehydroxylation of the kaolinite at a temperature between 400°C and 450°C. The peaks are broad and

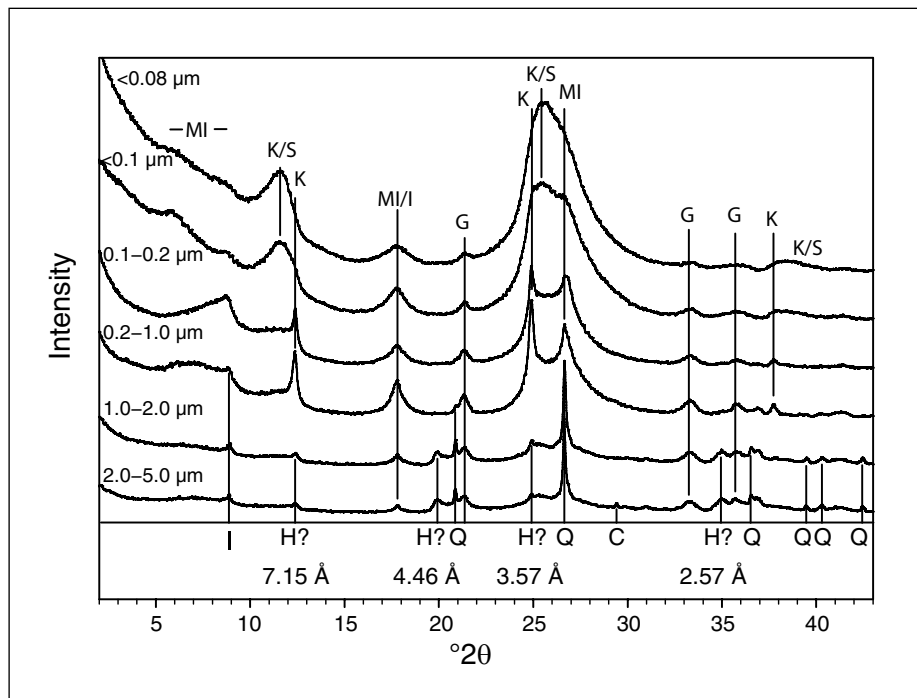


Figure 3. X-ray diffraction patterns for six different size ranges from Zone C (Ca-saturated, air-dried). MI = mixed layer illite/smectite; I = illite; K/S = interstratified kaolinite-smectite; K = kaolinite; H? = questionable halloysite; Q = quartz; G = goethite; C = calcite. The vertical lines extend through the range a given peak can be identified.

difficult to measure with perfect accuracy and precision, however, there appears to be a linear relationship between the shift in the KS $d_{001/002}$ peak and the increase in temperature from 25°C to 400°C (fig. 5).

Overnight exposure to a saturated atmosphere results in only partial rehydration and reexpansion of the structure (fig. 6). A linear relationship also exists for the shift of the KS $d_{001/002}$ peak in the rehydrated samples (fig. 5).

More time does not result in more rehydration. The sample heated to 375°C and reported in Figure 1 was kept at ambient humidity and rescanned by XRD three months later. The $d_{001/002}$ peak shift at 375°C is intermediate to the values measured at 350° and 400°C. However, after three months rehydration, the $d_{001/002}$ peak shift remained at a high value similar to the shift calculated for the 400°C sample (fig. 5).

Random orientation

As first noted by Schultz and others (1971), the diffraction pattern of a randomly oriented sample of interstratified kaolinite-smectite is dominated by broad hk reflections near 20°, 35°, 55°, and 62° 2θ (fig. 7). The single 060 peak occurs at a (fluorite-calibrated) position of 62.08° 2θ (1.495 Å) and has a full width-half maximum (fwhm) value of 0.95° 2θ . By comparison, Dudek and others (2006) report d_{060} and fwhm for a KS with 80 percent kaolinite layers, of 1.4923 Å and 0.842°, respectively.

Samples exchanged with Mg, Na, or K

Samples from the <0.08- μm fraction of Zone C were exchanged with Mg, Na, or K and scanned by XRD. For each case a replicate slide was prepared and scanned. The Mg-saturated pattern is essentially identical to the air-dried, Ca-saturated pattern reported in Figure 1. For both the Na- and K-saturated cases, the low angle illite/smectite peak becomes more prominent and shifts to about 8.51° 2θ (10.4 Å). For Na-saturation, the KS 001/002

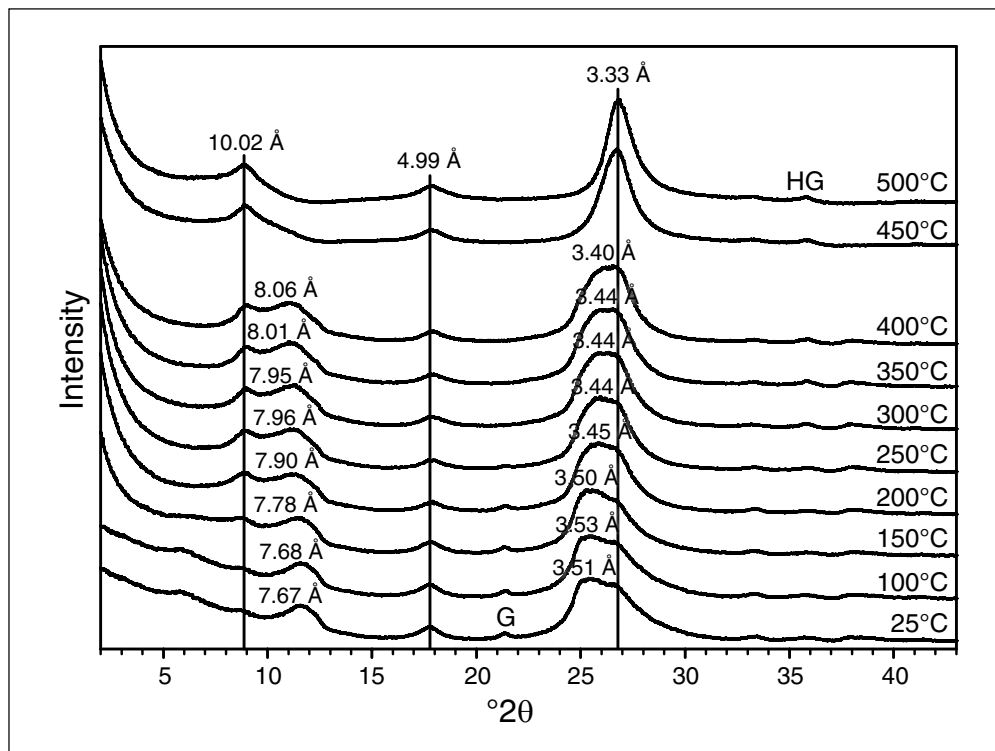


Figure 4. X-ray diffraction patterns for samples from the <0.1- μm fraction (Ca-saturated) of Zone C at temperatures from 100°C to 500°C. The 25°C pattern is the same as the one reported for Zone C in Figure 2 and is provided for reference. The KS $d_{001/002}$ and $d_{002/005}$ peaks are individually labeled with d-spacings. G = goethite; HG = goethite after heating.

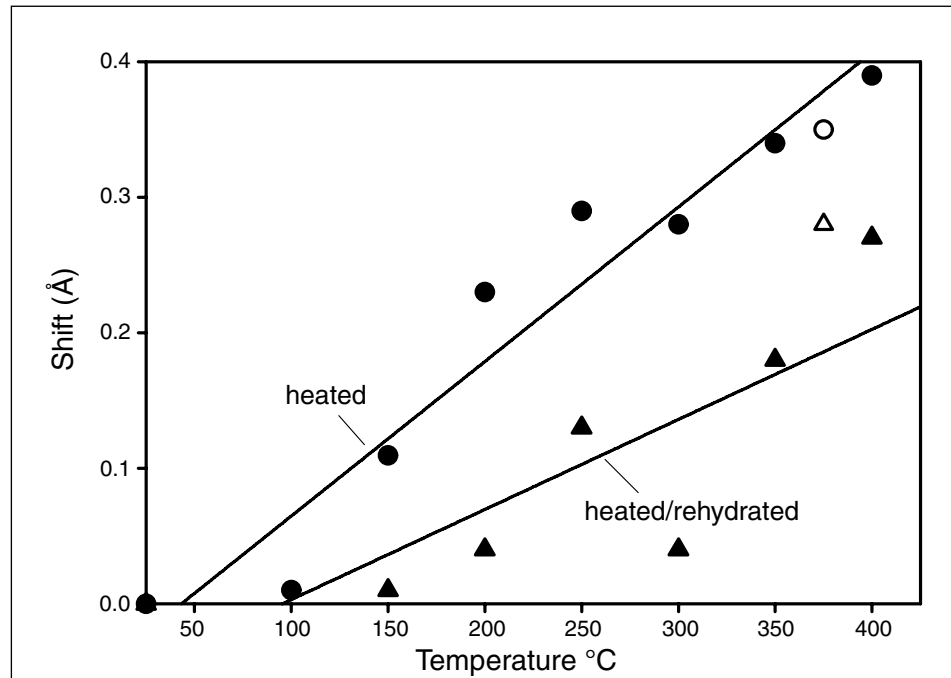


Figure 5. Shifts in the $KS_{001/002}$ peak as a function of temperature. Filled symbols are for the samples reported in Figures 4 and 6. Open symbols are for the sample heated to 375°C reported in Figure 1. Circles are for heated samples and triangles are for samples heated and then rehydrated overnight in a saturated atmosphere, except for the 375°C sample, which was held at ambient laboratory humidity for three months. Δd is calculated as the difference between $d_{001/002}$ at temperature and $d_{001/002}$ at 25°C. The best fit lines for the heated and the rehydrated groups have $r = 0.97$ and $r = 0.84$ respectively, and do not include the 375°C sample.

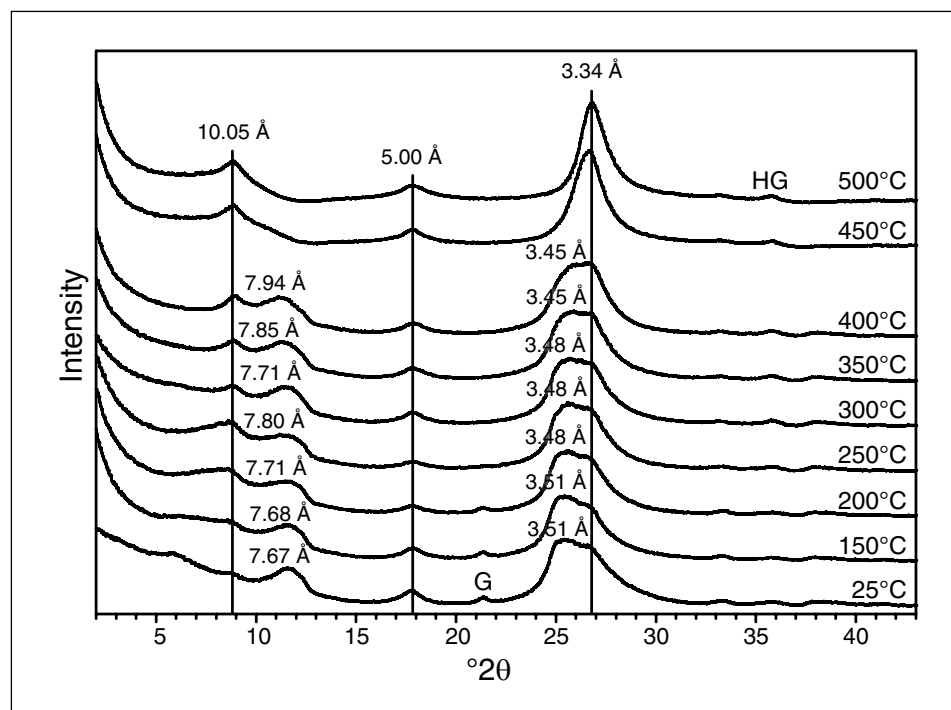


Figure 6. X-ray diffraction patterns for samples from the $<0.1\text{-}\mu\text{m}$ fraction (Ca-saturated) of Zone C at temperatures from 150°C to 500°C, after rehydration in a saturated atmosphere for a minimum of 24 hours. Labeling is the same as in Figure 4.

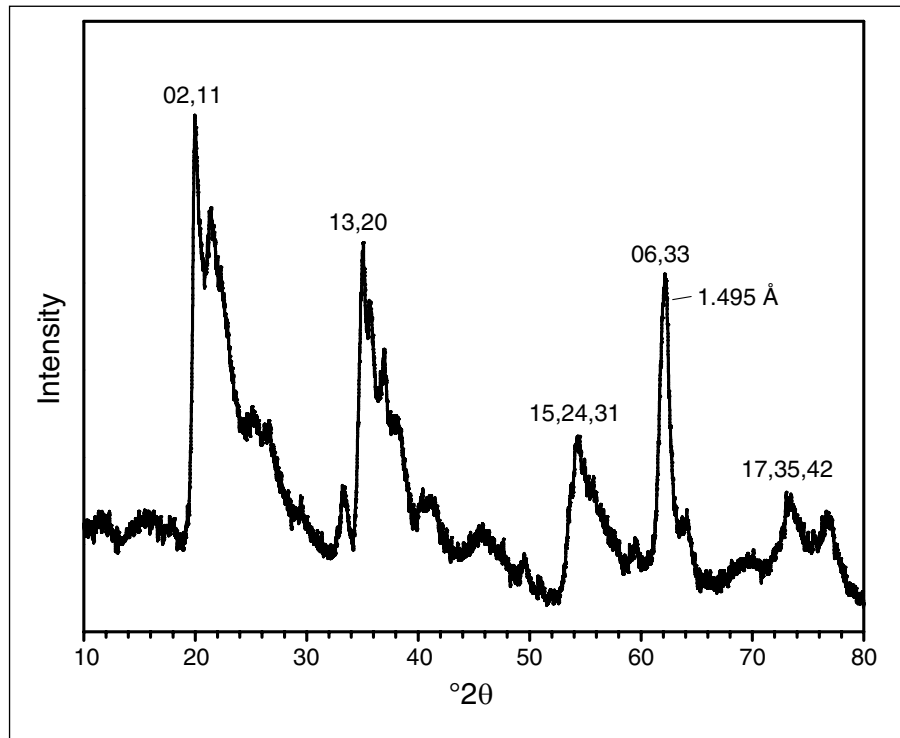


Figure 7. X-ray diffraction pattern of a side-mounted sample from Zone C, Ca-saturated, $<0.1\text{-}\mu\text{m}$ fraction. The pattern is dominated by broad hk bands which are labeled on the figure. Indexing based on information in Dudek and others (2006) and Brindley (1980). The value of $d(060)$ is 1.495 \AA .

is broader and shifts to 11.00° (8.04 \AA) and the KS 002/005 become somewhat stronger and shifts to 25.99° (3.43 \AA). For K-saturation, the KS 001/002 shifts to 10.87° (8.14 \AA) and the 002/005 shifts to 25.79° (3.45 \AA).

In another set of samples from the $<0.08\text{-}\mu\text{m}$ fraction of Zone C, samples first saturated with Mg, Na, or K were reexchanged with Ca. In each case the diffraction pattern returned to the pattern associated with the once-exchanged, air-dried, Ca-saturated case.

Chemistry

The results of EDX analysis on selected filter papers left over from the preparation of oriented XRD mounts is given in Table 1. The five sample pairs labeled with an "r" are independently prepared and analyzed replicates. These pairs provide a useful measure of analytic precision, with additional information concerning precision and accuracy of EDX analysis in our lab available

in Argast (2002). Zone A has less iron (Fe) than comparable samples from Zones B and C. Zone A also contains measurable sulfur (S), consistent with its higher organic content.

There is less iron in the $<0.08\text{-}\mu\text{m}$ fraction than there is in the $<0.1\text{-}\mu\text{m}$ fraction of Zone C. The difference in iron concentration is most easily explained as a result of less goethite in the $<0.08\text{-}\mu\text{m}$ fraction.

Calcium is the dominant exchange cation on the naturally occurring clay. Calcium is completely replaced when the sample is saturated with Mg, Na, or K.

Magnesium is present in the naturally occurring clay as both an exchange and a structural ion. The former is inferred from the observation that Mg concentration goes down in the Na, K, and Ca-saturated samples compared to the unexchanged samples. The latter is indicated by the inability to completely remove Mg by saturation with other ions.

Sodium was detected as an exchange ion in the naturally occurring samples from both size fractions of Zone C. The concentration is low and near our detection limits for Na.

Potassium is present at slightly higher concentration in the <0.1- μm fraction than in the <0.08- μm fraction. This slight difference in K concentration may be an analysis artifact, but is more likely the result of increased KS purity and, consequently, less discrete illite in the finest grain sizes.

The K concentration is not reduced by saturation with Mg, Ca, or Na and we conclude that none of the K in the naturally occurring clay is exchangeable. However, K can be exchanged for Ca, Mg, or Na; the K concentration was increased to approximately 3.4 to 3.5 weight percent K when the sample was saturated with a potassium chloride (KCl) solution.

The concentration of K in the unexchanged samples is about 1 percent. This requires the presence of approximately 10 to 15 percent discrete illite, or more as a mixed-layer, illite/smectite phase. Such concentrations of illite or mixed layer illite/smectite are consistent with XRD data (for example, fig. 3) that suggest the presence of low concentrations of illite or illite/smectite or both.

Samples first exchanged with Mg, Na, or K, and then reexchanged with Ca are indistinguishable from other Ca-exchanged samples. Permanent changes do not seem to be induced by saturating with different cations.

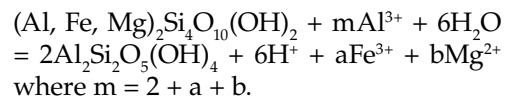
CONCLUSION

The Pipe Creek Sinkhole offers a unique view into midcontinent geology during the early Pliocene. Consequently, any clues that mineralogy reveals about climate have special importance. As discussed earlier, kaolinite-smectite is commonly associated with Mediterranean-type conditions. There is, however, considerable ambiguity in this association. We can safely say that the presence of interstratified kaolinite-smectite at Pipe Creek Sinkhole is at least consistent with tropical to subtropical conditions existing in the midcontinent of North America circa 5 million years ago.

This is the third published description of kaolinite-smectite found in or close to a terra rossa. It seems

likely that conditions favoring development of terra rossa also favor the development of kaolinite-smectite. High calcium concentrations may be critical. Terra rossa is, by definition, associated with limestone. Kaolinite-smectite also occurs commonly in soils developed on (Ca-rich) mafic rocks. The Pipe Creek kaolinite-smectite is Ca-saturated in its natural state, and in his experiments involving the synthesis of kaolinite-smectite from Wyoming smectite, Środoń (1980) notes that Ca-rich solutions strongly favor the development of kaolinite layers.

Środoń (1980) provides a proposed reaction for conversion of Wyoming smectite into interstratified kaolinite-smectite, specifically:



This proposed reaction releases iron and significantly decreases pH. At Pipe Creek Sinkhole, all samples contain goethite, which would precipitate from the free iron produced in the reaction; an increase in acidity is exactly the condition required to drive dissolution associated with the development of terra rossa. Organics could also produce acids to help dissolution.

Kaolinite-smectite is dominant in the <0.1- μm fraction and absent in the >0.1- μm fraction. Finding KS in only the finest fraction is a common observation (for example, Schultz and others, 1971). It is important, however, to recognize how easily the mineral assemblage can be misinterpreted if the wrong size fraction is selected. Our initial survey of the clay mineralogy at PCS was done on a standard <2- μm fraction and we missed the presence of KS because of the difficulty of recognizing KS when present as a minor constituent in a complex assemblage. This observational artifact is no doubt an important contributor to the apparent rarity of KS in the geologic record (see also Hughes and others, 1993) and indicates the need to routinely evaluate samples at more than one size interval.

Even if KS is recognized in the assemblage, evaluating the sample as a single <2- μm fraction could lead to a misinterpretation of the intimacy of the association between the interstratified kaolinite-smectite and kaolinite. Though found together in the same sample, KS and kaolinite exist in mutually exclusive size fractions (fig. 3).

It has been suggested that KS is a solid state, transitional intermediary produced in the weathering of smectite into kaolinite (for example, Buhmann and Grubb, 1991). Were this true at PCS, KS and kaolinite would most likely occur intimately associated in the same size fraction. That they are not suggests that KS is not a transitional intermediary at Pipe Creek.

Using the filter papers left over from XRD for chemical analysis by EDX proved straightforward and useful. The sample surface presented to the electron beam in the electron microscope was smooth and flat. The results were consistent and of good quality. The technique provides a simple-to-use method of chemically analyzing specific size ranges in any sample.

Special care is needed to routinely identify KS interstratified in complex clay assemblages. Kaolinite-smectite may very well be a much more common phase than generally acknowledged. Researchers in the future, especially in studies where clays are developed on or in close association with limestones, should pay particularly close attention to the possible existence of an interstratified kaolinite-smectite.

This contribution provides a basis for four lines of additional research:

1. There are few descriptions of interstratified KS in the literature, and three of the described occurrences are developed on or near terra rossa. Experimental data also suggest the importance of calcium in the development of interstratified kaolinite-smectite. The evidence indicates that a special relationship may exist between interstratified KS and soils developed on limestones or in other Ca-rich environments. Studies specific to this relationship would be welcome both to explain the origin of kaolinite-smectite and to explain the origin of terra rossa.
2. Discovered in 2000, the Gray Fossil Site in eastern Tennessee, like PCS, is thought to have formed through processes of limestone cave collapse and sinkhole development during the Miocene/Pliocene, and is another rare and valuable window into midcontinent geology (Wallace and Wang, 2004). Considerably larger than PCS, and from a slightly more southern locale, the Gray Site is an obvious target for detailed clay mineralogy including an

active search for, and characterization of, any interstratified kaolinite-smectite that might be found.

3. Consistent with the results of Dudek and others, (2006), it appears the width of the 060 XRD reflection might be useful for estimating the percentage of kaolinite layers in interstratified kaolinite-smectite. Not many randomly ordered XRD patterns of interstratified kaolinite-smectite have been reported in the literature. Future studies should include X-ray diffraction patterns of randomly mounted materials to confirm a relationship between composition and the 060 peak width.

4. Heating causes a change in the position of the KS $d_{001/002}$ peak. The peak shift is gradual and correlated to temperature in the range encountered during deep burial and diagenesis of sediments (fig. 5). It would be interesting to know if the gradual collapse of the layers with rising temperature is a universal property of interstratified kaolinite-smectite and if the slope of the correlation trend is predictably similar among interstratified kaolinite-smectites of differing compositions. If so, the possibility exists that interstratified kaolinite-smectite could be used as a paleotemperature indicator in burial sequences.

ACKNOWLEDGMENTS

Field work for this project was supported by National Science Foundation grant 0207182-EAR to James O. Farlow. Manuscript reviews by Walter A. Hasenmueller, Haydn H. Murray, and Nelson R. Shaffer are gratefully acknowledged.

REFERENCES

- Aleta, D. G. A., Tomita, K., and Kawano, M., 1999, Mineralogical and characterization studies of the mixed-layer kaolinite-smectite clay deposit in Liloan, Cebu province, Philippines: *Clay Science*, v. 11, no. 1, p. 11–29.
- Amouric, M., and Olives, J., 1998, Transformation mechanisms and interstratification in conversion of smectite to kaolinite—an HRTEM study: *Clays and Clay Minerals*, v. 46, no. 5, p. 521–527.
- Argast, A., 2002, The lower Proterozoic Fern Creek Formation, northern Michigan—mineral and bulk geochemical evidence for its glaciogenic origin:

- Canadian Journal of Earth Sciences, v. 39, no. 4, p. 481–492.
- Aspandiar, M. F., and Eggleton, R. A., 2002, Weathering of chlorite-I. reactions and products in microsystems controlled by the primary mineral: Clays and Clay Minerals, v. 50, no. 6, p. 685–698.
- Bertolino, S. R. A., Murray, H. H., and Depetris, P. J., 1991, Regular kaolinite-smectite (R1) from the Bermejo River basin, Argentina: Clays and Clay Minerals, v. 39, no. 6, p. 658–660.
- Boero, V., Premoli, A., Melis, P., Barberis, E., and Arduino, E., 1992, Influence of climate on the iron oxide mineralogy of terra rossa: Clays and Clay Mineralogy, v. 40, no. 1, p. 8–13.
- Boero, V., and Schwertmann, U., 1989, Iron oxide mineralogy of terra rossa and its genetic implications: Geoderma, v. 44, no. 4, p. 319–327.
- Brindley, G. W., 1980, Order-disorder in clay mineral structures, in Brindley, G. W., and Brown, G., eds., Crystal structures of clay minerals and their X-ray identification: Mineralogical Society (London) Monograph No. 5, p. 125–196.
- Brindley, G. W., Suzuki, T., and Thiry, M., 1983, Interstratified kaolinite-smectites from the Paris Basin; correlations of layer proportions, chemical compositions and other data: Bulletin de Mineralogie, v. 106, no. 4, p. 403–410.
- Buhmann, C., and Grubb, P. L. C., 1991, A kaolin-smectite interstratification sequence from a red and black complex: Clay Minerals, v. 26, no. 3, p. 343–358.
- Calvert, C., and Pevear, D., 1983, Paleopedogenic (?) mixed-layer kaolinite-smectite from 9000 ft in a Gulf Coast well, in 32nd Annual Clay Minerals Conference and 20th Meeting of the Clay Minerals Society, Programs and Abstracts, October 2–5, 1983, Buffalo, N.Y., v. 32, p. 50.
- Cho, H. D., and Mermut, A. R., 1992, Evidence for halloysite formation from weathering of ferruginous chlorite: Clays and Clay Minerals, v. 40, no. 5, p. 608–619.
- Corti, G., Fernández Sanjuro, M. J., and Cesare Ugolini, F., 1998, A randomly interstratified kaolinite-smectite from Galicia (NW Spain)—a new procedure for determination: Clays and Clay Minerals, v. 46, no. 6, p. 705–711.
- Cuadros, J., Delgado, A., Cardenete, A., Reyes, E., and Linares, J., 1994, Kaolinite/montmorillonite resembles beidellite: Clays and Clay Minerals, v. 42, no. 5, p. 643–651.
- Cuadros, J., and Dudek, T., 2006, FTIR investigation of the evolution of the octahedral sheet of kaolinite-smectite with progressive kaolinization: Clays and Clay Minerals, v. 54, no. 1, p. 1–11.
- Delvaux, B., and Herbillon, A. J., 1995, Pathways of mixed-layer kaolin-smectite formation in soils, in Churchman, G. J., Fitzpatrick, R. W., and Eagleton, R. A., eds., Clays controlling the environment, Proceedings 10th International Clay Conference, Adelaide, Australia, 1993: CSIRO Publishing, Melbourne, Australia, p. 457–461.
- Delvaux, B., Mestdagh, M. M., Vielvoye, L., and Herbillon, A. J., 1989, XRD, IR and ESR study of experimental alteration of Al-nontronite into mixed-layer kaolinite/smectite: Clay Minerals, v. 24, no. 4, p. 617–630.
- Drever, J. I., 1973, The preparation of oriented clay mineral specimens for X-ray diffraction analysis by a filter-membrane peel technique: American Mineralogist, v. 58, no. 5-6, p. 553–554.
- Dudek, T., Cuadros, J., and Fiore, S., 2006, Interstratified kaolinite-smectite—nature of the layers and mechanism of smectite kaolinization: American Mineralogist, v. 91, no. 1, p. 159–170.
- Durn, G., 2003, Terra rossa in the Mediterranean region—parent materials, composition and origin: Geologia Croatica, v. 56, no. 1, p. 83–100.
- Farlow, J. O., Sunderman, J. A., Havens, J. J., Swinehart, A. L., Holman, J. A., Richards, R. L., Miller, N. G., Martin, R. A., Hunt, R. M., Jr., Storrs, G. W., Curry, B. B., Fluegeman, R. H., Dawson, M. R., and Flint, M. E. T., 2001, The Pipe Creek Sinkhole biota, a diverse late Tertiary continental fossil assemblage from Grant County, Indiana: American Midland Naturalist, v. 145, no. 2, p. 367–378.
- Farlow, J. O., Richards, R., Garniewicz, R., Greenan, M., Wepler, W., Shunk, A., Ludvigson, G. A., and Argast, A., 2007, Occurrence and features of fossiliferous sediments of the Pipe Creek Sinkhole (late Neogene, Grant County, Indiana): Geological Society of America Abstracts with Programs, South-Central and North-Central Sections, v. 39, no. 3, p. 67.
- Fisher, G. B., and Ryan, P. C., 2006, The smectite-to-disordered kaolinite transition in a tropical soil chronosequence, Pacific coast, Costa Rica: Clays and Clay Minerals, v. 54, no. 5, p. 571–586.
- Grimley, D. A., Follmer, L. R., Hughes, R. E., and Solheid, P. A., 2003, Modern, Sangamon and Yarmouth soil development in loess of unglaciated southwestern Illinois: Quaternary Science Reviews, v. 22, no. 2-4, p. 225–244.
- Herbillon, A. J., Frankart, R., and Vielvoye, L., 1981, An occurrence of interstratified kaolinite-smectite minerals in a red-black soil toposequence: Clay Minerals, v. 16, no. 2, p. 195–201.
- Hughes, R. E., DeMaris, P. J., White, W. A., and Cowin, D. K., 1987, Origin of clay minerals in Pennsylvanian

- strata of the Illinois Basin, *in* Schultz, L. G., van Olphen, H., and Mumpton, F. A., eds., *Proceedings of the International Clay Conference*, Denver, Colo., July 28–Aug. 2, 1985, v. 8, p. 97–104.
- Hughes, R. E., Moore, D. M., and Reynolds, R. C., Jr., 1993, The nature, detection, occurrence, and origin of kaolinite/smectite, *in* Murray, H., Bundy, W., and Harvey, C., eds., *Kaolin genesis and utilization: The Clay Minerals Society Special Publication Number 1*, p. 291–323.
- Lynch, F. L., 2000, Weathering of clay minerals in soils in semi-tropical south central Texas: *Geological Society of America Abstracts with Programs*, v. 32, no. 7, p. 366.
- Maliva, R. G., and Siever, R., 1988, Diagenetic replacement controlled by force of crystallization: *Geology*, v. 16, no. 8, p. 688–691.
- Merino, E., 2005, Origin of associated terra rossa and karst by replacement: *Geological Society of America Abstracts with Programs*, v. 37, no. 7, p. 257.
- Moore, D. M., and Reynolds, R. C., Jr., 1997, *X-ray diffraction and the identification and analysis of clay minerals*, 2nd ed.: New York, Oxford University Press, 378 p.
- Nurcholis, M., and Tokashiki, Y., 1998, Characterization of kaolin/smectite mixed layer mineral in paleudult of Java island: *Clay Science*, v. 10, no. 4, p. 291–302.
- Patrier, P., Beaufort, D., Mas, A., and Traineau, H., 2003, Surficial clay assemblage associated with the hydrothermal activity of Bouillante (Guadeloupe, French West Indies): *Journal of Volcanology and Geothermal Research*, v. 126, no. 1-2, p. 143–156.
- Polyak, V. J., and Güven, N., 2000, Clays in caves of the Guadalupe Mountains, New Mexico: *Journal of Cave and Karst Studies*, v. 62, no. 2, p. 120–126.
- Proust, D., Caillaud, J., and Fontaine, C., 2006, Clay minerals in early amphibole weathering—tri- to dioctahedral sequence as a function of crystallization sites in the amphibole: *Clays and Clay Minerals*, v. 54, no. 3, p. 351–362.
- Reynolds, R. C., Jr., and Reynolds, R. C., III, 1996, Newmod—the calculation of one-dimensional X-ray diffraction patterns of mixed-layer clay minerals [computer program]: Hanover, New Hampshire.
- Righi, D., Terribile, F., and Petit, S., 1999, Pedogenic formation of kaolinite-smectite mixed layers in a soil toposequence developed from basaltic parent material in Sardinia (Italy): *Clays and Clay Minerals*, v. 47, no. 4, p. 505–514.
- Sakharov, B. A., and Drits, V. A., 1973, Mixed-layer kaolinite-montmorillonite—a comparison of observed and calculated diffraction patterns: *Clays and Clay Minerals*, v. 21, no. 1, p. 15–17.
- Schultz, L. G., Shepard, A. O., Blackmon, P. D., and Starkey, H. C., 1971, Mixed-layer kaolinite-montmorillonite from the Yucatán Peninsula, Mexico: *Clays and Clay Minerals*, v. 19, no. 3, p. 137–150.
- Środoń, J., 1980, Synthesis of mixed-layer kaolinite/smectite: *Clays and Clay Minerals*, v. 28, no. 6, p. 419–424.
- Środoń, J., 1999, Nature of mixed-layer clays and mechanisms of their formation and alteration: *Annual Review of Earth and Planetary Sciences*, v. 27, p. 19–53.
- Sudo, T., and Hayashi, H., 1956, A randomly interstratified kaolinite montmorillonite in acid clay deposits in Japan: *Nature*, v. 178, no. 4542, p. 1,115–1,116.
- Thanachit, S., Suddhiprakarn, A., Kheoruenromme, I., and Gilkes, R. J., 2006, The geochemistry of soils on a catena on basalt at Khon Buri northeast Thailand: *Geoderma*, v. 135, p. 81–96.
- Thomas, A. R., 1989, A new mixed layer clay mineral—regular 1:1 mixed layer kaolinite/smectite: *Programs and Abstracts, 26th Annual Meeting Clay Minerals Society*, Sept. 25–28, 1989, Sacramento, Calif., v. 26, p. 69.
- Wada, K., and Kakuto, Y., 1983, Intergradient vermiculite-kaolin mineral in a Korean ultisol: *Clays and Clay Minerals*, v. 31, no. 3, p. 183–190.
- Wallace, S. C., and Wang, X., 2004, Two new carnivores from an unusual late Tertiary forest biota in eastern North America: *Nature*, v. 431, no. 7008, p. 556–559.
- Wiewióra, A., 1973, Mixed-layer kaolinite-smectite from lower Silesia, Poland—final report, *in* *Proceedings of the International Clay Conference*, June 23–30, 1972, Madrid, Spain: Madrid, Division de Ciencias, p. 75–88.
- Wilson, M. J., and Cradwick, P. D., 1972, Occurrence of interstratified kaolinite-montmorillonite in some Scottish soils: *Clay Minerals*, v. 9, no. 4, p. 435–437.
- Yerima, B. P. K., Calhoun, F. G., Senkayi, A. L., and Dixon, J. B., 1985, Occurrence of interstratified kaolinite-smectite in El Salvador vertisols: *Soil Science Society of America Journal*, v. 49, no. 2, p. 462–466.

Course of the Tertiary Teays River Southwest of Lake Erie Lowlands, USA: Evidence from Petrologic and Lead Isotopic Characteristics of Pebbles Found in the Northern Indiana Pipe Creek Sinkhole

By Jack A. Sunderman, E. Troy Rasbury, and Sidney R. Hemming

ABSTRACT

In the early spring of 1996, thousands of metaquartzite pebbles and a few cobbles were discovered in a paleosinkhole in northern Indiana, a few miles south of the drift-covered Teays Valley. The rounded metaquartzite clasts occurred in diamictons located beneath glacial outwash and till that covered the sinkhole. Some of the deepest pebble-bearing diamictons contained vertebrate fossils indicating burial ages of ~5 Ma (millions of years before present) (Farlow and others, 1998).

The pebble-bearing beds had unconformable contacts with the overlying glacial drift and contained well-sorted and well-rounded pebbles. In addition, the microfabric features of the sinkhole pebbles closely resembled those found in quartzite-bearing gravels east of the southern Blue Ridge, in bedrock of the southern Blue Ridge, and in gravels of Teays Valley remnants west of Charleston, West Virginia.

Microfabric features of the metaquartzite pebbles differed significantly from microfabric features found in other potential sources: 1) glacial drift within the sinkhole, and 2) glacial drift derived from the Canadian Shield, above the sinkhole.

Lead (Pb) isotope data from quartz pebbles of the Pipe Creek paleosinkhole and from gravels of the southern Blue Ridge and Teays Valley further demonstrate that the sinkhole pebbles very likely were not derived from the glacial drift. The Pb isotope characteristics of the rounded sinkhole pebbles define an array of data consistent with Grenvillian crystallization ages, and are similar to those of quartzites found in southern Blue Ridge bedrock and associated gravels. In contrast, quartzites from Pleistocene gravels and till found in and above the paleosinkhole have Pb isotope characteristics that define an array of data consistent with published ~2.0 Ga (billions of years before present) of crystallization ages of quartzites

in Canadian Shield bedrock north and northeast of Lake Erie. A very striking characteristic of quartzes found in the Canadian Shield and in the glacial drift is that they both have high and variable ages determined by differences in thorogenic Pb (differences in thorium/lead content), while the sinkhole pebbles, southern Blue Ridge, and Teays River quartzes have virtually no differences in thorogenic Pb.

The petrographic and Pb isotopic data thus suggest that the sinkhole metaquartzite pebbles and cobbles were ultimately derived from the southern Blue Ridge Mountains. The most parsimonious explanation is that the pebbles were transported to northern Indiana from the Blue Ridge area >5 Ma by a preincision version of the Teays River, because transportation to this area would not have been possible after its incision. This also implies that the course of the Teays River was westward across northern Indiana.

During this time, repeated flooding across the upland surface apparently transported pebbles to the sinkhole, producing at least four pebble-bearing layers. Eventually, the Teays River incised its bedrock valley, which is now recognized from the Appalachian Mountains across southern West Virginia, Ohio, northern Indiana, and into Illinois. After these events occurred, Wisconsin glaciers modified the Teays Valley to some extent, and eventually buried its northern and western parts with glacial till and outwash, now found in unconformable relationships with the pebble-bearing sediments of the Pipe Creek Sinkhole.

INTRODUCTION

Previous studies of the Teays River

Drill records, seismic studies, and geomorphic studies have been used to identify a buried Late Tertiary bedrock valley across glaciated rocks southwest of the Lake Erie Lowlands in Ohio, northern Indiana, and parts of Illinois. The valley has been called the Teays Valley, after an unglaciated and abandoned section of the Teays Valley in western West Virginia. As so identified, the Teays Valley extends from its modern New River equivalent in North Carolina across parts of Virginia, West Virginia, Ohio, northern Indiana, and to Illinois (fig. 1), where (as the Mahomet Valley) it joins the ancestral Mississippi River Valley (Tight, 1903; Stout and Schaaf, 1931; Fidler, 1943; Horberg, 1945, 1956; Ver Steeg, 1946; Fridley, 1950; Wayne, 1956; Manos, 1961; Rhodehamel and Carlston, 1963; Thornbury, 1965; Gray, 1982; Bruns and others, 1985; Bartholomew and Mills, 1991; Bleuer, 1991; Bonnett and others, 1991; Goldthwait,

1991; Kempton and others, 1991; Teller and Goldthwait, 1991). The drift-covered Teays Valley crosses northern Indiana about 10 km (6.2 miles) north of the Pipe Creek paleosinkhole (Gray, 1982; Bleuer, 1991) (fig. 1).

Until recently it was generally accepted that the Teays River and its tributaries were the major drainage system for the east-central United States during late Tertiary time. The Teays River was believed to have functioned until late Pleistocene time, when damming of the river and burial of the northern parts of its valley by glaciers established the modern route of the Ohio River (Wayne, 1952; Thornbury, 1965, p. 139–141, 214–217; Goldthwait, 1991; Teller and Goldthwait, 1991).

However, an opposing model of pre-Ohio River drainage in this area suggests that the Tertiary Teays River continued northward from central Ohio into the Lake Erie Lowland, and that the deeply incised Teays Valley that crosses northwestern Ohio and

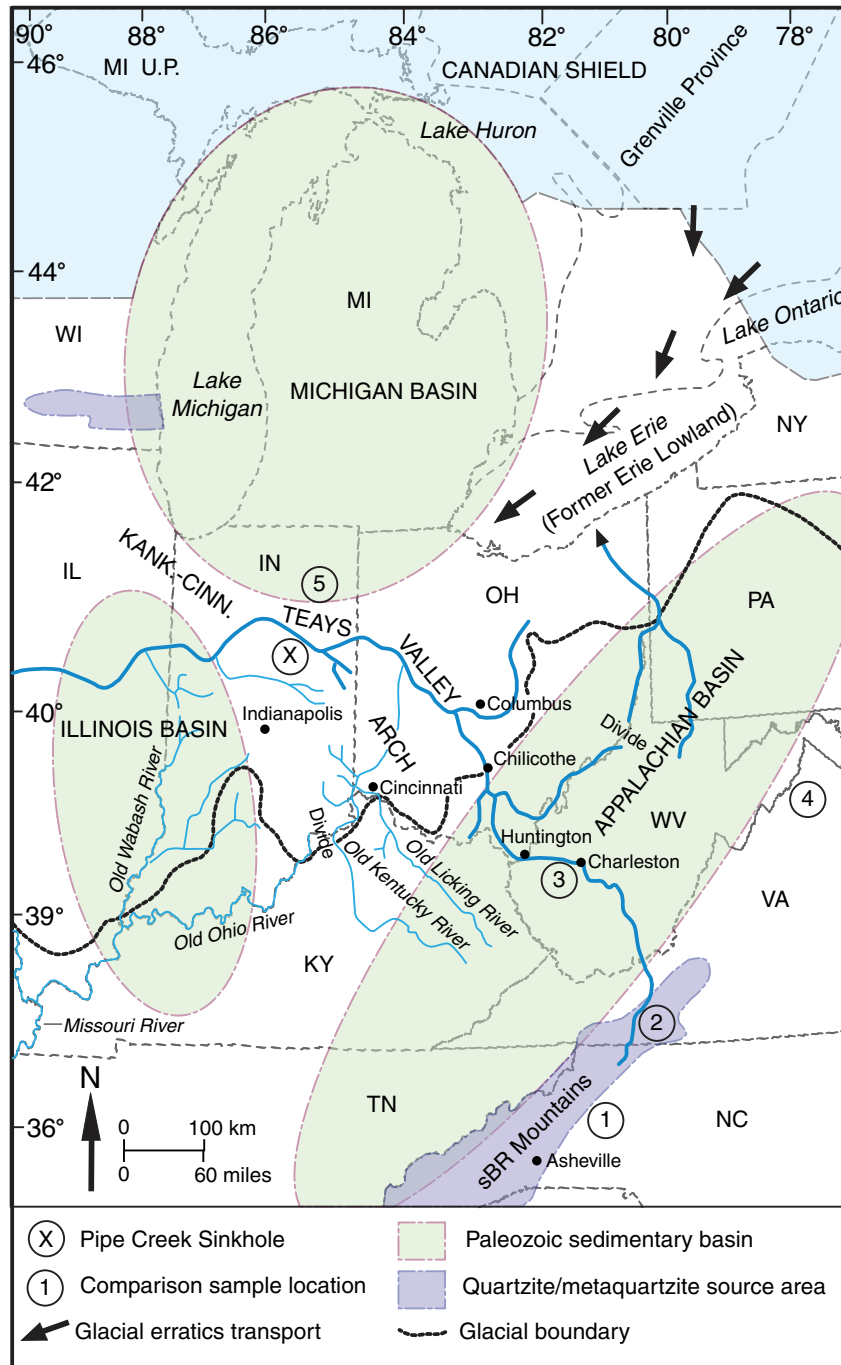


Figure 1. Geologic map of northeastern United States, showing location of the Pipe Creek Sinkhole and locations of possible sources of the sinkhole bed (Sb) metaquartzite (Mq) pebbles and cobbles. Locations of samples are shown by the numbered circles: (1) Inner Piedmont (IP) stream gravels; (2) southern Blue Ridge (sBR) bedrock; (3) Teays Valley (TV) stream gravels; (4) northern Blue Ridge (nBR) bedrock; (5) Fort Wayne, Indiana, (FW) glacial outwash gravels; and (X) the Pipe Creek Sinkhole, with preglacial and overlying glacial sediments.

Three major sedimentary basins essentially surround the sinkhole site, suggesting the Mq sources lie beyond the basins, in either the Appalachian Mountains or the Canadian Shield (CS). The path of the Teays River valley suggests a possible preincision transport route for the Sb Mq exotics to northern Indiana and beyond, and the elongate former Erie Lowland (dark arrows) suggests a general transport route for CS glacial erratics to the Pipe Creek Sinkhole.

northern Indiana was produced later by Pleistocene meltwater streams (Coffey, 1958; Gray and others, 1991; Melhorn and Kempton, 1991). This model also has been supported by Granger and others (2001), who suggested that the "Teays River" of western Ohio and northern Indiana was an ice-marginal river that was newly formed or integrated by glaciers ~2 Ma. These suggestions were based on measurements of radioactive decay of cosmogenic ^{26}Al and ^{10}Be found in sediments of Mammoth Cave, Kentucky, ~400 km (~250 miles) south of the Pipe Creek Sinkhole, and also based on the views presented by Gray (1991).

Discovery of the Pipe Creek Sinkhole and its Tertiary sediments

In the spring of 1996, unconsolidated Tertiary sediments containing thousands of rounded metaquartzite (Mq) pebbles and cobbles were found in a complex paleosinkhole discovered in the Pipe Creek Jr. Limestone Quarry of north-central Indiana (fig. 1). The quarry is developed primarily in a large limestone reef, located in the southwest corner of Grant County, about 15 km (9 miles) southwest of Marion (figs. 1 and 2A). The paleosinkhole was buried beneath Wisconsin-age glacial drift, and was not anticipated. During early excavation of the sinkhole numerous pebbles and cobbles were transported with other sediments to a spoil pile near the quarry. Fortunately, some of the pebble-bearing sediments were left undisturbed, and have been the basis for much of this study. However, most of the original sinkhole sediments have now been removed by continued excavation, fossil retrieval, weathering, and erosion. For convenience, the metaquartzite-bearing beds and related nonglacial Pipe Creek Sinkhole sediments are here referred to as the "sinkhole beds" (Sb). (See Appendix for a guide to abbreviations used herein.)

The discovery of the metaquartzite pebbles and cobbles in the sinkhole beds introduces several topics relevant to the course of the Tertiary Teays River: (1) the age of the metaquartzite grains, (2) their provenance,

(3) their time and means of transport to the Lake Erie Lowlands of the United States, (4) their time and means of transport and deposition into the sinkhole, and (5) the incision of the nearby Teays Valley.

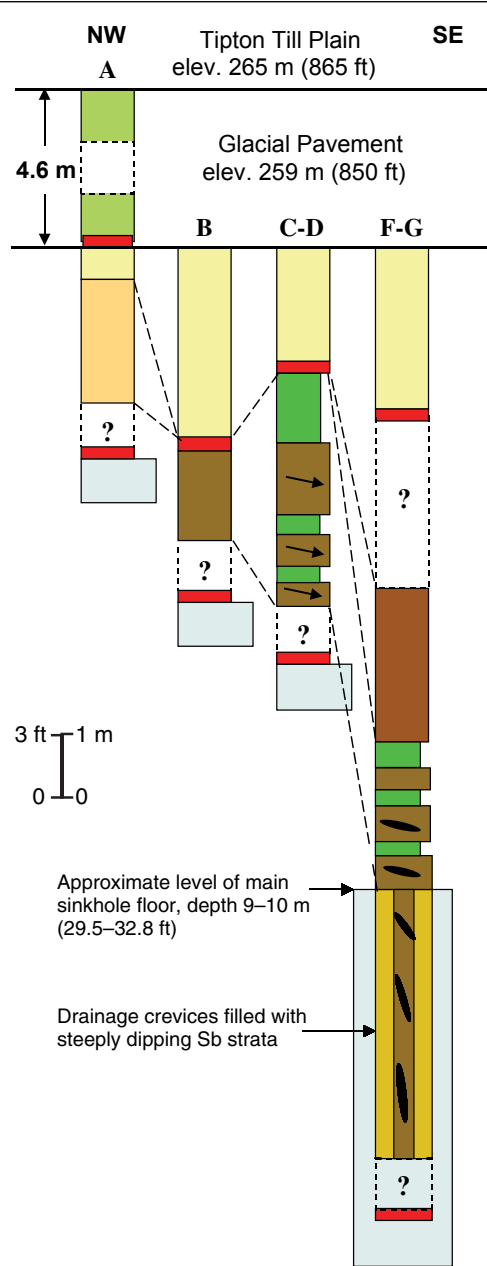
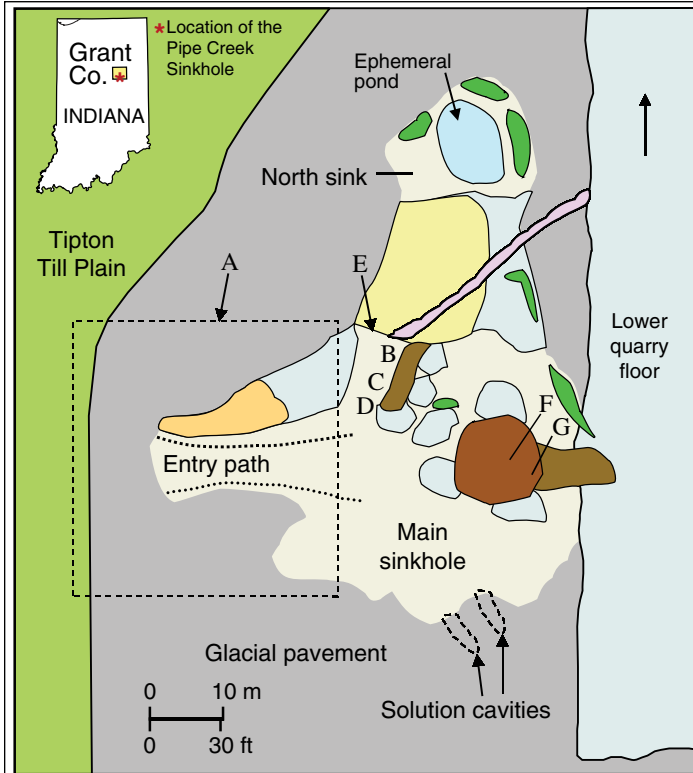
RELATED GEOLOGIC FEATURES

Local glacial drift. When first observed, the Pipe Creek paleosinkhole was partly filled with a few meters of silty clay till of the ~20,000-year-old Wisconsin Trafalgar Formation, and several meters of bouldery sand and gravel outwash of the ~10,000-year-old Lagro Formation. Lagro clay till also covered the sinkhole and the adjoining glacial pavement to a depth of ~4 m (~13 ft) (Wayne and Thornbury, 1955; Wayne, 1956) (figs. 1, 2A, and 3A). The glacial drift contained faceted and striated igneous and metamorphic erratics derived from the Canadian Shield (CS) north or northeast of Lake Erie and transported here by the Lake Erie Glacial Lobe (fig. 1) (Wayne and Thornbury, 1955). The drift also contained angular clasts of limestone and chert derived from the reef (fig. 2B).

Surrounding bedrock structures. The Pipe Creek Jr. Quarry lies near the crest of the northwestern Kankakee branch of the Cincinnati Arch, and is surrounded by the Michigan, Illinois, and Appalachian Basins (fig. 1), all of which are filled with several kilometers of unmetamorphosed Paleozoic sedimentary rocks. The arches between the basins contain similar, but thinner, Paleozoic sediments (Dorr and Eschman, 1977). Beyond the major Paleozoic basins, Precambrian quartzite-bearing metamorphic rocks are exposed in both the Canadian Shield ~650 km (~404 miles) north and northeast of the Pipe Creek Sinkhole, and in the Appalachian Mountains ~750 km (~466 miles) east and southeast of the sinkhole.

Other east-central pebble-bearing sediments. South of the glacial boundary (fig. 1), uplands and high stream terraces associated with Tertiary bedrock surfaces (Mitchell Plain in southern Indiana, Lexington Peneplain in Kentucky and Tennessee)

Figure 2 (on opposite page). Geologic map and stratigraphic sections of the sinkhole area. A) Geologic map of Pipe Creek Sinkhole and surrounding features, based on aerial and field photographs, and from data obtained from 1996 through 2005. The dash-lined area "A" was used to construct the upper part of vertical "Section A," which includes glacial sediment. B) Stratigraphic sections showing differences in sinkhole sediments at locations shown on the map. Section A (constructed from information inside rectangular dashed line on map) shows relationships of preexcavation Pleistocene drift to the overlying sinkhole sediments. Sections B and C-D were constructed from well-preserved sediments, and those in section F-G were constructed from sinkhole bed surface exposures and subsurface exposures produced by excavation of solution crevices.



LEGEND

Pleistocene (Wisconsin)

- TILL (Lagro Fm.). Gray, clay-rich. Contains faceted and striated igneous, metamorphic, and sedimentary clasts (fig. 3A).
- GRAVEL AND SAND OUTWASH (Lagro Fm.). Gravel contains igneous, metamorphic, and sedimentary clasts (fig. 3B).
- TILL (Trafalgar Fm.). Tan, silty, hard. Contains scattered small igneous, metamorphic, and sedimentary clasts.

-----UNCONFORMITY-----

Tertiary (Early Pliocene, Swayzee Beds)

- DIAMICTON-2 (Dm2). Brown-black, massive. Contains clay and silt, with angular chert and limestone clasts and rounded metaquartzite clasts intermixed with plant and animal fossils (fig. 3F, G).
- CRINOIDAL SAND AND CLAY, INTERBEDDED. Sand is coarse, white to yellow, mainly fragments of crinoid columns. Clays are yellow-brown to red-brown, waxy and kaolinitic. Vertical pattern indicates steeply dipping strata (fig. 3C-G).
- DIAMICTON-1 (Dm1). Red-brown, with angular chert and limestone clasts, and rounded metaquartzite clasts. Unit is interbedded with crinoidal sand and clay. Brown-black fossil-bearing lenses associated with Dm2 appear only in deep part of main sinkhole (fig. 3B, C, G).

-----UNCONFORMITY-----

Late Silurian (Wabash Formation)

- REEF LIMESTONE. White flank beds contain crinoid debris and other marine fossils. Isolated blocks are breakdown, gray indicates glacial pavement, and pink shows pisolite dike (fig. 3B).
- DIP OF BEDDING. Orientation of stratified beds shown by arrows in section C-D and by fossil-bearing lenses in section F-G.

are blanketed with paleosols and alluvial sediments known as Lafayette gravels and Irvine gravels, some of which contain exotic pebbles interpreted as metaquartzites that originated in the southern Blue Ridge Mountains (Potter, 1955a, 1955b; Potter and Pryor, 1961; Ray, 1965; McDowell and Newell, 1986; McGrain, 1986).

In addition, a paleosinkhole known as the Gray Fossil Site, discovered in northeastern Tennessee in 2000, has yielded Late Tertiary (~5 Ma) fossils somewhat similar to those found in the Pipe Creek Sinkhole (Parmalee and others, 2002; Wallace and others, 2002; Shunk, 2003; Smith, 2003; Wallace and Wang, 2004; Shunk and others, 2006). This Tennessee paleosinkhole also has yielded sand-size metaquartzite grains that have been interpreted as derived from the nearby southern Blue Ridge Mountains (Shunk, 2003; Smith, 2003; Shunk and others, 2006), and transported there by small local streams.

Vein quartz pebbles. A few vein quartz pebbles found in the Pipe Creek Sinkhole are similar to vein quartz pebbles found in Lower Pennsylvanian conglomerates of eastern Ohio, in Kentucky, and in southern Indiana, but they are easily distinguished from the Sb metaquartzite pebbles and cobbles.

SINKHOLE BEDS AND GLACIAL SEDIMENTS

Stratigraphy

Most of the Tertiary sediments in the southern part of the sinkhole were eroded and replaced by glacial sediments, then removed during early quarrying, leaving only the northern part of the sinkhole available for study (figs. 2 and 3). The remaining

Pipe Creek Sinkhole pebbles and cobbles occurred in two types of diamictons. The oldest (diamicton-1 = Dm1) consisted of gray-brown clay that contained well-rounded metaquartzite pebbles and cobbles intermixed with angular clasts of local chert and limestone. In the northwestern corner of the sinkhole, at least four Dm1 beds were interstratified with thin layers of carbonate sand and clay of local derivation (fig. 3C, D, E). In this part of the sinkhole, glacial sediments overlay and truncated the Dm1 beds unconformably (fig. 3D).

In the lower northeastern part of the sinkhole, another sediment (diamicton-2 = Dm2) occurred above Dm1 beds (figs. 2 and 3A, F, G). The Dm2 beds were gray-black and consisted of local clay containing metaquartzite pebbles and cobbles intermixed with sand, chert, and parts of fossil plants and animals (Sunderman and others, 1997; Farlow and others, 1998; Swinehart and others, 1999; Farlow and others, 2001; Martin and others, 2002) (fig. 3F, G). The dark color and fossils of this sediment suggests the former presence of an ephemeral pond that attracted animals and provided water for plants.

Petrography of hand specimens

Virtually all the sinkhole pebbles and cobbles are well rounded (shown by circles in fig. 3B, C, G; fig. 4), and have thin exterior oxidized zones, clear quartzose interiors, and apparent metamorphic textures. In contrast, all the angular clasts (Krumbein, 1941) found in both diamictons (shown by rectangles in fig. 3B, C) consisted only of local chert and limestone) and all of the clasts in the overlying glacial drift had angular shapes, faceted and striated surfaces, various colors, and numerous igneous and metamorphic lithologies (figs. 2B, 3B).

Figure 3. Field photographs of the Pipe Creek Sinkhole and surrounding features. A) Main sinkhole during first week of excavation, showing surrounding glacial pavement (GP), south vertical wall (VW), east-dipping bedding-plane wall (BW), Wisconsin Trafalgar silty till (ST), detached limestone blocks (LB), lower quarry floor (QF) on which sediment was being dumped, Wisconsin Lagro clay till (CT), and Tipton Till Plain (TP). (Dark van on glacial pavement gives scale.) B) Tertiary-Pleistocene Unconformity (TPU) preserved in sediments filling solution crevice developed in pisolite dike (PD). Sinkhole bed (Sb) red-brown diamicton-1 (Dm1) is overlain unconformably by Lagro boulder gravel (BG). Dm1 contains local clasts of angular chert and limestone (within rectangles) and rounded exotic metaquartzite pebbles (within circles). (Pocketknife gives scale.) C) Sb brown Dm1 interstratified with yellow-white crinoidal sand (CrS) and red-brown kaolinitic clay (KC). Local clasts and exotic metaquartzite pebbles indicated by rectangles and circles, as in Figure 3B. (Hammer gives scale.) D) Southwest extension of Figure 3C. Tertiary/Pleistocene unconformity (TPU) exposed adjacent to detached limestone block (LB). Interlaminated Sb yellow-white crinoidal sand and red-brown kaolinitic clay (CrS/KC) truncated and overlain by quartz sand of Wisconsin Lagro Fm. (QS). (Pocketknife gives scale.) E) Three sequences of Sb crinoidal sand and kaolinitic clay (CrS/KC) slumped and differentially distorted in solution crevice of reef limestone (RL). (Bar gives scale; see 3G.)

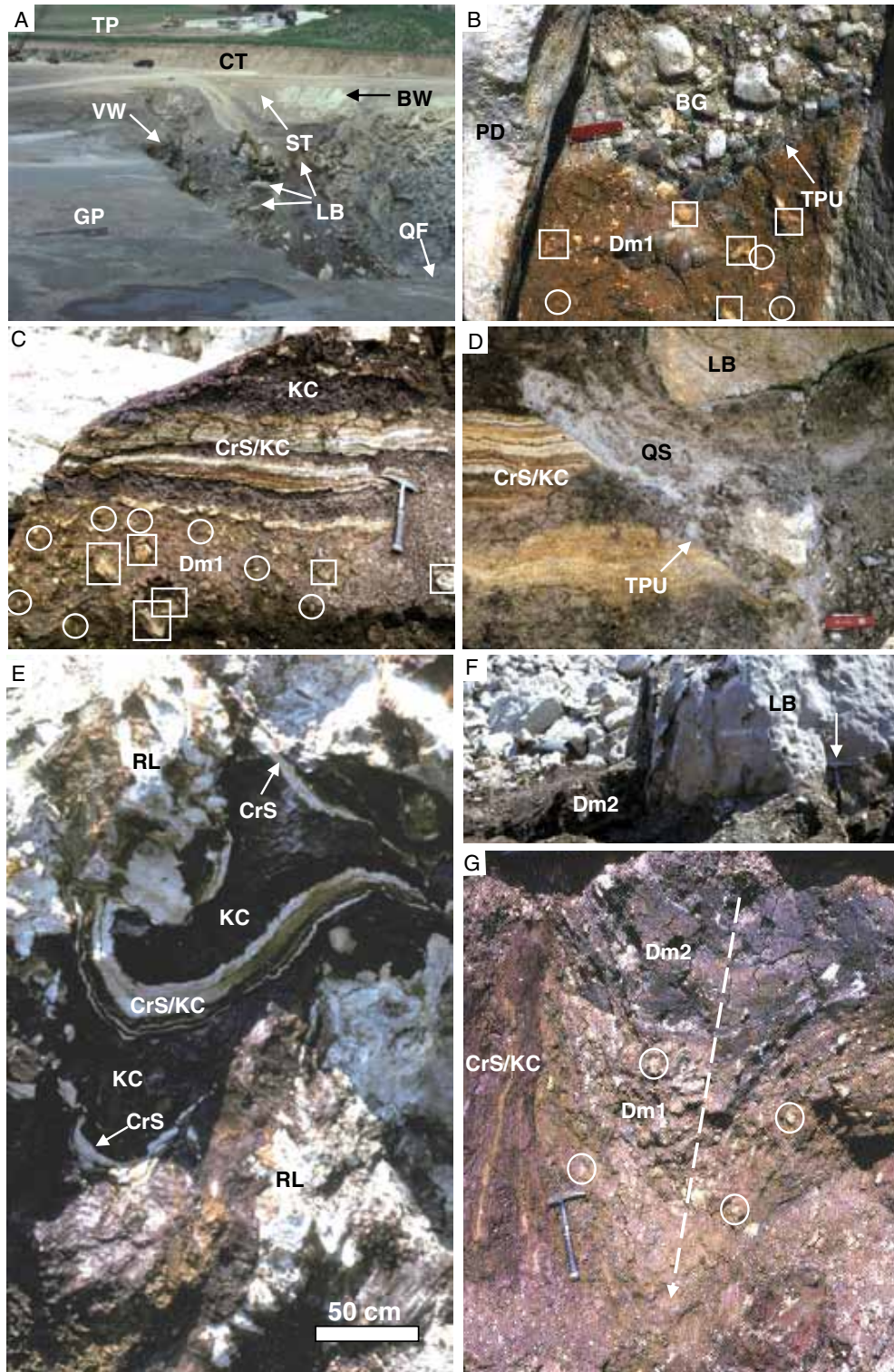


Figure 3 (cont.). Field photographs of the Pipe Creek Sinkhole and surrounding features. F) Sb gray-black unstratified diamicton-2 (Dm2), containing randomly intermixed metaquartzite pebbles and Early Pliocene fossil fragments (Farlow and others, 2001), deposited in lower part of sinkhole, adjacent to reef limestone boulder (LB). (Arrow points to hammer for scale.) G) Slumped cavity fill near and below level of photo F, exposed by excavation. Sb CrS/KC interstratified pebble-bearing (circled) sediments stratigraphically overlain by brown Dm1 and fossil-bearing gray-black Dm2. (Arrow gives approximate axis of fold produced during slumping, and hammer gives scale.)



Figure 4. Photograph of metaquartzite pebbles, showing smoothed surfaces, near-perfect rounding, and shapes (spheroids, rods, discs, and blades, top to bottom) typical of long-distance stream transport (Krumbein, 1941).

POSSIBLE PEBBLE SOURCES

Sample collections

To compare potential source materials with the Pipe Creek Sinkhole pebbles, samples were collected from rock outcrops, stream gravels, and glacial deposits derived from potential bedrock sources (fig. 1, sample sites = circled numbers 1–5). The last two types (stream gravels and glacial deposits) were used to increase the effective size and representation of the potential source areas (Eriksson and others, 2001).

To represent southern Blue Ridge rocks, samples were collected from Catawba River terrace gravels in the Inner Piedmont, just east of the Blue Ridge crest in North Carolina (site 1) (Goodwin and Johnson, 1970); from Cambrian Chilhowee Group bedrock in the southern Blue Ridge (site 2) (Stose and Stose, 1944); and from gravels in an abandoned section of the Teays Valley in West Virginia (site 3). To represent northern Blue Ridge rocks, samples were collected from Cambrian Chilhowee Group bedrock in northern Virginia and southern Maryland (site 4). To represent Canadian Shield quartzites that occur near Lake Erie, samples were collected from Erie Lobe outwash gravels at Fort Wayne, Indiana (site 5), and from Erie Lobe till and outwash gravels at the Pipe Creek Sinkhole (labeled “X”). To compare the Sb vein quartz pebbles with possible sources,

similar pebbles were obtained from basal Pennsylvanian pebble conglomerates in eastern Ohio, eastern Tennessee, and southwestern Indiana (fig. 1).

Sample analyses

Micrographic features

Micrographic features of 38 sinkhole pebbles and 40 comparison samples from sites 1 through 5 (fig. 1) were analyzed. Site 6, in the Upper Peninsula of Michigan, was not used because a transport stream from there to the Pipe Creek Jr. Quarry has not been discovered.

The micrographic features were identified in thin sections, then assigned to one of five categories, with features shown in Figures 5, 6, and 7, and identified with abbreviations and arrows: 1) DE (distorted extinctions) – sweeping undulatory and patchy; 2) PO (preferred orientations) – lattice and shape; 3) IC (irregular contacts) – sutured, serrated, and mortared; 4) DG (detrital grain features) – detrital grains, point contacts, and detrital-sericitic matrix; and 5) ME (massive extinctions) – massive crystal features extending over most of the thin section, with small (DI) (dispersed inclusions) closely spaced throughout the entire thin section. (The photomicrographs of Figures 5 through 7 were taken with crossed Nicholls at the same magnification, resulting in horizontal view dimensions of ~10 mm. Micrographic features and categories referred to in Figures 5 through 7 are described in the methods section of the text, and are used for graphic comparisons of samples in Figure 9 [microfeature graph].)

Categories 1 through 3 were established to characterize highly metamorphosed quartz arenites (metaquartzites), category 4 to characterize slightly or moderately metamorphosed clastic rocks that retained sedimentary rock characteristics, and category 5 to characterize milky vein quartz. Percents of the micrographic features were then determined and compared graphically (fig. 8) (Skolnick, 1965; Groshong, 1988; Wu and Groshong, 1991).

Extension microfractures called Fairbairn lamellae (Fairbairn, 1941) and planes and bands of inclusions called Tuttle lamellae and ghost Tuttle lamellae (Tuttle, 1949) also occurred in some samples, but did not distinguish the categories and are not shown on the charts.

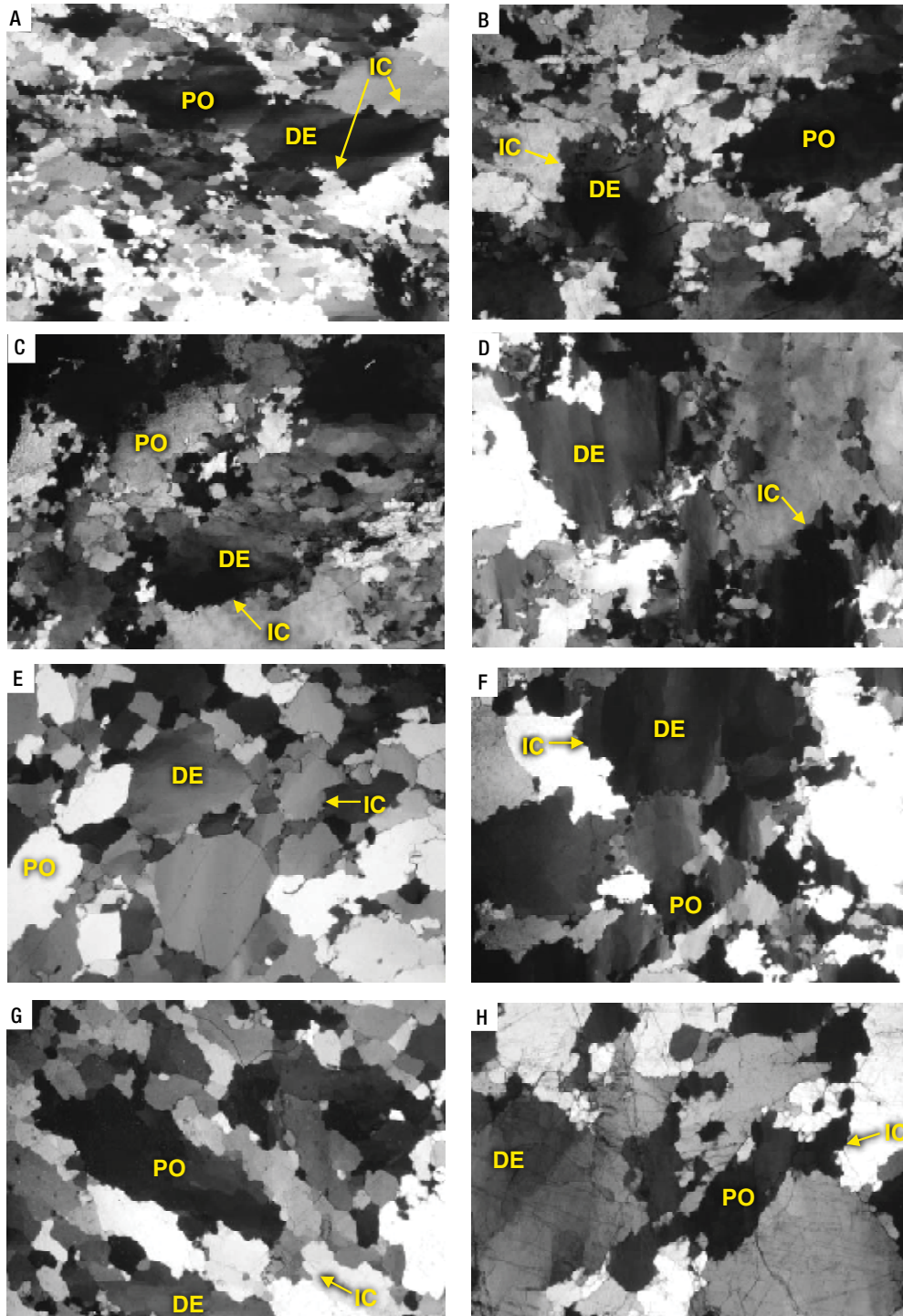


Figure 5. Photomicrographs of sinkhole bed (Sb) metaquartzite (Mq) pebbles and potential source rocks from the southern Blue Ridge (sBR) area. A–C) Sb Mq pebbles exhibiting distorted extinctions (DE), preferred orientations (PO), and irregular crystal contacts (IC). D–H) Rocks from the sBR drainage area exhibiting micrographic features (DE, PO, IC) similar to those of the Sb Mq pebbles. Sample D is from sBR bedrock, E and F from Inner Piedmont (IP) stream cobbles and boulders, and G and H from Teays Valley (TV) stream pebbles and cobbles (see also figs. 1 and 3).

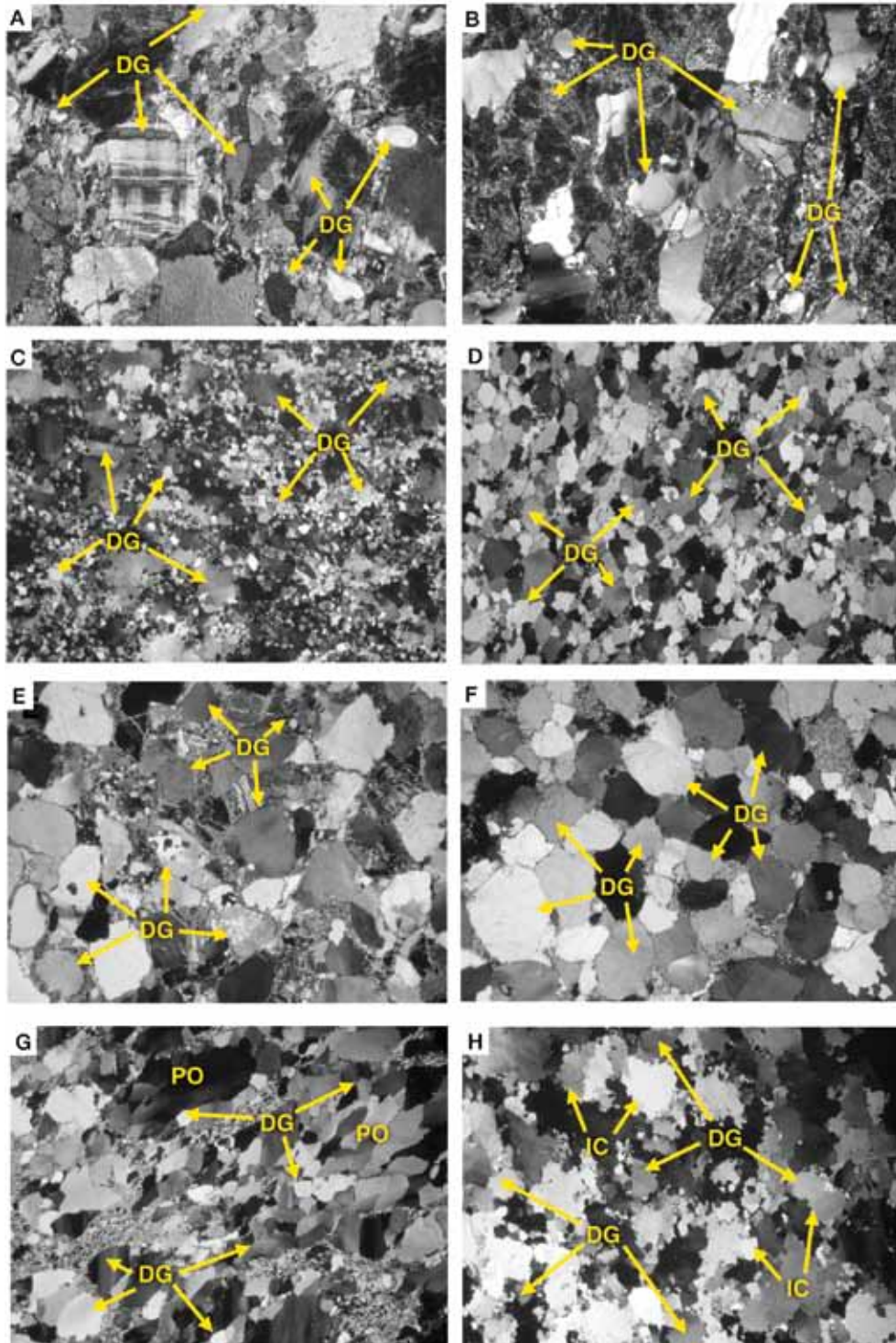


Figure 6. Photomicrographs of rocks from northern Blue Ridge (nBR) and Canadian Shield (CS) areas (see also Fig. 5A–C). A–B) Obtained from nBR bedrock, both with detrital grains (DG), detrital/sericitic matrix and a variety of minerals (quartz, feldspars, biotite). C–D) Northern Wisconsin Precambrian bedrock and Upper Peninsula of Michigan Precambrian bedrock, both with detrital grains (DG). E–H) Precambrian glacial cobbles and boulders derived from CS Lake Erie region, collected from Late Wisconsin glacial till and outwash at the sinkhole site, all with detrital grains (DG). (Note that some grains of sample G exhibit preferred orientations (PO), and some grains of sample H exhibit irregular (sutured) contacts (IC).

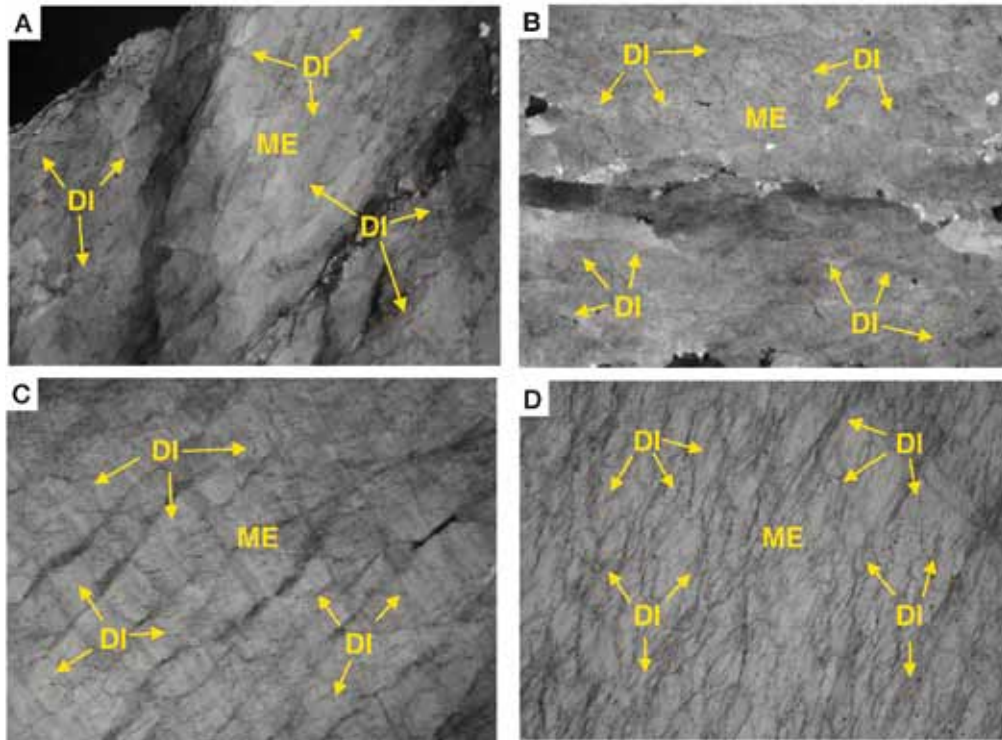


Figure 7. Photomicrographs comparing micrographic features of sinkhole bed (Sb) vein quartz (Vq) pebble with those of pebbles from lower Pennsylvanian quartz pebble conglomerates. A) Sb Vq pebble exhibiting mass crystal features (universal mass extinction and disseminated inclusions). B–D) Milky vein quartz pebbles from basal Pennsylvanian conglomerates (Pc) exhibiting mass crystal features similar to those of the Sb Vq pebble. Specimen B is from eastern Tennessee, C from eastern Ohio, and D from southern Indiana.

Micrographic interpretations

Micrographic features of the sinkhole pebbles (fig. 5A–C) indicate metamorphism (Skolnick, 1965; Groshong, 1988; Carozzi, 1993), suggesting derivation from a provenance located beyond the three sedimentary basins that surround the Pipe Creek Sinkhole (fig. 1).

The compositions and textures of samples from the southern Blue Ridge area (fig. 5D–H) are similar to those of the Pipe Creek Sinkhole metaquartzite pebbles and cobbles (fig. 8), suggesting that this area is the provenance of the sinkhole grains (Groshong, 1988; Wu and Groshong, 1991; Carozzi, 1993; Farrar, 2001). In addition, many of the Pipe Creek pebbles and southern Blue Ridge samples have elongate textures, possibly from directed stress during thrust faulting, a common characteristic of rocks in the southern Blue Ridge area.

Vein quartz interpretations

A few of the sinkhole pebbles consist of milky-white vein quartz (Vq) that in thin sections show large crystals >20 mm in diameter and have widely disseminated small inclusions (fig. 8B). These features indicate that the vein quartz pebbles also originated in distant source areas. Their features are similar to those of basal Pennsylvanian vein quartz pebbles from southern Indiana, eastern Ohio, and eastern Tennessee, suggesting they have similar origins. The sinkhole vein quartz pebbles thus could have been derived from the same provenance area as the sinkhole metaquartzite pebbles (Hadley and Nelson, 1971; Unrug and Unrug, 1990), or from secondary basal Pennsylvanian conglomerates located between the sinkhole metaquartzite provenance area and the sinkhole.

In contrast, samples from the northern Blue Ridge (fig. 6A, B) and from the Canadian Shield (fig. 6C–H) all contain recognizable detrital grain features, in-

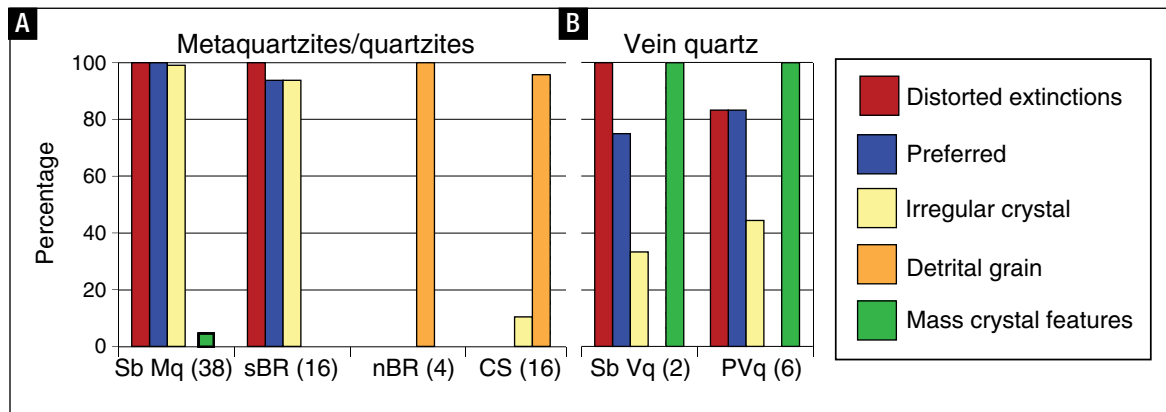


Figure 8. Graphs comparing percentages of micrographic features exhibited by sinkhole bed (Sb) erratics and potential sources. The numbers of samples used are given in parentheses adjacent to specimen names, and the locations of sample sites are indicated on Figure 1, by numbers 1–6, and by an X for the sinkhole site. A) Sinkhole beds metaquartzite (Sb Mq) and southern Blue Ridge (sBR) specimens show similar percentages of properties, but the properties of northern Blue Ridge (nBR) and Canadian Shield (CS) specimens are significantly different. B) Sb vein quartz (Vq) pebbles and P Vq specimens show similar percentages of properties.

dicating lower levels of metamorphism than the pebbles and cobbles of the Pipe Creek Sinkhole (fig. 5A–C).

Lead isotope analysis

To test the possibilities that the sinkhole pebbles were derived from the Canadian Shield or from Blue Ridge sources, the following 26 samples were analyzed: 8 sinkhole pebbles, 2 samples from Inner Piedmont (IP) gravels, 7 from southern Blue Ridge (sBR) bedrock, 5 from Teays Valley (TV) gravels, and 4 from northern Blue Ridge (nBR) bedrock. For comparison, the following 25 Canadian Shield samples were analyzed: 20 samples from Erie Lobe outwash gravels at Fort Wayne, Indiana, and 5 from Erie Lobe glacial outwash and till at the Pipe Creek Quarry.

The samples were subjected to single clast Pb/Pb analysis, and the resulting data plotted on Pb/Pb diagrams (fig. 9). The samples were crushed and aliquots cleaned ultrasonically with 1 N HCl for 30 minutes. The cleaned pieces were hand-picked to avoid discoloration and placed in clean Savillex vials for dissolution. The samples were dissolved in approximately 1 ml of concentrated HF mixed with HNO₃ on a hotplate for 2 to 3 days. After dissolution, the vials were uncapped, the solution dried down and then redissolved in 6 N HCl for standard Pb anion exchange chemistry (Krogh, 1973). The samples were not spiked, so the concentrations are not known, but the Pb blank during the interval of the analyses was less than 100 mg and the sample sizes are all greater than 100 mg. Quartz has a wide range

in Pb concentrations, with lowest measured concentrations (Hemming and others, 1994) around 0.05 ppm. Thus, considering the aliquot size, and with the common Pb ratios measured, the blank will have no significant impact. Samples were analyzed on a Finnigan MAT 262 multi-collector mass spectrometer at Stony Brook. Measurements were made in static mode. Pb was loaded on Re single Re filaments with an H₃PO₄-silica-gel loading solution. Fractionation was monitored through multiple runs of SRM 982 and for the intervals of analyses for this study was 0.08% +/- 0.04 per AMU, and this correction is made for the reported ratios.

Lead isotope interpretations

Pb isotope diagrams (fig. 9) show data collected for this study. The ²⁰⁷Pb/²⁰⁴Pb versus ²⁰⁶Pb/²⁰⁴Pb data from Inner Piedmont gravels, Late Paleozoic bedrock, Teays Valley gravels, Appalachian bedrock, and Pipe Creek Sinkhole pebbles scatter about a 1.1 Ga reference line, whereas data from the overlying glacial sediments scatter about a 2.0 Ga reference line and show dramatically more radiogenic values. ²⁰⁸Pb/²⁰⁴Pb data from the Inner Piedmont, Late Paleozoic, Teays Valley, Appalachians, and the Pipe Creek Sinkhole pebbles are nearly invariant and average 38.52 ± 0.8 Ga. In contrast, data from the overlying glacial till show high and extremely variable ²⁰⁸Pb/²⁰⁴Pb values ranging from 35.58 to 105.98 Ga. To emphasize the similarity of the ²⁰⁷Pb/²⁰⁴Pb versus ²⁰⁶Pb/²⁰⁴Pb data of the Inner Piedmont, Late Paleozoic, Teays Valley, Appalachians, and Pipe Creek

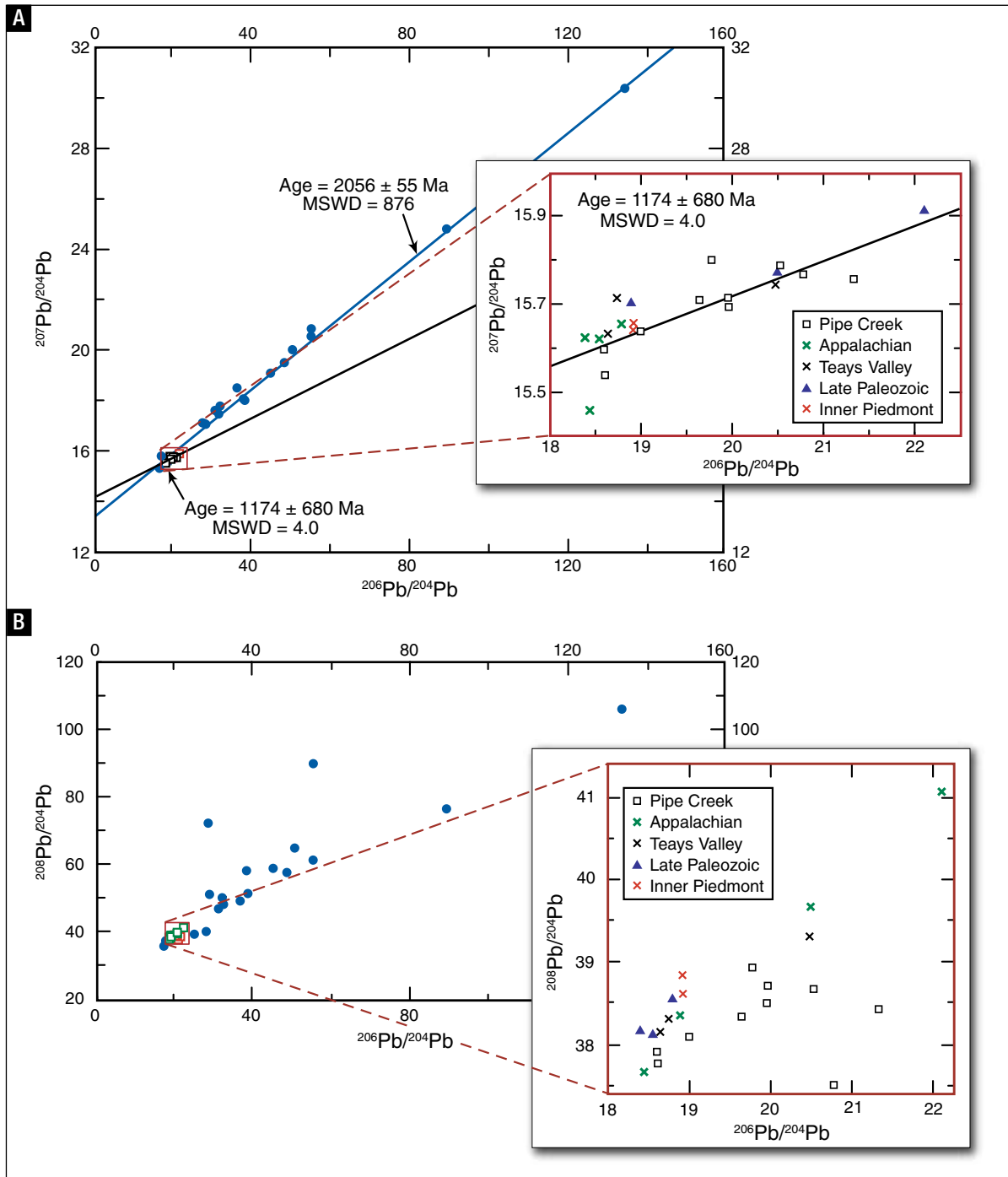


Figure 9. Pb isotope diagrams showing data collected for this study: A) $^{207}\text{Pb}/^{204}\text{Pb}$ versus $^{206}\text{Pb}/^{204}\text{Pb}$ data from the Inner Piedmont, Late Paleozoic, Teays Valley, Appalachians, and Pipe Creek Sinkhole scatter about a 1.1 Ga reference line, whereas data from the overlying glacial sediments scatter about a 2.0 Ga reference line and show dramatically more radiogenic values. B) $^{208}\text{Pb}/^{204}\text{Pb}$ data are nearly invariant from the Inner Piedmont, Late Paleozoic, Teays Valley, Appalachians, and the Pipe Creek Sinkhole (averaging 38.52 ± 0.8), whereas data from the glacial till overlying the paleosinkhole shows high and extremely variable $^{208}\text{Pb}/^{204}\text{Pb}$ values, ranging from 35.58 to 105.98.

The normal (small) and enlarged $^{207}\text{Pb}/^{204}\text{Pb}$ versus $^{206}\text{Pb}/^{204}\text{Pb}$ diagrams (red rectangles) show only the Inner Piedmont, Appalachian, Late Paleozoic, Teays Valley, and Pipe Creek Sinkhole data.

paleosinkhole, their diagrams are enlarged and outlined in red.

Together, the plots of Figure 9 show that the sBR sample data are consistent with the Sb Mq pebble data, and that the CS sample data are highly distinct from that data. In addition, the interpreted ~1.0 Ga signature established for the Sb metaquartzite pebbles is consistent with published Pb isotope data from the Appalachian region (Sinha and others, 1996) and is consistent with published ages of plutonic rocks of the Grenville Province of the southern Appalachians (Bartholomew and Lewis, 1984; Sinha and others, 1996; Eriksson and others, 2001).

PEBBLE/COBBLE TRANSPORT

Transport agent

The rounding, shaping, and nearly perfect lithologic sorting of the sinkhole metaquartzite pebbles and cobbles (figs. 3 B, C, G, and 4) indicate that: (1) they were transported to Indiana by a major stream; (2) they were deposited near the sinkhole as well-sorted stream gravels; and (3) the transporting stream was not associated with glaciation. The composition, texture, and repetition of the stratified pebble-bearing diamicton-1 beds suggest that the Mq stream gravels eventually became mixed with clays derived from nearby paleosols, and with angular clasts of local reef chert and limestone. The repetition of these diamicton beds also suggests that the mixtures were periodically transported to the sinkhole essentially without sorting, perhaps in the form of debris flows (Sunderman and others, 1998).

Time of transport. The random mixing of Sb pebbles and cobbles with indigenous fossils such as snakes, frogs, toads, and turtles in the gray-black diamicton-2 indicates that the Sb clasts were deposited in the sinkholes either prior to or during the time the organisms lived there, ~5 Ma (Dm2 in figs. 2 A, B, and 3 F, G) (Farlow and others, 1998; 2001). This time of sedimentation provides a minimum age limit for transport of the exotics to northern Indiana (at least ~5 Ma), but does not provide a maximum age limit. This contradicts a conclusion by Granger and others (2001) that the Teays River in Indiana was an ice marginal river that was newly formed by glaciers ~2 Ma.

INCISION OF THE “TEAYS VALLEY” IN INDIANA

This study also provides evidence for incision of the Teays Valley in Indiana. The similarity of the sinkhole metaquartzites and southern Blue Ridge rocks (which include samples from the abandoned Teays Valley of West Virginia), and the location of the sinkhole beds ~12 km (~7 miles) south of the Teays Valley in Indiana together suggest transport of the Sb pebbles and cobbles to Indiana by a preincision version of the Teays River. The ~259-m (~850-ft) elevation of the glacially eroded bedrock surface at the sinkhole site (figs. 2 and 3A) also gives a minimum elevation for the surface across which the pebbles and cobbles were transported to Indiana.

The presence of drainage cavities and steeply dipping unconsolidated sinkhole beds in the bottom of the main sinkhole (figs. 2 and 3) suggests that the sinkhole could have acted as a “swallow hole” for underground drainage of the valley or its tributaries. The presence of these features implies that incision of the Teays Valley in northern Indiana began sometime before or during development of the sinkhole, >5 Ma. This age is compatible with a ~5.7 Ma date determined for initial incision of the Cumberland River, which flows westward south of the glacial boundary in Kentucky and Tennessee (Anthony and Granger, 2004), and also is compatible with the ~7 Ma maximum age of the highest gravels in old courses of the New River headwaters of the Teays River system in southwestern Virginia (Bartholomew and Mills, 1991).

CONCLUSIONS

Stratigraphic relations and petrologic characteristics of the sinkhole beds prove their pre-Wisconsin, nonglacial origin, in agreement with published ~5 Ma ages of fossils found in these sediments. The Pb/Pb isotopic signature of ~1.0 Ga for the sinkhole metaquartzite pebbles indicates initial crystallization of their mineral components in a Grenvillian terrain, suggesting derivation from a Grenvillian Appalachian source. Petrographic features of the metaquartzites suggest metamorphism under directed compressional stress, characteristics typical of southern Blue Ridge bedrock. Also, rounding of the pebbles and cobbles prove their stream transport

from a distant source; and petrographic similarities with the southern Blue Ridge sample group (fig. 6) suggest a southern Blue Ridge provenance.

The proximity of the sinkhole site to the incised Teays Valley in Indiana suggests transport of the exotics to Indiana by a preincision version of the Teays River. The presence of the metaquartzite pebbles and cobbles in the sinkhole strongly suggests that the Tertiary Teays River flowed westward across Indiana rather than northward into the Lake Superior Lowland (Coffey, 1958; Gray, 1991; Melhorn and Kempton, 1991), and that the incision of the Teays Valley in Indiana was a westward continuation of the preglacial incision of the Teays Valley that occurred in Virginia, West Virginia, and southern Ohio (Ver Steeg, 1946; Rhodehamel and Carlston, 1963; Thornbury, 1965, p. 139–141; Bonnett and others, 1991; Goldthwait, 1991.)

Petrologic and petrographic similarities of the sinkhole vein quartz pebbles and basal Pennsylvanian pebbles (figs. 7 and 8B) suggest the origin of these grains from such secondary sources. Other possible sources are vein quartz bedrock and vein quartz pebble conglomerates of the southern Blue Ridge Mq provenance area (Hadley and Nelson, 1971; Unrug and Unrug, 1990).

In summary, 1) the provenance of the sinkhole metaquartzites was the southern Blue Ridge Province of the Appalachian Mountains; 2) a preincision version of the Teays River transported the metaquartzite pebbles and cobbles to northern Indiana >5 Ma, initially depositing them on an erosion surface at greater than 259 m (850 ft) elevation, and comparable to the Lexington Penplain of Kentucky; 3) the Tertiary Teays River later incised the Teays Valley across northern Indiana, with possible later modifications by Pleistocene meltwater streams; and 4) vadose development of the Pipe Creek Sinkhole probably was initiated by incision of the Teays Valley during Late Miocene time, >5 Ma.

The provenance of the Sb Vq pebbles is problematic. They could have been derived from primary or secondary vein quartz pebble sources in the southern Blue Ridge area (Simpson and Eriksson, 1989), or from secondary vein quartz pebble sources such as the Pennsylvanian Sharon Conglomerate in Ohio.

ACKNOWLEDGEMENTS

Ray Rich, Area Manager, and Ron Lewis, Quarry Superintendent, provided access to the Pipe Creek Sinkhole, and Jonathan Havens, company Geologist, provided informative discussions on the geology of the sinkhole. Anne Argast helped with photomicrography, Greg Nelson gave advice on petrographic analyses, and Clarence Tennis gave help in production of thin sections and illustrations. William Blackburn carried out exploratory microprobe analyses of pebbles, Nelson Shaffer provided analyses of clays from the sinkhole, and Pat Catanzaro drafted an early version of the geologic map and the current version of the Pb/Pb figure. Mark Carter, Leonard Weiner, and Peter Lemiszki provided help in identifying and collecting specimens from the southern Blue Ridge region. Ned Bleuer, Leon Follmer, and John Kempton provided early reviews of the manuscript, and Michael Velbel provided information that supported our effort to determine the provenance and transport of the sinkhole pebbles and the course of the Teays River southwest of the Lake Erie Lowlands of the United States.

REFERENCES

- Anthony, D. M., and Granger, D. E., 2004, A Late Tertiary origin for multilevel caves along the western escarpment of the Cumberland Plateau, Tennessee and Kentucky, established by Cosmogenic ²⁶Al and ¹⁰Be: *Journal of Cave and Karst Studies*, v. 66, no. 2, p. 46–55.
- Bartholomew, M. J., and Lewis, S. E., 1984, Evolution of the Grenville massifs in the Blue Ridge province, southern and central Appalachians, *in* Bartholomew, M. J., and others, eds., *The Grenville event in the Appalachians and related topics: Geological Society of America Special Paper 194*, p. 229–254.
- Bartholomew, M. J., and Mills, H. H., 1991, Old courses of the New River—its late Cenozoic migration and bedrock control inferred from high-level stream gravels, southwestern Virginia: *Geological Society of America Bulletin*, v. 103, no. 1, p. 73–81.
- Bleuer, N. K., 1991, The Lafayette Bedrock Valley System of Indiana; concept, form, and fill stratigraphy, *in* Melhorn, W. N., and Kempton, J. P., eds., *Geology and hydrogeology of the Teays-Mahomet Bedrock Valley System: Geological Society of America Special Paper 258*, p. 51–77.

- Bonnett, R. B., Noltimier, H. C., and Sanderson, D. D., 1991, A paleomagnetic study of the early Pleistocene Minford Silt Member, Teays Formation, West Virginia, *in* Melhorn, W. N., and Kempton, J. P., eds., *Geology and hydrogeology of the Teays-Mahomet Bedrock Valley System: Geological Society of America Special Paper 258*, p. 9–18.
- Bruns, T. M., Logan, S. M., and Steen, W. J., 1985, Map showing bedrock topography of the Teays Valley [central and eastern parts], north-central Indiana: Indiana Geological Survey Miscellaneous Maps 43 and 44, scale 1:100,000.
- Carozzi, A. V., 1993, *Sedimentary petrography*: Englewood Cliffs, N.J., Prentice Hall, 263 p.
- Coffey, G. N., 1958, Major glacial drainage changes in Ohio: *Ohio Journal of Science*, v. 58, no. 1, p. 43–49.
- DeWolf, C. P., and Mezger, K., 1994, Lead-isotope analyses of leached feldspars- constraints on the early crustal history of the Grenville-Orogen: *Geochimica et Cosmochimica Acta*, v. 58, no. 24, p. 5,537–5,550.
- Dorr, J. A., Jr., and Eschman, D. F., 1977, *Geology of Michigan: The University of Michigan Press and John Wiley and Sons Canada*, 476 p.
- Eriksson, K. A., Campbell, I. H., Palin, J. M., and Allen, C. M., 2001, The Grenville Superorogeny revealed by detrital zircons in Appalachian rivers: *Geological Society of America Abstracts with Programs*, v. 33, no. 6, p. A-29.
- Fairbairn, H. W., 1941, Deformation lamellae in quartz from the Ajibik Formation, Michigan: *Geological Society of America Bulletin*, v. 52, no. 8, p. 1,265–1,278.
- Farlow, J. O., Sunderman, J. A., Holman, J. A., Swinehart, A. L., and Havens, J. J., 1998, Pipe Creek Sinkhole, a Late Tertiary terrestrial biota from Grant County, Indiana: *Society of Vertebrate Paleontology Program with Abstracts*, p. 40A.
- Farlow, J. O., Sunderman, J. A., Havens, J. J., Swinehart, A. L., Holman, J. A., Richards, R. L., Miller, N. G., Martin, R. A., Hunt, R. M., Jr., Storrs, G. W., Curry, B. B., Fluegeman, R. H., Dawson, M. R., and Flint, M. E. T., 2001, The Pipe Creek Sinkhole biota, a diverse Late Tertiary continental fossil assemblage from Grant County, Indiana: *The American Midland Naturalist*, v. 145, no. 2, p. 367–378.
- Farrar, S. S., 2001, The Grenvillian Goochland terrane-thrust slices of the Late Neoproterozoic Laurentian margin in the southern Appalachians: *Geological Society of America Abstracts with Programs*, v. 33, no. 6, p. A-28.
- Fidlar, M. M., 1943, The preglacial Teays Valley in Indiana: *Journal of Geology*, v. 51, no. 6, p. 411–418.
- Fridley, H. M., 1950, *The Geomorphic history of the New-Kanawha River System: West Virginia Geological and Economic Survey Report of Investigations*, no. 7, 12 p.
- Garipey, C., and Allegre, C. J., 1985, The lead isotope geochemistry and geochronology of late-kinematic intrusives from the Abitibi greenstone belt, and the implications for Late Archean crustal evolution: *Geochimica et Cosmochimica Acta*, v. 49, no. 11, p. 2,371–2,383.
- Goldthwait, R. P., 1991, The Teays Valley problem; a historical perspective, *in* Melhorn, W. N., and Kempton, J. P., eds., *Geology and hydrogeology of the Teays-Mahomet Bedrock Valley System: Geological Society of America Special Paper 258*, p. 3–8.
- Goodwin, B. K., and Johnson, G. H., 1970, Guidebook to the Geology of the Upland Gravels near Midlothian, Virginia: Eleventh Annual Field Conference of the Atlantic Coastal Plain Geological Association, 15 p.
- Granger, D. E., Fabel, D., and Palmer, A. N., 2001, Pliocene-Pleistocene incision of the Green River, Kentucky, determined from radioactive decay of cosmogenic ²⁶Al and ¹⁰Be in Mammoth Cave sediments: *Geological Society of America Bulletin*, v. 113, no. 7, p. 825–836.
- Gray, H. H., 1982, Map of Indiana showing topography of the bedrock surface: Indiana Geological Survey Miscellaneous Map 36, scale 1:500,000.
- Gray, H. H., 1991, Origin and history of the Teays drainage system- the view from midstream, *in* Melhorn, W. N., and Kempton, J. P., eds., *Geology and hydrogeology of the Teays-Mahomet Bedrock Valley System: Geological Society of America Special Paper 258*, p. 43–49.
- Groshong, R. H., Jr., 1988, Low-temperature deformation mechanisms and their interpretation: *Geological Society of America Bulletin*, v. 100, no. 9, p. 1,329–1,360.
- Hadley, J. B., and Nelson, A. E., 1971, Geologic map of the Knoxville quadrangle, North Carolina, Tennessee, and South Carolina: U.S. Geological Survey Miscellaneous Investigations Map I-654, scale 1:250,000.
- Hemming, S. R., McLennan, S. M., and Hanson, G. N., 1994, Lead isotopes as a provenance tool for quartz-examples from plutons and quartzite, northeastern Minnesota, USA: *Geochimica et Cosmochimica Acta*, v. 58, no. 20, p. 4,455–4,464.
- Horberg, C. L., 1945, A major buried valley in east-central Illinois and its regional relationships: *Journal of Geology*, v. 53, no. 5, p. 349–359.
- Horberg, C. L., 1956, Preglacial erosion surfaces in Illinois: *Journal of Geology*, v. 54, no. 3, p. 179–192.
- Kempton, J. P., Johnson, W. H., Heigold, P. C., and Cartwright, K., 1991, Mahomet Bedrock Valley in east-central Illinois; topography, glacial drift stratigraphy, and hydrogeology: Boulder, Colo., Geological Society of America Special Paper 258, p. 91–124.
- Krogh, T. E., 1973, A low-contamination method for hydrothermal decomposition of zircon and extraction

- of U and Pb for isotopic age determinations: *Geochimica et Cosmochimica Acta*, v. 37, no. 3, p. 485–494.
- Krumbein, W. C., 1941, Measurement and geological significance of shape and roundness of sedimentary particles: *Journal of Sedimentary Petrology*, v. 11, no. 2, p. 64–72.
- Manos, C., 1961, Petrography of the Teays-Mahomet Valley deposits: *Journal of Sedimentary Petrography*, v. 31, no. 3, p. 456–465.
- Martin, R. A., Goodwin, H. T., and Farlow, J. O., 2002, Late Neogene (Late Hemphillian) rodents from the Pipe Creek Sinkhole, Grant County, Indiana: *Journal of Vertebrate Paleontology*, v. 21, no. 1, p. 137–151.
- McDowell, R. C., and Newell, W. L., 1986, Quaternary System, in McDowell, R. C., ed., *The geology of Kentucky—a text to accompany the geologic map of Kentucky*: U.S. Geological Survey Professional Paper 1151-H, p. H49–H53.
- McGrain, P., 1986, Economic geology, in McDowell, R. C., ed., *The geology of Kentucky—a text to accompany the geologic map of Kentucky*: U.S. Geological Survey Professional Paper 1151-H, p. H59–H64.
- Melhorn, W. N., and Kempton, J. P., 1991, The Teays System; a summary, in Melhorn, W. N., and Kempton, J. P., eds., *Geology and hydrogeology of the Teays-Mahomet Bedrock Valley System*: Geological Society of America Special Paper 258, p. 125–128.
- Parmalee, P. W., Klippel, W. E., Meylan, P. A., and Holman, J. A., 2002, A Late Miocene-Early Pliocene population of *Trachemys* (Testudines: Emydidae) from east Tennessee: *Annals of Carnegie Museum*, v. 71, p. 233–239.
- Potter, P. E., 1955a, The petrology and origin of the Lafayette gravel, part 1—mineralogy and petrology: *Journal of Geology*, v. 63, no. 1, p. 1–38.
- Potter, P. E., 1955b, The petrology and origin of the Lafayette gravel, part 2—geomorphic history: *Journal of Geology*, v. 63, no. 2, p. 115–132.
- Potter, P. E., and Pryor, W. A., 1961, Dispersal centers of Paleozoic and later clastics of the upper Mississippi Valley and adjacent areas: *Geological Society of America Bulletin*, v. 72, no. 8, p. 1,195–1,250.
- Ray, L. L., 1965, Geomorphology and Quaternary geology of the Owensboro quadrangle, Indiana and Kentucky: U.S. Geological Survey Professional Paper 488, 72 p., 1 plate.
- Rhodehamel, E. C., and Carlston, C. W., 1963, Geologic history of the Teays Valley in West Virginia: *Geological Society of America Bulletin*, v. 74, no. 3, p. 251–274.
- Shunk, A. J., 2003, Evidence for an abrupt latest Miocene-earliest Pliocene climate shift preserved in a sinkhole paleolake at the Gray Fossil Site, northeastern Tennessee: Knoxville, University of Tennessee, master's thesis, 79 p.
- Shunk, A. J., Driese, S. G., and Clark, G. M., 2006, Latest Miocene to earliest Pliocene sedimentation and climate record derived from paleosinkhole fill deposits, Gray Fossil Site, northeastern Tennessee, USA: *Palaeogeography, Palaeoclimatology, Palaeoecology*, v. 231, nos. 3–4, p. 265–278.
- Simpson, E. L., and Eriksson, K. A., 1989, Sedimentology of the Unicoi Formation in southern and central Virginia—evidence for late Proterozoic to early Cambrian rift-to-passive margin transition: *Geological Society of America Bulletin*, v. 101, no. 1, p. 42–54.
- Sinha, A. K., Hogan, J. P., and Parks, J., 1996, Lead isotope mapping of crustal reservoirs within the Grenville superterrane—I. central and southern Appalachians, in Basu, A., and Hart, S., eds., *Earth processes—reading the isotopic code*: Geophysical Monograph 95, p. 293–305.
- Skolnick, H., 1965, The quartzite problem: *Journal of Sedimentary Petrology*, v. 35, no. 1, p. 12–21.
- Smith, S. A., 2003, Sedimentation, pedogenesis, and paleodrainage straddling the Neogene-Quaternary boundary; a perspective from an infilled sinkhole lake, the Gray Fossil Site, northeastern TN: Knoxville, University of Tennessee, master's thesis, 66 p.
- Spencer, K. J., 1987, Isotopic, major and trace element constraints on the sources of granites in an 1800 Ma igneous complex near St. Cloud, Minnesota: State University of New York at Stony Brook, Ph.D. thesis, 194 p.
- Stose, G. W., and Stose, A. J., 1944, The Chilhowee group and Ocoee series of the southern Appalachians: *American Journal of Science*, v. 242, no. 7, p. 367–390.
- Stout, W., and Schaaf, D., 1931, The Minford silts of southern Ohio: *Geological Society of America Bulletin*, v. 42, no. 3, p. 605–620.
- Sunderman, J. A., Farlow, J. O., and Havens, J. J., 1997, Preglacial sinkhole, Pipe Creek Jr. Quarry, northern Indiana—geology and geomorphic history: Indiana Academy of Science 113th Annual Meeting Programs and Abstracts, p. 78, 79.
- Sunderman, J. A., Farlow, J. O., and Havens, J. J., 1998, Tertiary sediments and fossils from northern Indiana Pipe Creek Jr. Sinkhole site: *Geological Society of America Abstracts with Programs*, v. 30, no. 2, p. 74.
- Swinehart, A. L., Miller, N. G., Farlow, J. O., and Sunderman, J. A., 1999, Palaeoenvironment of the Pipe Creek Sinkhole (Tertiary, Hemphillian) as indicated by plant fossils: Indiana Academy of Sciences 115th Annual Meeting Program and Abstracts, p. 44, 45.
- Teller, J. T., and Goldthwait, R. P., 1991, The Old Kentucky River; a major tributary to the Teays River, in Melhorn, W. N., and Kempton, J. P., eds., *Geology and hydrogeology of the Teays-Mahomet Bedrock Valley System*: Geological Society of America Special Paper 258, p. 29–41.

- Thornbury, W. D., 1965, Regional geomorphology of the United States: New York, John Wiley and Sons, 609 p.
- Tight, W. G., 1903, Drainage modifications in southeastern Ohio and adjacent parts of West Virginia and Kentucky: U. S. Geological Survey Professional Paper 13, 111 p.
- Tuttle, O. F., 1949, Structural petrology of planes of liquid inclusions: *Journal of Geology*, v. 57, no. 4, p. 331–356.
- Unrug, R., and Unrug, S., 1990, Paleontological evidence of Paleozoic age for the Walden Creek Group, Ocoee Supergroup, Tennessee: *Geology*, v. 18, no. 11, p. 1,041–1,045.
- Ver Steeg, K., 1946, The Teays River: *Ohio Journal of Science*, v. 46, no. 6, p. 297–307.
- Wallace, S. C., Nave, J. W., and Burdick, K. M., 2002, Preliminary report on the recently discovered Gray Fossil Site (Miocene), Washington Co., Tennessee, with comments on observed paleopathologies—the advantages of a large sample: *Journal of Vertebrate Paleontology*, v. 22, no. 3, p. 117.
- Wallace, S. C., and Wang, X., 2004, Two new carnivores from an unusual late Tertiary forest biota in eastern North America: *Nature*, v. 431, no. 7008, p. 556–559.
- Wayne, W. J., 1952, Pleistocene evolution of the Ohio and Wabash Valleys: *Journal of Geology*, v. 60, no. 6, p. 575–585.
- Wayne, W. J., 1956, Thickness of drift and bedrock physiography of Indiana north of the Wisconsin glacial boundary: *Indiana Geological Survey Report of Progress* 7, 70 p.
- Wayne, W. J., and Thornbury, W. D., 1955, Wisconsin stratigraphy of northern and eastern Indiana: 5th Biennial Pleistocene Field Conference, p. 1–34.
- Wu, S., and Groshong, R. H., 1991, Low-temperature deformation of sandstones, southern Appalachian fold-thrust belt: *Geological Society of America Bulletin*, v. 103, no. 7, p. 861–875.

APPENDIX

Abbreviation	Meaning
BG	Lagro boulder gravel
BW	east-dipping bedding-plane wall
CrS	crinoidal sand
CS	Canadian Shield
CT	Wisconsin Lagro clay till
DE	distorted extinctions
DG	detrital grain features
DI	dispersed inclusions
Dm1	diamicton-1
Dm2	diamicton-2
FW	Fort Wayne, Indiana
GP	glacial pavement
IC	irregular contacts
IP	Inner Piedmont
KC	kaolinitic clay
LB	detached limestone blocks/ limestone boulder
ME	massive extinctions
Mq	metaquartzite
nBR	northern Blue Ridge
Pc	Pennsylvanian conglomerates
PD	pisolite dike
PO	preferred orientations
QF	lower quarry floor
QS	quartz sand
RL	reef limestone
Sb	sinkhole bed
sBR	southern Blue Ridge
ST	Wisconsin Trafalgar silty till
TP	Tipton Till Plain
TPU	Tertiary-Pleistocene Unconformity
TV	Teays Valley
VQ	vein quartz
VW	south vertical wall